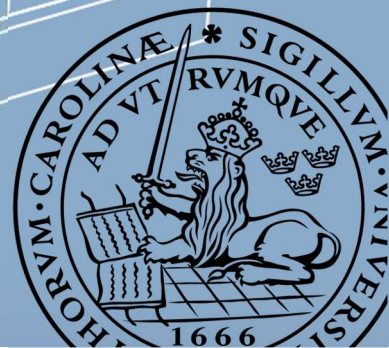


Sensitivity and Uncertainty Analysis of Building Parameters

Integrating Energy, Daylight and Thermal Comfort

Tian Tan, Magdalena Szumanska

Master thesis in Energy-efficient and Environmental Building Design
Faculty of Engineering | Lund University



Lund University

Lund University, with eight faculties and a number of research centers and specialized institutes, is the largest establishment for research and higher education in Scandinavia. The main part of the University is situated in the small city of Lund which has about 112 000 inhabitants. A number of departments for research and education are, however, located in Malmö. Lund University was founded in 1666 and has today a total staff of 6000 employees and 47 000 students attending 280-degree programmes and 2 300 subject courses offered by 63 departments.

Master Programme in Energy-efficient and Environmental Building Design

This international programme provides knowledge, skills and competencies within the area of energy-efficient and environmental building design in cold climates. The goal is to train highly skilled professionals, who will significantly contribute to and influence the design, building or renovation of energy-efficient buildings, taking into consideration the architecture and environment, the inhabitants' behavior and needs, their health and comfort as well as the overall economy.

The degree project is the final part of the master programme leading to a Master of Science (120 credits) in Energy-efficient and Environmental Buildings.

Examiner: Denis Johannson (Division of Building Services)

Supervisor: Saqib Javed (Division of Building Services), Iason Bournas (Division of Energy and Building Design), Frederik Blum Winther (Rambøll)

Front page picture source: illustrated by Tian Tan (building belongs to Rambøll).

Keywords: Sensitivity Analysis, Uncertainty Analysis, Energy Performance, Daylight, Thermal Comfort

Thesis: EEBD - # / 19

Abstract

The objective of this thesis was to perform multi-disciplinary sensitivity and uncertainty analysis of the building parameters integrating thermal comfort, energy and daylight. The case study of a Danish office building was used for performing the simulations. The study evaluated the suitability of developed methodology for further usage in the early design stages of the building projects. A literature review was conducted to summarize existing methods for sensitivity and uncertainty analysis as well as to identify the most commonly used variables. Eighteen building parameters such as window types, opaque constructions insulation thicknesses, infiltration rate, ventilation rate, setpoint and setback temperatures, internal gains, and surface optical properties were tested. Total energy consumption, number of rooms complied with Danish Building Regulations thermal comfort requirements and spatial daylight autonomy, were used as the result indicators. After validation of the statistical model of Pearson's method, Spearman's rank-order correlation method was chosen for this study. Both the sampling method and sample size were carefully determined for the generation of sampling. Results of the study included the most crucial parameters for the case building optimization. In addition, the results showed the quantification of the uncertainty in according to the results. Filtering the best-performing multi-disciplinary results led to the identification of the best performance input regions according to the input parameters. A significant outcome of the study was development of DIVA code and Python code in IES VE which could be further readjusted and reused based on the consultant needs.

Acknowledgements

We would like to take the opportunity to express our sincere gratitude towards our supervisors, Frederik Blum Winther from Rambøll, Saqib Javed from Division of Building Services and Iason Bournas from the Division of Energy and Building Design. Without your constant support, guidance, and encouragement it would not have been possible to complete this thesis to the best of our ability.

We also extend our special thanks to Rambøll Denmark for initiating the project and providing consultations and all necessary tools for successful completion of the project.

Moreover, we would like to acknowledge Maria Wall, the director of the Energy-efficient and Environmental Building Design (EEBD) Master's Programme, and all the course teachers for giving us an opportunity to be a part of the EEBD Program and sharing their valuable knowledge.

Additionally, we are grateful to Marwan Abugabbara for sharing his knowledge of statistical methods.

Finally, words cannot express our appreciation and gratitude towards our parents Bogdan and Elzbieta Szumanscy, and Yongjun and Jian, as well as our boyfriends Claus and Shen. Thank you for your continuous support, encouragement, and providing us the opportunity to dedicate 100 % of our time towards reaching our goal of achieving a master's degree in Sweden.

2019, Helsingborg

Tian Tan and Magdalena Szumanska

Contents

Abstract	i
Acknowledgements	iii
Abbreviations	vii
Figure list	ix
Table list	xiii
1 Introduction	1
1.1 Background	1
1.2 Aim and objectives	1
1.3 Scope and limitations	2
1.4 Research methods	2
1.5 Disposition of the thesis	3
2 Literature review	5
2.1 Case studies for sensitivity and uncertainty analysis	5
2.2 Statistical methods for sensitivity and uncertainty analysis	9
2.2.1 Uncertainty analysis	9
2.2.2 Sensitivity analysis	9
2.2.3 Sensitivity analysis methods	10
2.2.4 Sensitivity and uncertainty analysis sampling	13
3 Methodology	17
3.1 Building base case	18
3.2 Input parameters	20
3.3 Output parameters	25
3.3.1 Daylight	25
3.3.2 Thermal comfort	26
3.3.3 Energy	27
3.4 Generation of samples:	27
3.5 Daylight analysis	29
3.5.1 General workflow	29
3.5.2 Assumptions	30
3.5.3 Detailed workflow	30
3.6 Development of script in VEScript Python Editor	34

3.6.1	Steps in coding the VEScripts	34
3.6.2	Limitations in the VEScript Python Editor	42
3.7	Data processing in R	45
3.8	Overall results in Design Explorer	47
4	Results	49
4.1	Sensitivity analysis	49
4.1.1	Energy & Thermal comfort	50
4.1.2	Daylight	67
4.2	Uncertainty analysis	69
4.2.1	Energy & Thermal comfort	69
4.2.2	Daylight	77
4.3	Overall Results	79
5	Discussion.....	83
6	Conclusions and Future Work	87
	Summary	89
	References	91
	Appendix	99
	Appendix A: Literature review of other sensitivity analysis methods	99
	Appendix B: Python script for IES VE	101

Abbreviations

Statistical quantities:

FAST	Fourier Amplitude Sensitivity Testing
DSA	Differential Sensitivity Analysis
MCA	Monte Carlo Analysis
SSA	Stochastic Sensitivity Analysis
SRC	Standardised Regression Coefficients
SRRC	Standardised Rank Regression Coefficients
PRC	Partial Correlation Coefficient
PRCC	Partial Rank Correlation Coefficient
ACS	Adaptive Component Selection
UA	Uncertainty Analysis
SA	Sensitivity Analysis
MARS	Multivariate adaptive regression splines screening

General:

PPD	Predicted percent dissatisfied
COP	Coefficient of performance
WWR	Window to wall ratio [%]
SW	Smart windows
UDI	Useful daylight illuminance
ach	Air changes
SHD	Overhang depth [m]
SHGC	Solar heat gain coefficient
T	Temperature [$^{\circ}$ C]

SCoP	Seasonal coefficient of performance
SSEER	Seasonal energy efficiency ratio
sDA	Spatial daylight autonomy
PMV	Predicted mean vote

Nomenclature:

AF_{vent}	Window area fraction for natural ventilation
α	Solar absorptance
α_{wall}	Solar absorptance of wall
T_{vis}	Visible transmittance [%]

Figure list

Figure 1. Schematic representation of Sensitivity and Uncertainty Analysis.....	10
Figure 2. Schematic workflow for performing Sensitivity and Uncertainty analysis.....	17
Figure 3. North Façade, South Façade and Top view.....	18
Figure 4. Process of sample generation.....	27
Figure 5. Daylight simulations workflow.....	29
Figure 6. Daylight simulation model (left) glazing ratio variation on top floor (right).....	30
Figure 7. Floor plan for sDA simulations.....	31
Figure 8. Python code for reading Excel data.....	35
Figure 9. Python code for getting opaque constructions.	35
Figure 10. Python code setting properties for constructions.	36
Figure 11. Python code for changing window properties.....	36
Figure 12. Python code for getting daily profile from database.....	37
Figure 13. Python code for storing information of daily profile.....	37
Figure 14. Python code for overwriting daily profile.....	37
Figure 15. Python code for changing set points.....	38
Figure 16. Python code for getting templates database.....	38
Figure 17. Python code for getting template number.....	39
Figure 18. Internal gains database.....	40
Figure 19. Python code for getting internal gains and air exchanges database.....	40
Figure 20. Python code for adding gains and air exchanges.....	41
Figure 21. Python code for removing gains and air exchanges.....	41
Figure 22. Python code for extraction of the results.....	42
Figure 23. Example of faulty function in the VEScript Python Editor.....	43
Figure 24. Python code for reading room ids.....	44
Figure 25. Python code for assigning templates to rooms.....	44
Figure 26. Python code for writing data to Excel.....	45
Figure 27. Python code for checking number of overheating hours in problematic rooms..	45
Figure 28. Flow chart for interpretation of the results.....	49
Figure 29. Scatter plots showing correlation between wall insulation thickness and total energy consumption, and heating and cooling demand.....	51

Figure 30. Scatter plots showing correlation between roof insulation thickness and total energy consumption, and heating and cooling demand.....51

Figure 31. Scatter plots showing correlation between floor insulation thickness and total energy consumption, and heating and cooling demand.....52

Figure 32. Scatter plots showing correlation between inlet air temperature and total energy consumption, and heating and cooling demand53

Figure 33. Scatter plots showing correlation between infiltration and total energy consumption, and heating and cooling demand53

Figure 34. Scatter plots showing correlation between auxiliary ventilation and total energy consumption, and heating and cooling demand.54

Figure 35. Scatter plots showing correlation between heating setpoint and total energy consumption, and heating and cooling demand.55

Figure 36. Scatter plots showing correlation between heating setback and total energy consumption, and heating and cooling demand.55

Figure 37. Scatter plots showing correlation between cooling setpoint and total energy consumption, and heating and cooling demand56

Figure 38. Scatter plots showing correlation between cooling setback and total energy consumption, and heating and cooling demand.56

Figure 39. Scatter plots showing correlation between type of occupancy profile and total energy consumption, and heating and cooling demand.....57

Figure 40. Scatter plots showing correlation between occupancy rate and total energy consumption, and heating and cooling demand57

Figure 41. Scatter plots showing correlation between g-value of window a and total energy consumption, and heating and cooling demand.58

Figure 42. Scatter plots showing correlation between lighting gains and total energy consumption, and heating and cooling demand.....59

Figure 43. Scatter plots showing correlation between g-value of window and total energy consumption, and heating and cooling demand59

Figure 44. Scatter plots showing correlation between thickness of building envelope materials and thermal comfort.....60

Figure 45. Scatter plots showing correlation between inlet air properties and thermal comfort.61

Figure 46. Scatterplot showing correlation between setback / setpoints temperature and thermal comfort.62

Figure 47. Scatterplot showing correlation between type of occupancy profile/ occupancy rate and thermal comfort.....62

Figure 48. Scatterplot showing correlation between window *g*-value, lighting gains, equipment gains and thermal comfort.....63

Figure 49. Spearman's coefficient for total energy consumption.64

Figure 50. Spearman's coefficient for thermal comfort.64

Figure 51. Spearman's coefficient for heating demand.65

Figure 52. Spearman's coefficient for cooling demand.65

Figure 53. Scatter plots showing correlation between floor reflectance, ceiling reflectance and spatial daylight autonomy.....67

Figure 54. Scatter plots showing correlation between reflectance of wall, *T_{vis}* of different window types and spatial daylight autonomy.68

Figure 55. Density plot for total energy consumption results based on 400 simulated samples.70

Figure 56. Density plot for heating demand results based on 400 simulated samples.70

Figure 57. Density plot for cooling demand results based on 400 simulated samples.70

Figure 58. Density plot of results representing number of rooms complying with requirements set in thermal comfort section (Less than 100hr in period from April to October, with operative temperature exceeding 26 °C).....71

Figure 59. Favorable input span for wall insulation thickness in 117, 118 and 31 samples..71

Figure 60. Favorable input span for roof insulation thickness in 117, 118 and 31 samples..72

Figure 61. Favorable input span for floor insulation thickness in 117, 118 and 31 samples.72

Figure 62. Favorable input span for inlet air temperature in 117, 118 and 31 samples.....73

Figure 63. Favorable input span for infiltration rate in 117, 118 and 31 samples.....73

Figure 64. Favorable input span for auxiliary ventilation rate in 117, 118 and 31 samples..73

Figure 65. Favorable input span for heating setpoint in 117, 118 and 31 samples.....74

Figure 66. Favorable input span for heating setback in 117, 118 and 31 samples.74

Figure 67. Favorable input span for cooling setpoint in 117, 118 and 31 samples.75

Figure 68. Favorable input span for cooling setback in 117, 118 and 31 samples.75

Figure 69. Favorable input span for occupancy profile type in 117,118 and 31 samples.75

Figure 70. Favorable input span for occupancy rate in 117, 118 and 31 samples.....76

Figure 71. Favorable input span for g-value of window in 117, 118 and 31 samples.....76

Figure 72. Favorable input span for lighting gains in 117, 118 and 31 samples.....77

Figure 73. Favorable input span for equipment gains in 117, 118 and 31 samples.....77

Figure 74. Density plot representing distribution of Spatial Daylight Autonomy results in simulated population.....78

Figure 75. Favorable input ranges for ceiling and floor reflectance, meeting the criterion of sDA over 82.27 %.....78

Figure 76. Favorable input ranges for wall reflectance and window Tvis, meeting the criterion of sDA over 82.27 %.....79

Figure 77. Parallel coordinate plot for 400 samples.....80

Figure 78. Parallel coordinate plot for remaining samples after adding the first filter.....80

Figure 79. Parallel coordinate plot for remaining samples after adding the second filter.....80

Figure 80. Parallel coordinate plot for remaining samples after adding the third filter.....81

Figure 81. Parallel coordinate plot for the optimum approach.....81

Table list

Table 1. Literature research summarizing choice of input / output parameters and different methods used for sensitivity/ uncertainty analysis in buildings.	5
Table 2. Summary of global methods (<i>n</i> means number of parameters).....	11
Table 3. Probability Distributions based on applicability in building simulation analysis. ...	14
Table 4. Opaque construction for base case.	18
Table 5. Base case glazed constructions.....	19
Table 6. Thermal templates assigned for the base case.	19
Table 7. Opening types.....	20
Table 8. HVAC settings.	20
Table 9. Input parameters for parametric studies including distributions and ranges.	21
Table 10. Type of windows chosen for parametric studies.	22
Table 11. Types of profiles used in the project.	23
Table 12. Tolerance level for different calculational periods.....	26
Table 13. Determination of the minimum sample size based on different accuracy levels...	28
Table 14. Transmissivity values used for DIVA simulations.....	32
Table 15. Raytrace quality settings; Source: [85].....	33
Table 16. Template number and index assigned in the base case model.....	39
Table 17. Evaluation of correlation strength.	46
Table 18. Evaluation of significance level.	47
Table 19. Pearson's determination coefficient.	50
Table 20. Ranking of the most important parameters in the building optimization process.	66
Table 21. Comparison of coefficients in Spearman's and Pearson's method.	67
Table 22. Ranking of coefficients affecting daylight.	68
Table 23. Summary of the data.....	69
Table 24. Uncertainty Results parameters for sDA _{300,50} output.....	78

1 Introduction

This chapter presents the theoretical background, objectives, and scope of the project. It also details research methods, project deliverables, and research limitations.

1.1 Background

The building industry is under continuous development and several changes in legislation and building codes concerning energy efficiency have been implemented in recent times [1]. Reducing the building's energy consumption and optimizing its energy performance are the two key-target areas for both architects and engineers. Prediction of the building's energy consumption is not only a significant step towards finalizing the design process but is also central for classifying the building based on its energy performance. Building simulations aiding the decision-making process are widely used in the latter stages of the design process. However, due to the time required for modelling and computation, and due to the uncertainties in the design input parameters, benefits of using building simulations in the initial design stages of the construction projects are still limited. Consequently, statistical methods have been frequently used in both practice and research [2-4] for predicting the energy consumption of the buildings and for assessing the impact of the design input parameters on the simulation results.

As requirements on energy demands are becoming more stringent with every new change in buildings regulations [5], early decision making in a project lifecycle can lead to better time-efficiency in solving design challenges. Sensitivity and uncertainty analysis can be used to identify the order in which the design parameters should be addressed, and to quantify how uncertainties in modelling inputs may affect the model outputs [6]. Majority of the case studies reported in the literature [7-9] have performed sensitivity and uncertainty analysis considering only one design objective, for example, minimising the energy demands of a building. A relatively small number of studies have investigated energy, thermal comfort and daylight at the same time [6]. Only a handful of studies have used a holistic design approach to the building design process. For example, Iason et al. [10] suggested a methodology for analysing multiple objectives from the early design stage to the final design stage of a building. The 'holistic design approach' also provides a significant motivation for performing multi-disciplinary sensitivity and uncertainty analysis.

1.2 Aim and objectives

Firstly, this study aimed to develop a methodology for performing multi-disciplinary sensitivity and uncertainty analysis for energy, daylight and thermal comfort. The main task of this objective was to create scripts in two different building simulation tools DIVA and IES-VE for automating the simulations of daylight, energy performance and thermal comfort, respectively. The codes developed in this project shall be able to be used in real-life projects. Secondly, another objective of this work was to identify the design parameters for the studied case, which should be focused upon by the design team, and to determine their sensitivity. Thirdly, ranges of expected energy consumption values of the investigated building, dependent on the uncertainty of input parameters, were determined. Fourthly, this work aimed

to determine if performing uncertainty and sensitivity analysis in the early design stages of a project could lead to time-savings in the later stages of the design process. Finally, the study aimed to find out how different design variables influence the multi-disciplinary results and how these variables can be evaluated to obtain the best solution in the early design stages of the building projects.

The main research outcomes of this thesis project are:

- Identification of the most important design input variables and their sensitivity ranking,
- Quantification of the influence of the design input variables on the multi-disciplinary output indices,
- Interpretation of the multi-disciplinary results and suggestions for decision-making.

1.3 Scope and limitations

This work has used Spearman's rank-order method for assessing the correlations between variables. Due to the excessive computational time required for running the samples, the geometrical complexity of the model and the limitations of the VEScript python editor, the number of initial design input variables considered for the study was limited. For daylight simulation, only one floor was chosen for investigations. The energy and thermal comfort evaluations were, however, performed for the whole building. No surrounding buildings nor vegetation were included in the models. The IES VE energy model did not include detailed design of the HVAC system. However generic system, used for building simulations, was specified in Apache.

1.4 Research methods

The work was carried out using the following research methods:

- Literature review: Previous research projects on sensitivity and uncertainty analysis for single and multi-objective assessment were investigated to identify the trends in the choice of input / output values,
- Modelling: Scripts in VE Python API and DIVA were created to automatize the process of performing multiple simulations,
- Simulation: Simulations were performed to produce daylight, thermal comfort, and energy performance data,
- Statistical analysis: Post-processing of results, statistical analysis (using Excel VBA, 'R' programming language) and graphical visualization of extracted data (using Tableau, 'R' and Excel) were carried out to answer the main research questions.

1.5 Disposition of the thesis

The thesis report begins with the literature review summing up available methods for sensitivity and uncertainty analysis as well as the current state of research in the building design context. The methodology chapter presents the description of the methods used for the thesis work, with a special focus on the script development for performing multi-disciplinary sensitivity and uncertainty analysis. It also includes a description of the base case building used for the energy, daylight and thermal comfort simulations. The results and discussion chapters present the outcomes of the sensitivity and uncertainty analysis for the case building. Ranking of the most important parameters and recommendations for favourable input ranges are also defined in this chapter. The results of the study are placed in the broader context of multidisciplinary evaluations including daylight, energy, and thermal comfort. Finally, last chapter highlights future work possibilities including further development of scripts and usage of different sensitivity and uncertainty analysis methods.

2 Literature review

The literature review was divided into two parts. The first part aimed to summarize the current state of research concerning sensitivity and uncertainty analysis with different objectives, while the second part was focused on the different statistical methods suitable for performing Monte Carlo simulations. Based on the literature review, a list of dependent and independent variables for creation of data matrix, was generated.

2.1 Case studies for sensitivity and uncertainty analysis

Table 1 presented below, provides a summary of the previous research works in the area of sensitivity and uncertainty analysis and identifies the most commonly used statistical methods for building parameters sensitivity and uncertainty analysis, together with the most frequently analyzed input and output variables.

Table 1. Literature research summarizing choice of input / output parameters and different methods used for sensitivity / uncertainty analysis in buildings.

Input variables	Output variables	Research area	Type of study	Aim of research	Ref.
89 input variables, for example: wind pressure difference coefficients, room air temperature distribution, outdoor climatic conditions, heat gains from people, lighting and equipment, control of solar shadings and windows	TO-performance indicator (The number of hours in a year when more than 10 % occupants feel dissatisfied)	Thermal comfort	Uncertainty analysis (Bayesian node method), Sensitivity analysis (Latin Hypercube sampling)	Thermal comfort assessment performance of a four-storey office building in The Netherlands.	[11]
24 variables including: building height, length, width, rotation, view factor of the ground, ground reflectivity, insulation thickness, glazing ratio, weather parameters, setpoint temperature, ventilation rates, variables concerning occupancy and building environment	Yearly heating loads, Heating load per m ³ , Heating power, Summer comfort factor	Thermal comfort, Energy needs	Sensitivity analysis (Morris method and FAST)	Thermal comfort and heating / cooling loads assessment	[3]

General methodology for performing Sensitivity analysis and Uncertainty analysis (different methods)	Not specified	Holistic approach	Sensitivity analysis	-	[12]
Infiltration rate at 50 Pa, ventilation system heat recovery, U-value of different building components, window type, sunscreen type, energy pricing scenarios, workmanship errors, internal heat gains, temperature set points	Net-present cost based on effectiveness and robustness	Methodology for incorporation of different sensitivity and uncertainty analysis methods and case study focusing on cost	Uncertainty analysis and Sensitivity analysis (meta-models)	Building performance analysis and multidimensional optimization of semi-detached residential house	[13]
70 input parameters (for example): thermal conductivity of materials, thermostat setpoints, ground reflectivity, surface convection coefficients, solar radiation, heat gains	Energy consumption, Peak power demand, Maximum / minimum / mean swing of temperature, Mean radiant temperature, Dry resultant temperature	Thermal comfort, energy	Sensitivity analysis: DSA, MCA, SSA methods	Passive solar, single-zone buildings tested for application of different Sensitivity analysis methods	[14]
Exemplary parameters: weather conditions physical properties of building materials, internal heat gains (occupancy, metabolic rate, equipment, lighting, setpoint temperature), interventions in building fabric and systems, infiltration rate, chiller COP, boilers efficiency	Annual heating energy, Annual cooling energy, Carbon emissions	Thermal comfort and adaptation to climate change	Sensitivity analysis: SRC and ACS methods; Uncertainty analysis	University building renovation scenarios assessed regarding changing climate conditions	[15]

8 chosen parameters: location, façade, orientation, window control, WWR, SW, internal heat gains, thermal mass, airtightness rating at 75 Pa	Heating / cooling / total / lighting energy consumption, Peak loads improvements: heating / cooling / total, UDI, PPD	Thermal and visual comfort	Sensitivity analysis (global main index)	Office building with EC façade assessed holistically to support building design decision-making process	[10]
U-values of building components, ACH, heat recovery, thermal bridges	Annual heating energy per m ² floor area, Cost-benefit analysis based on sampling results	Review of different sensitivity analysis methods, assessment of compliance with standards	Sensitivity analysis (Sobol' sampling) and Uncertainty analysis	3 case studies combining cost-benefit calculation and bps	[2]
Orientation, U_{Wall} , U_{Roof} , U_{Floor} , U_{Win} , solar heat gain coefficient, window frame thickness, $Therm_{control}$, ventilation and infiltration rate, occupation, metabolic rate, clothing level	Annual heating energy consumption, Predicted mean vote index	Energy, Thermal comfort	Sensitivity analysis	Sensitivity analysis of Building parameters and occupancy parameters effects in residential buildings	[16]
Window shading size, window width, window length, windows infiltration rate, doors infiltration rate, $AF_{ventilation}$, $U_{ExtWall}$, $U_{IntWall}$, $U_{FirstFloor}$, U_{Roof} , SHD, $\alpha_{ExtWall}$, α_{Roof} , α_{Floors} , thickness of floor slab	Heating / cooling / fans energy consumption, Total degree hours, Global objective, Cooling degree hours, Heating degree hours	Energy, Thermal comfort	Sensitivity analysis	Building design optimization using Sensitivity analysis and genetic algorithm	[17]
Orientation, window to wall ratio, skylight to roof ratio, U_{Wall} , U_{Roof} , $U_{Skylight}$, U_{Win} , U_{Floor} , C_{Floor} , C_{Roof} , C_{Wall} , $\alpha_{ExtWall}$, SHGC, T_{vis} , infiltration, glazing, floor, parapet, corner linear transmittance	Hourly discomfort index, Cooling energy, Annual electricity energy	Energy, Thermal comfort	Sensitivity analysis	Sensitivity analysis and optimization of building design in subtropical regions	[18]

Orientation, window to wall ratio, overhang depth, SHGC, insulation, infiltration rate, insulation thickness, window resistance, $T_{slabFloor}$, infiltration, sensible heat recovery effectiveness, air distribution effectiveness, heating and cooling setpoints, $T_{coolair}$, $T_{heatair}$	Energy consumption, Predicted mean vote index	Energy, Thermal comfort	Sensitivity analysis	Sensitivity analysis throughout the building design process	[19]
Window to wall ratio, window type, space aspect ratio, insulation, $T_{Shading}$, $\alpha_{front\ shade}$, $\alpha_{back\ shade}$	UDI, Lighting energy consumption, Heating / cooling energy	Energy, Daylight	Sensitivity analysis, Uncertainty analysis	Performance of Office room with automated shading	[20]
Window to wall ratio, U_{Wall} , U_{Win} , solar heat gain coefficient, side fins degree surface reflectance	Energy consumption, Daylight factor, Overtemperature	Energy, Thermal comfort, Daylight	Sensitivity analysis	Informed decision supported by Sensitivity analysis in multidimensional design space	[6]
Location, orientation, window to wall ratio smart windows, Smart windows rule-based controls, thermal mass, infiltration rate	Energy consumption, Peak energy demand, UDI, PPD	Energy, Thermal comfort, Daylight	Sensitivity analysis	Office building with smart windows: Sensitivity analysis of design parameters on 3 aspects	[10]
Aspect ratio, window to wall ratio, number of floors, orientation, overall scale, U-values: wall roof, window, solar heat gain coefficient, lighting peak density, equipment peak density	Heating energy use, Cooling energy use, Electricity use	Energy	Sensitivity analysis: SRC, FAST TGP, Morris	Comparison of the suitability of different Sensitivity analysis methods in assessing building energy performance	[21]

Reflectance of surfaces: floor, wall, ceiling, ground, frames	Total Annual Illumination, Useful Daylight Illuminance, Daylight Autonomy, Daylight Factor	Daylight	Sensitivity analysis: Morris	Sensitivity analysis studying the impact of reflectance values	[22]
---	--	----------	------------------------------	--	------

The reviewed scientific literature provides state-of-the-art in multi-disciplinary sensitivity and uncertainty analysis. It can be noted that the majority of the previous literature on sensitivity and uncertainty analysis of buildings, focused only on one or two output indices, with thermal comfort being the most popular choice. Only a few studies reported in the literature have implemented a holistic approach including energy, thermal comfort, and daylight simultaneously. No unified trends regarding choices of input parameters and methods are evident. Selection is highly dependent on available time and resources for project implementation. The number of input parameters varies between 4 and 89 or more, among the reviewed literature. Based on the literature review, there is no clear pattern indicating which parameters should be prioritised. Nevertheless, a minimum number of samples is necessary for the chosen statistical method.

2.2 Statistical methods for sensitivity and uncertainty analysis

2.2.1 Uncertainty analysis

The uncertainty in the output results can be classified based on what causes the differences among them [23]. According to de Wit [11], uncertainty can be divided into categories of specification, modelling, scenario and numerical. Therefore, it is important to distinguish between different uncertainty sources before choosing an appropriate method for statistical quantification. The type of the uncertainty influence the choice of the method for solving the design problem, providing the right results data and generating suitable conclusions. Various types of uncertainties can be directly linked with each other. This is due to the lack of precise determination of certain behaviors of occupants or other factors, for example, the infiltration rate. The correct quantification of the related inputs is needed to obtain reliable results [2] both in sensitivity and uncertainty analysis. Several research works focused on uncertainty analysis [8, 10, 19, 20], however, different methods for quantification of the results were used

2.2.2 Sensitivity analysis

Sensitivity analysis has been widely applied in the context of building energy modelling to assess how uncertainties in the input parameters may influence the results [26]. The main reason for performing the sensitivity analysis is to identify the input parameters which have the largest influence on the results. Moreover, performing sensitivity analysis can also determine the design variables which do not affect the results. These insignificant parameters could be excluded from the main focus of optimization in the design projects [27]. Sensitivity analysis can even be used to better understand the relationship between inputs and outputs and to detect errors in the model [26]. According to Tian [25], sensitivity analysis methods can be divided into local and global approaches. The local sensitivity analysis approach is

focused on the influence of uncertain parameters over the user-defined point in the data sets, whereas the global analysis refers to these uncertainties over the whole input space [25, 2]. Even though the global approach is generally considered more reliable for data interpretation, it requires a high computational effort to perform the analysis. This leads to the fact that both local and global approaches are widely used in practice. Monte Carlo based techniques are typically used to compare uncertainties with normal distributions to the parameters defined in ranges. Figure 1 presents the schematic representation of sensitivity and uncertainty analysis.

Sensitivity and uncertainty analysis

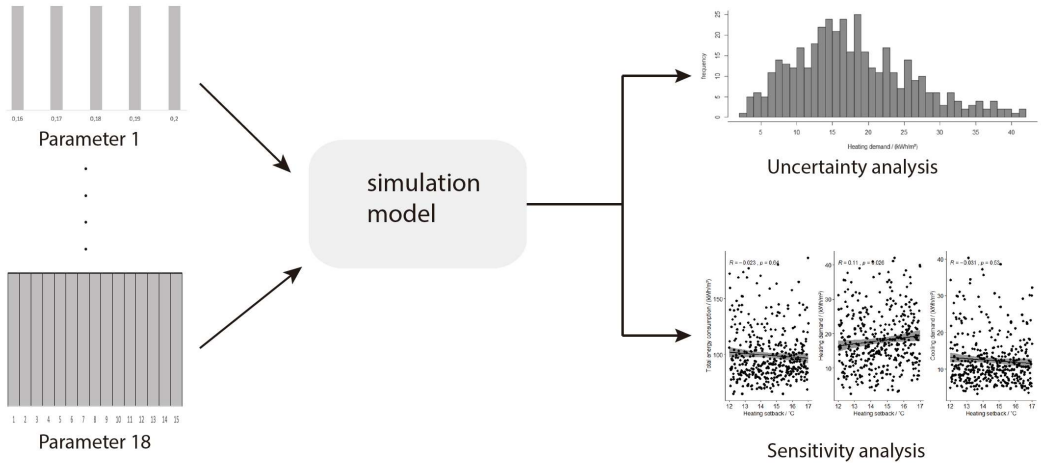


Figure 1. Schematic representation of Sensitivity and Uncertainty Analysis.

2.2.3 Sensitivity analysis methods

Sensitivity Analysis methods can also be evaluated by different quantification categories. According to Heiselberg [28], three main classes of sensitivity analysis methods are screening methods, local sensitivity methods, and global sensitivity methods. Hamby [29] assigned the sensitivity analysis methods into ten one-factor-at-a-time-methods, four methods dividing or segmenting input parameters into two or more empirical distributions based on the partitioning of the output distribution, and ten methods based on generation of sample of input matrix and associated output vector. Mokhatari and Frey [27] noted that there is no formal guidance / evaluation matching specific sensitivity analysis methods to the specific type of scientific problems. However, they suggested general guidance on sensitivity analysis of the probabilistic risk models.

2.2.3.1 Local methods

Local sensitivity analysis explores the design space around data points (or base case) and does not include the possible interactions between them [26, 30]. Therefore, the local method is quite limited in comparison to global method therefore decreases the accuracy of the outcomes. Local sensitivity analysis belongs to the one-factor-at-a-time methods (OFAT / OAT). According to Delgarm [31], each variable is changed once at a time over the whole design space, while all the other parameters are kept fixed. The same process is repeated for each

variable. The one-factor-at-a-time method is assessed using gradients or partial derivatives of the output variables when the function of outputs is available [2, 31].

2.2.3.2 Global methods

In general, the global methods, summarized in Table 2, include regression methods, screening methods, variance-based methods, and meta-model methods. Each method differs in terms of suitability of statistical model, sample size, sampling method, and sensitivity index.

Table 2. Summary of global methods (n means number of parameters).

Methods	Regression methods	Screening methods	Variance-based methods	Meta-model methods	Reference
Number of model evaluations	$10n$	$2n-10n$	$100n-1000n$	$1000n$	[24, 32]
Computational cost	Cheap	Cheap	Very expensive	Very expensive	[30, 33]
Accuracy	moderate	moderate	high	high	[30, 4]
Sampling method	LHS, Monte Carlo	Morris	Sobol, FAST	Sobol, FAST	[4, 30]
Sensitivity indices	Regression coefficient Correlation coefficient	μ : main effect σ : interaction with other factors or the nonlinear effects	First-order sensitivity index Total-effect index"	First-order sensitivity index Total-effect index"	[30, 4]
Linear model	✓				[30]
Monotonic model	✓				[30]
Non-monotonic model		✓	✓	✓	[30]
Interaction effects and non-linear effects		✓	✓	✓	[30]
Field	Sensitivity analysis, Uncertainty analysis	Sensitivity analysis	Sensitivity analysis, Uncertainty analysis	Sensitivity analysis, Uncertainty analysis	[30, 4]

Regression methods have low computational costs as they are easy to implement and fast to compute [30]. Screening methods are suitable when the aim of the analysis is to exclude unimportant parameters from a large number of inputs [34]. Screening methods, variance-based methods or meta-modeling methods are recommended to recognize non-linearity and interaction effects [35]. Meta-modeling methods are recommended for cross-platform simulations, as they are computationally efficient and faster to get the predictive results [30]. Meta-modeling methods are suitable when the model is complex and computationally intensive. Additionally, they are better for performing quantitative sensitivity analysis, design

space exploration and optimization, as time of running detailed model is much longer than time of running meta-model [30]. Kristensen and Petersen [36] noted that Morris (screening) method, which requires a significantly smaller number of samples, can provide as accurate results as Sobol' (variance-based and meta-model) method for ranking of parameters importance. In this thesis work, regression methods were preferred by the authors due to the time limitations of the project and limited computational power for performing complex and time-consuming simulations. Regression methods, which include linear regression and correlation method, will be explained in detail in the following sections. Description of other sensitivity analysis methods is presented in Appendix A.

Linear Regression:

Linear Regression methods include Standardized Regression Coefficient (SRC), Standardized Rank Regression Coefficient (SRRC), Partial Correlation Coefficient (PRC), and Partial Rank Correlation Coefficient (PRCC). SRC is commonly used in the field of building energy assessment since it is easier to understand and fast to compute [30]. The computational cost for SRC is moderate compared to Morris and Sobol' method [33]. A higher SRC value indicates a higher significance of the variable, and a negative SRC value suggests that the outputs values will change in opposite direction compared to the changes in inputs [21]. Menberg et al. [33] suggested that the distinction between non-influential and influential parameters increases with the number of samples tested. An SRC of 0.01 is a threshold to indicate that the results are robust and meaningful. If SRC is lower than 0.01, the values of SRC will vary according to different sample sizes [33].

However, SRC is not reliable if the statistical model is highly non-linear. Besides, it is valid only when the inputs are not correlated. If there exists a correlation between inputs, PRC should be used instead. PRC and SRC will give similar results else wise [30]. The coefficient of determination (R^2) should be calculated for the linear model. $R^2 = 0.7$ indicates that the outcome of the building model sufficiently fit into the regression model. If R^2 is lower than 1 even for a sufficient number of samples, it reveals the presence of significant non-linear effects and interactions between the parameters [33]. The SRRC can be implemented when R^2 value is low since it is suitable for a non-linear but monotonic model. The monotonic model means the relations between variables have similar trend directions but at probably inconstant rates [86]. As mentioned by Anh-Tuan and Sigrid, to calculate SRRC, the input and output parameters are replaced by their ranks and regression is calculated based on them. Detailed SRC and SRRC functions are explained in reference [4].

Correlation:

Correlation methods include Pearson's correlation, Kendall rank correlation, Spearman's correlation, and Point-biserial correlation. Pearson's method measures the linear correlation coefficient between input X and output Y . However, this sensitivity index can only be applied to the linear model. Pearson's correlation is applicable when the two correlated variables are measured on a continuous scale. If at least one variable has discrete values, then Spearman's correlation should be used. More details on the suitability of each correlation coefficient are provided further down in Section 3.7. In the case of the monotonic function, Spearman's method should be considered. Spearman's method is based on the ranking of input variables instead of the raw values of Pearson which is similar to SRRC and PRCC [4].

2.2.4 Sensitivity and uncertainty analysis sampling

2.2.4.1 Sampling method

The choice of the sampling method is a very important step in performing sensitivity and uncertainty analysis. Special attention must be paid to samples distribution within the created data matrix. The more uniform spread of design iteration is, the more accurate the results are [2]. Sampling methods such as random sampling, cluster sampling, stratified sampling, and systematic sampling are commonly used for performing sensitivity analysis.

Different sensitivity analysis methods require specific sampling methods associated with them. For example, traditional Morris sampling technique (factorial sampling) is a one-parameter-at-a-time (OAT) method, which means only one parameter is varied in each sample. Sobol' method requires sampling based on Sobol' sequences which is a quasi-random low-discrepancy sampling approach [36]. Regression and meta-modeling methods can use both random sampling methods, e.g. Monte Carlo sampling, or quasi-random methods, such as Latin Hypercube sampling (stratified sampling category). Compared to random sampling methods, quasi-random sampling methods more quickly provide evenly distributed samples covering the design space [35]. The reason is that quasi-random stratified methods initially divide the parameter space into equal areas and then select the random samples within these multi-dimensional areas [33, 36].

2.2.4.2 Probability distributions

According to Burhenne [2], probability distributions affect the quantification of uncertainties in the project inputs. Since the probability density function (PDF) affects the results of sensitivity analysis, it should be carefully selected [38]. Particularly attention should be paid to sensitivity measures for variance-based and density-based methods since the results are related to an output probability distribution [39]. In addition, the PDF affects results since shape of distribution is influenced by any potential parameter correlations and is model-specific. The PDF can be generally categorized into several types of distributions, including uniform and non-uniform, among others. The uniform distribution is called non-informative and can be implemented for any sensitivity analysis method. Non-uniform distribution is called informative and can only apply to specific sensitivity analysis methods [36]. Some sensitivity analysis methods require certain PDFs. For example, Morris and Regional Sensitivity Analysis (Monte Carlo filtering) should have uniform input distribution [35]. On the contrary, some probability density functions are limited to specific sensitivity analysis methods. For example, if there are both uniform and non-uniform distributions, Sobol' method should be selected rather than Morris or Local methods, as it can consider the shape of parameter distributions, range and correlated effects simultaneously [36]. Burhenne [2] has reported that uniform, normal and log-normal distributions are the most commonly used types. However, this does not indicate the applicability of the aforementioned types to every single project. The choice of the right probability distribution is dependent on the uncertainties of inputs and their types.

Table 3. Probability distributions based on the applicability in building simulations analysis.

Input parameters	Distribution	Type	Examples	Reference
x,y	Uniform	Continuou	Lack of specific background knowledge about input parameters for example efficiency, overhang projection ratio	[2, 40]
μ, σ	Normal	Continuous	Setpoints temperature, useful when physical quantities are measured (for example, length)	[41]
α, β	Beta	Continuous	Efficiency of heat recovery	[41]
ω^2, θ	Log-normal	Continuous	Non-negative parameters (material's density, metabolic rate, air change, U-values)	[42]
x,y,z	Triangular	Continuous	Applicable for variables between uniform and normal distribution	-
x,y	Uniform	Discrete	Number of occupants / inhabitants, sky radiation, shading coefficient	[2, 43]
$0 \leq p \leq 1$	Bernoulli	Discrete	Fixed number of trials with a fixed probability of succeeding. Has only two outcomes, therefore limited applicability in case of building projects.	[44]
p, n, q	Binomial	-	Related to Bernoulli distribution where each trial is independent. Limited applicability.	[45]
u, k, c	Weibull	-	Commonly used to model tropospheric wind speed	[46]

Table 3 presents the different types of probability distributions. Normal distribution means the value of input parameters will have equal probability around a mean value (e.g. setpoint temperature). Log-normal distribution means higher values will be more probable than lower values (e.g. U-values and infiltration rate). Beta distribution means higher values will be less probable than lower values (e.g. efficiency of heat recovery) [41]. Parameter distributions are used in the detailed design phase when the uncertainty is included in the fixed parameter values chosen in the early design stage. Besides, they are applied when the values are fixed as expected or preferred, for example, Eggebø [48] chose normal distribution based on the new Norwegian energy standard for TEK 10 (NS3031) and applied a standard deviation of $\pm 10\%$. In addition, when the uncertainty of the existing building stock needs to be reflected, different types of probability distribution functions can be used [36].

2.2.4.3 Sampling size

Several methods for determining minimum sample size exist such as conventional rules, statistical power methods, cross-validation approaches [49]. Determination of sample size is a crucial point in the sensitivity and uncertainty analysis to yield accurate results. Too small sample group might result in biased data, not going far beyond the analyzed base case, thus rejecting the validity of the performed analysis. The necessary sample size is linked to the goal of the development project and the required accuracy of results. According to Brooks and Barcikowski, the sample sizes which are not large enough are prone to type II error [49].

In the effect-size method, there is an inverse correlation between the size of the sample and the effect size meaning that with the decrease of effect size there is an increase in the number of samples [50].

The sampling size considers many factors such as input variables, the range of variables, the distribution in range, building type or the HVAC system [37]. Loepky et al. [51] recommended $10 * n$ (n being the number of inputs in this section) as a sampling number for the regression method. In any case, the sampling size should be large enough which enables input convergence for the sensitivity indices [27]. The Morris method recommends r (the number of trajectories) * $(n+1)$ [24]. It usually sets r between 5 to maximum 15 [51]. On the other hand, Willems et al. [52] concluded that while $r = 25$ manages to clearly differentiate between influential and non-influential factors, it still does not suffice to stabilize the factor ranking. Variance based methods, such as Sobol indices require having $m * (2n+2)$ number of samples, whereas m is the number of evaluations according to the individual effect. The variable m can usually take any values such as 16, 32, 64 (and so on), which leads to larger sampling and therefore higher computational cost [4]. Tian [53] applied sequential method to determine the number of samples required for convergence. In addition, the Sobol' method has proven to determine convergence faster than the SRC method.

3 Methodology

The main goal of the project was to explore the most significant building design parameters for the case building by means of sensitivity analysis. The project objectives also included an assessment of how the design inputs affect different results by performing an uncertainty analysis. Schematic workflow for the project work is shown in Figure 2.

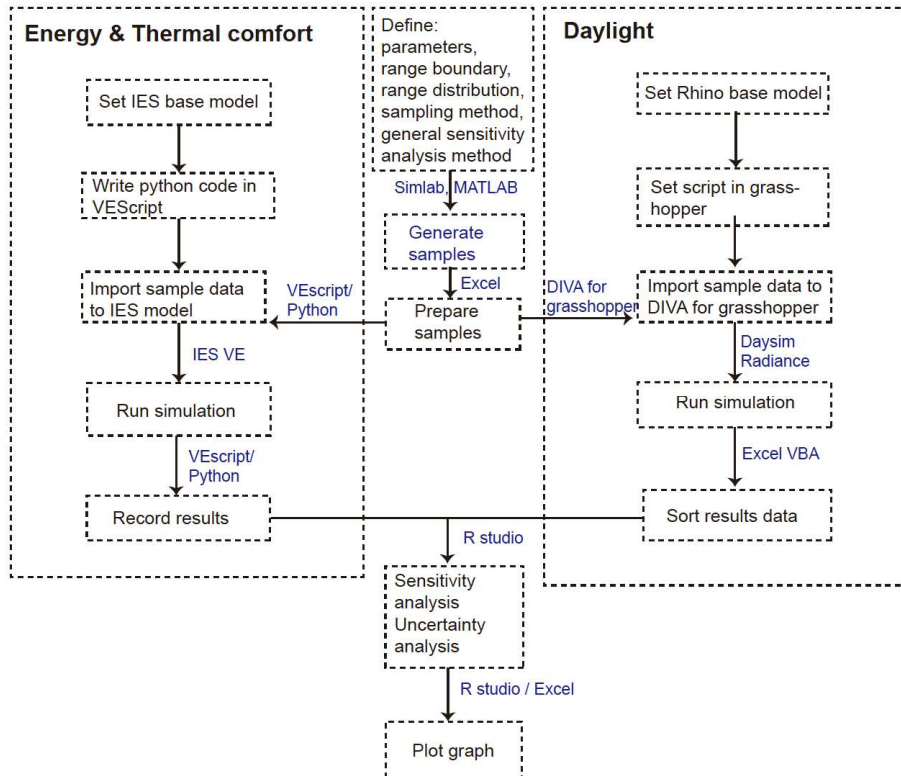


Figure 2. Schematic workflow for performing sensitivity analysis and uncertainty analysis.

Among the various available statistical methods, correlation methods were chosen for performing sensitivity and uncertainty analysis in the current project. Pearson's correlation coefficient was used for evaluating the strength of linear association between paired input and output values, whereas, SPEAR, which is a non-parametric test, was used when Pearson's method was not suitable [27]. The statistical approach for energy and thermal comfort included running multiple simulations based on randomly generated samples (SimLab 2.2). This was executed by implementing python codes in IES VE Script Python Editor (software build-in). A similar methodology was used for daylight analysis with the difference of performing simulations in DIVA. The methodology, including samples generation, development of python and DIVA codes for automatization of simulations and selection of methods for data interpretation, is aiming to be applicable for future building optimization projects. Workflow for performing sensitivity and uncertainty analysis, which is presented in Figure 2 for the project case, is described in detail in the following sections.

3.1 Building base case

The initiator of this research project was company Rambøll, with main headquarters located in Copenhagen, Denmark. In this study, the chosen base case was a newly built office located in Nordhavn (coastal part of Copenhagen) with an approximated floor area of 29,403 m². The approximated heated area is 25,994 m² and the total window area is 6,337 m². The ground and the first floors are fully glazed and are open for public. The office floors spread from the second floor up to the twelfth floor of the building. External glazing area is varying according to different azimuths in the façade. The window to wall ratio varies between 54 % in the north to 34 % in the south. An atrium is located in the centre of the building and is covered by a roof skylight on the top. The building includes a basement floor located underground and a sky lounge on the thirteenth floor. Northern, southern and top view of the building are shown below in Figure 3.

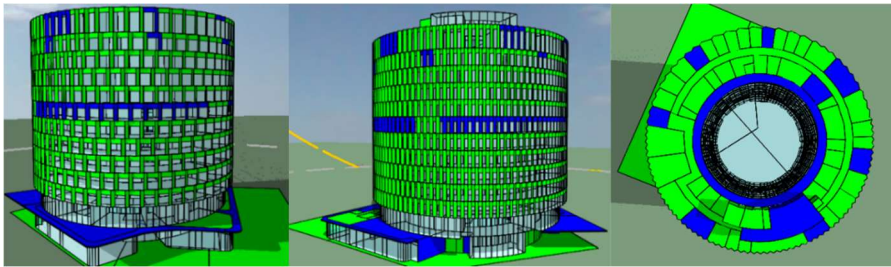


Figure 3. North Façade, South Façade and Top view of the case study building.

In reference to shading strategies, internal shading devices have been added to the rooms from the southwest to the southeast. The shading is operating in the discrete mode, which means that the shading is fully raised when the incident irradiance variable is lower than 200 W/m² and the shading is fully lowered when the incident irradiance variable is higher than 300 W/m². The opaque and glazed constructions used in the model are presented in Table 4 and Table 5.

Table 4. Opaque construction for base case.

Opaque Constructions	U-value [W/(m ² K)]	Assigned for
External Wall-1	0.709	3 rd to 11 th floor
External Wall-2	0.725	2 nd floor
External Wall-3	0.716	12 th floor
External Wall-4	0.150	Sky lounge and the ground floor
Internal Wall	0.568	All floors
Ground Floor	0.103	Basement floor
Exposed Floor-1	0.150	1 st and 2 nd floor
Exposed Floor-2	0.709	3 rd to 11 th exposed floor (twisted)
Exposed Floor-3	0.715	12 th exposed floor (twisted)
Internal Floor / Ceiling	0.978	All floors
Roof-1	0.150	Basement, ground and top floor
Roof-2	0.700	3 rd to 12 th floor exposed roof (twisted)
Roof-3	0.707	2 nd floor exposed roof (twisted)
Roof-4	0.180	Ground atrium part

Table 5. Base case glazed constructions.

Glazed construction	U-value [W/(m ² K)]	g-value	Assigned for
External Window	0.638	0.350	All
Roof-light	1.508	0.774	All
Internal Window-1	1.051	0.349	Rooms surrounding atrium
Internal Window-2	4.081	0.813	Internal windows between rooms

Table 6 presents ten thermal templates which were assigned to different types of rooms. The heating and cooling operation profiles were adjusted to the building working hours, with a setpoint temperature of 21 °C for heating and 23 °C for cooling. In the table, MS stands for the maximum sensible gain, and ML stands for the maximum latent gain.

Table 6. Thermal templates assigned for the base case.

Template	Heating-cooling setpoint temperature	Internal gains	Infiltration rate	Auxiliary ventilation
Atrium	21-23 °C	-	0.2 l/s/m ²	-
Auditorium	21-23 °C	People = 1.5 m ² /person MS: 6 W/person Equipment = 900 W+8 W/m ² Lighting = 6 W/m ²	0.2 l/s/m ²	9.4 l/s/person
Auditorium - Cloakroom	21-23 °C	People = 124 MS: 83 W/person ML: 30 W/person Lighting = 6 W/m ²	0.2 l/s/m ²	9.4 l/s/person
Canteen	21-23 °C	People = 1.5 m ² /person MS: 100 W/person ML: 43 W/person Lighting = 6 W/m ²	0.2 l/s/m ²	11.3 l/s/person
Heated rooms	21 °C	Lighting = 6 W/m ²	0.3 ach	-
Meeting rooms	21-23 °C	People = 2.5 m ² /person MS: 100 W/person ML: 43 W/person Equipment = 24 W/m ² Lighting = 6 W/m ²	0.2 l/s/m ²	11.3 l/s/person
Non-heated rooms	-	-	0.3 ach	-
Office	21-23 °C	People = 8 m ² /person MS: 100 W/person ML: 43 W/person Equipment = 12.5 W/m ² Lighting = 7 W/m ²	0.2 l/s/m ²	7 l/s/person 0.7 l/s/m ²
Print room	21-23 °C	-	5 ach	-
Sky lounge	21-23 °C	People = 49 MS: 100 W/person ML: 43 W/person Lighting = 6 W/m ²	0.2 l/s/m ²	11.3 l/s/person

Since the majority of the windows cannot be opened, a mechanical HVAC system is used for providing ventilation inside of the building. The properties and the location of the opening types are shown in Table 7. Ground floor includes windows which can be manually opened by the room users, therefore energy and thermal simulations included possibility of the natural ventilation.

Table 7. Opening types.

Opening type	Opening percentage [%]	Placement
Windows opening 1	10.3	Ground floor northern and southern entrance
Windows opening 2	6.5	Ground floor main entrance
Windows opening 3	1.6	External skylight
Windows not openable	0.0	Whole building except above areas

The generic HVAC system for the whole building was assigned and the settings are presented in Table 8. The ventilation airflow rate was demand-controlled, i.e., changing accordingly to the occupancy rate.

Table 8. HVAC settings.

Category	Parameter	Value	Unit
Heating	Seasonal efficiency of heat source	3.50	kW/kW
	SCoP of entire heating system	3.00	kW/kW
	Ventilation heat recovery	0.85	-
Cooling	Seasonal efficiency of cool source	2.50	kW/kW
	SSEER of entire cooling system	2.00	kW/kW
Auxiliary energy	System-specific fan power	1.50	W/1/s

3.2 Input parameters

According to de Wit [11], there is no existing database specifying input parameters for building sensitivity and uncertainty analysis. Therefore, all inputs for the current project were initially determined based on the literature review, previous knowledge, and discussions with experts. These inputs are presented in Table 9. The initial list consisted of eighteen parameters divided into five groups: configuration of façade design, construction quality, system design, internal gains, and material surface optical properties. It is important to highlight that along the course of the project, several constraints on input parameters appeared due to the limitations of the software combined with the complex geometry of the building. Description of python limitations in IES VE resulting in the limitations to the input parameters is presented in Section 3.6.

Table 9. Input parameters for parametric studies including distributions and ranges.

Category	Parameter	Distribution	Range	Units
Configuration of Façade design	Wall insulation thickness	Uniform	0.01 - 0.25	m
	Roof insulation thickness	Uniform	0.16 - 0.20	m
	Floor insulation thickness	Uniform	0.20 - 0.45	m
	Glazing type	Discrete	1, 2, 3, 4, 5 (Table 10)	-
Construction quality	ACH at 50 Pa (blower door test)	Discrete	0.179, 0.279, 0.379, 0.479, 0.579	ach
System design	Auxiliary ventilation rate	Discrete	9.5, 12.5, 14.5, 16.5, 18.5	l/s/person
	Inlet air temperature	Discrete	14, 15, 16, 17, 18	°C
	Indoor heating setpoint	Uniform	18 - 22	°C
	Indoor heating setback	Uniform	12 - 17	°C
	Indoor cooling setpoint	Uniform	23 - 26	°C
	Indoor cooling setback	Uniform	26 - 30	°C
	Occupancy profile type	Discrete	1, 2, 3, 4, 5 (Table 11)	-
Internal heat gains	Occupancy	Discrete	8, 10, 12, 14, 16	m ² /person
	Lighting	Discrete	5, 7, 9, 11, 13	W/m ²
	Equipment	Discrete	10.0, 12.5, 15.0, 17.5, 20.0	W/m ²
Material surface optical properties	Reflectance of Ceiling	Discrete	0.7, 0.8, 0.9	-
	Reflectance of Walls	Discrete	0.5, 0.6, 0.7, 0.8	-
	Reflectance of Floor	Discrete	0.2, 0.3, 0.4	-

The U-value of the opaque constructions is a significant factor in the building façade design. Building regulations for various climates, in terms of U-value, may have different requirements. For example, according to Swedish Building Regulation BBR [54], the U-value of external walls, ground slabs and roof structures for new building should be lower than 0.18 W/(m²K), 0.15 W/(m²K) and 0.13 W/(m²K), respectively, whereas according to the Danish Building Regulations 2018 [1], they should be less than 0.3 W/(m²K), 0.2 W/(m²K) and 0.2 W/(m² K), respectively. The U-values of existing external roof and ground structures fulfill the Danish building code requirements in the case building. According to BR18 [1], the approximate insulation thicknesses for external walls, ground slabs, and roof structures are 150 mm, 150 mm and 200 mm, respectively. Therefore, different insulation thicknesses for different opaque constructions were tested and are presented in Table 9.

Window properties, such as heat conductivity, solar heat gain coefficient, and light transmittance, affect energy, daylight and thermal comfort in different ways. Previous sensitivity analysis studies have analyzed these properties separately and concluded that the g -value is more important than the U -value of the window [38, 8, 35]. Sherman and Bre investigated window type as an independent variable which included all window properties [55, 56]. However, due to the limitation of VEScript explained in Section 3.6, only the glazing type of the outer pane was tested among different window types in this project. The properties of the middle pane and inner pane remained the same as in the existing case. The U -value for all the tested window types was the same, i.e. $0.638 \text{ W}/(\text{m}^2\text{K})$. The properties for window types are listed in Table 10.

Table 10. Type of windows chosen for parametric studies.

Window Type	Outer pane glazing type	g -value	Reflectance	Light transmittance
w-1	Planiclear	0.700	0.078	0.720
w-2	Planitherm	0.580	0.200	0.689
w-3	Cool Lite Xtreme 60-28	0.260	0.600	0.524
w-4	SKN 174 II	0.340	0.380	0.601
w-5	Cool Lite Xtreme 70-33	0.300	0.400	0.610

The airtightness of the building envelope can significantly affect the building energy performance as well as the indoor air quality. Higher infiltration rate results in the increase of the total energy demand (higher heating and cooling) and potentially leads to unpleasant draught [57]. In addition, during summertime, warm and humid air leaking might condense on the cooler part of the construction, which may result in mould and consequently harms the structure [57]. The Swedish passive house airtightness should be below 0.3 l/s/m^2 at 50 Pa. In a conventional building [58], the air permeability value varies around 0.8 l/s/m^2 at 50 Pa. Nevertheless, in the existing buildings, the air leakage value falls within the large range of 0.1 l/s/m^2 to over 30 times the standard value of 0.8 l/s/m^2 from the former Swedish Building Regulation [54, 58]. The airtightness depends on the quality of workmanship, the continuousness of airtight layer in the constructions, age of the building and number of floors [58]. In the project base case model, the infiltration rate was assigned to different thermal templates resulting in an overall building infiltration value of 0.179 ach, equal to approximately 0.2 l/s/m^2 . Different air change values were tested with the purpose of determining the sensitivity of the parameter.

The auxiliary ventilation airflow rate is used for constantly allowing fresh air in the building, to keep the CO_2 concentration at a low level. Higher ventilation rate can significantly limit the CO_2 concentration which benefits people's health. However, in a cold climate, it might result in higher heating demand in winter but less cooling need in the summer. The desired indoor climate is specified in terms of the desired air quality for a designed building. CIBSE Guide A Table 1.5 [59] and ASHRAE Handbook Fundamentals 2009 Chapter 16.10 [60] suggest airflows of 10 l/s/person for office rooms. Danish Standard 447 [61] and BR18 [1] specifies that flow needs shall be determined based on the size and the usage of the rooms.

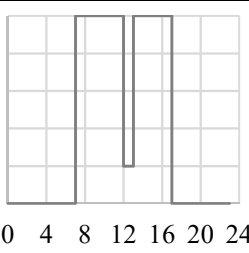
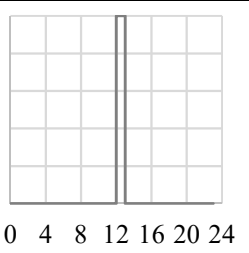
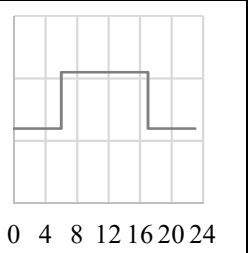
The auxiliary ventilation rate in the investigated building varies between 7 l/s/person , 9.4 l/s/person , and 11.3 l/s/person in different thermal templates. However, in order to have a general value for the whole building, the overall auxiliary ventilation was calculated as 9.5 l/s/person (plus addition for the heated floor area) based on the occupancy rate in each

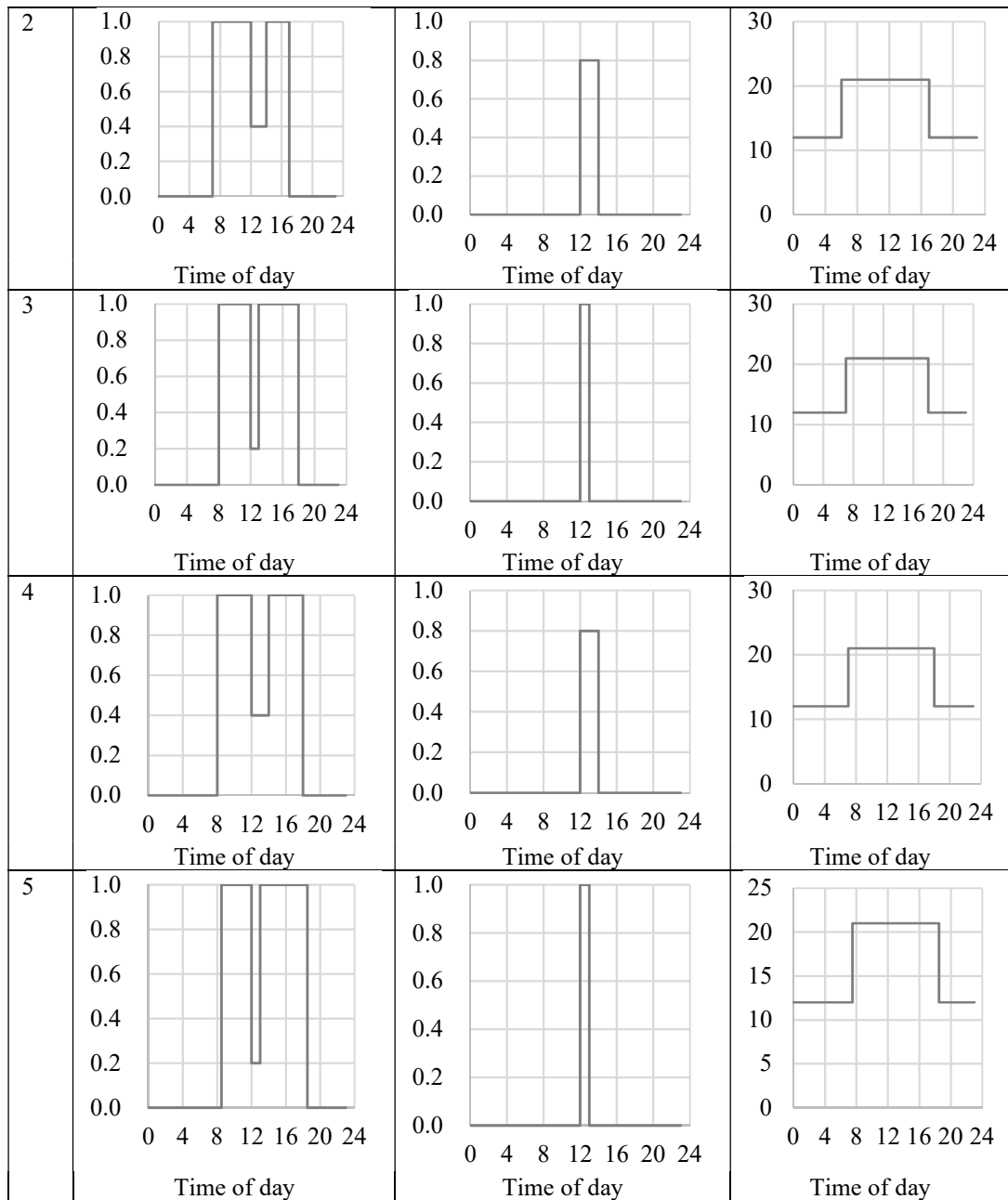
template. The testing options of auxiliary ventilation rates, are in reference to ASHRAE standards [62] and decision of project authors. Different ventilation rates were tested for the sensitivity and uncertainty study. When using outside air for free cooling, a higher supply air temperature may result in less mechanical cooling, less terminal box reheating and higher fan power consumption [63]. Optimizing the supply air temperature can help to decrease energy consumption [64]. Therefore, the inlet air temperature was considered as a parameter for testing. Prior research [63] has shown that the supply air temperature should be related to the outside temperature. For example, the ‘outdoor temperature-compensated supply air temperature’, also described as supply air temperature as a function of outdoor temperature, is commonly used when the VAV system is applied. However, with the aim of testing values above and below the base case (16 °C), discrete values between 14 - 18 °C for inlet air temperature were tested. The airflow was varying according to the occupancy schedule.

Setpoint temperature is used to maintain the air temperature of the rooms when occupied. On the contrary, setback temperature is used outside of the occupied hours. The typical heating setpoint temperature is around 21 - 22 °C and the cooling setpoint temperature is 23 - 24 °C [65]. However, if the setpoint temperature is closer to the outside temperature, the energy required for heating and cooling is decreased [65]. According to the ANSI / ASHRAE Standard 55 [66], the heating setpoint temperature of 66 - 80 °F (18.9 - 21.1 °C) and the cooling setpoint temperature of 74 - 78 °F (23.5 - 25.5 °C) are accepted by 80 percent of the building occupants. The ASHRAE standard also recommends having 55 °F (12.8 °C) as heating setback temperature and 82 °F (27.8 °C) as cooling setback temperature. However, in order to test more possibilities, the ranges presented in Table 9 were used.

Different occupancy schedules result in various HVAC, lighting, and equipment operating times, which may lead to diverse energy consumption results. However, there is a lack of research investigating this parameter in the sensitivity analysis. Therefore, the occupancy profile type was included in the input parameters list. The length of working hours was kept the same as the base case. However, the starting point of the working day and the length of the lunch break were varying. Five types of tested profiles are listed in Table 11.

Table 11. Types of profiles used in the project.

Type	Office occupancy profile	Canteen profile	Heating setpoint profile
1	 <p>1.0 0.8 0.6 0.4 0.2 0.0</p> <p>0 4 8 12 16 20 24</p> <p>Time of day</p>	 <p>1.0 0.8 0.6 0.4 0.2 0.0</p> <p>0 4 8 12 16 20 24</p> <p>Time of day</p>	 <p>30 20 10 0</p> <p>0 4 8 12 16 20 24</p> <p>Time of day</p>



Internal gains are the sensible and latent heat generated by the internal sources such as people, lighting or equipment. They can result in different temperature and relative humidity conditions in rooms [67]. The internal gains contribute to the reduction of the heating demand in winter, meanwhile, they can increase the cooling demand in summer. In order to know how the internal gains influence both the energy demand and thermal comfort, different occupancy rates, and lighting and equipment gains were chosen for the sensitivity analysis. Building Research Established [67] have suggested that 12 - 16 m²/person would be the occupancy rate for general office building. Since the base case was 8 m²/person, 8 - 16 m²/person with an interval of 2 m²/person was selected as the test range.

The Building Research Established [67] suggested that lighting load should be between 8 - 12 W/m², whereas Rees [68] indicated that lighting gains should fall within range of 10 - 15 W/m². Additionally, lighting of 5 W/m², lower than existing case of 7 W/m² was tested, with an assumption of implementing efficient LED lighting. In accordance with the guidelines [67, 68], the tested range was finalized to be between 5 - 13 W/m² with an interval of 2 W/m². An assumption of the equipment gains given by the Building Research Established was 12 - 15 W/m² [67], while Rees suggested a range of 7.8 - 21.5 W/m² for the equipment gains [68]. In order to test values above and below the base case (12.5 W/m²), range between 10 - 20 W/m² with an interval of 2.5 W/m² was chosen.

To maximize daylight usage, the reflectance of the internal surfaces should be investigated in the initial design stage [22]. Highly reflective surfaces often have a lighter color. They can brighten up space by absorbing less daylight than the darker surfaces [69]. Brembilla et al. [22] performed a sensitivity analysis of the reflectance affecting the daylight performance. Research has shown that reflectance of the surfaces plays a significant role in climate-based daylight modelling evaluations. In addition, it has been found by Wilson [70] that the illuminance level can be increased by 50 % if the mean reflectance is changed from 0.4 to 0.6, and can be increased 100 % if the mean reflectance is changed to 0.7. However, according to the European Standard EN 12464-1 [71], reflectance recommendations for ceiling, wall and floor are 0.7 - 0.9, 0.5 - 0.8 and 0.2 - 0.4, respectively. For the surrounding and ground, the reflectance values of 0.44 and 0.2 are suggested. However, from preliminary simulation runs, it was observed that the daylight simulation may take a longer time than the energy simulation. Therefore, in order to increase the number of samples to be tested while avoiding time restrictions, a decision to use a fixed amount of daylight simulations was taken. By using discrete values for reflectance, the results led to 180 possibilities in total.

3.3 Output parameters

Determination of the output parameters is correlated with the current Danish Building Regulations 2018 [1], DS 474 and CIBSE guide A [59]. All the specific requirements, as well as the choice of parameters for each investigated category, will be presented in the following sub-sections.

3.3.1 Daylight

Danish Building Regulations 2018 [1] mentions the following requirements for the daylight in new buildings.

- Working rooms must have sufficient access to daylight ensuring sufficient level of lighting in the rooms,
- 10 % rule: Sufficient access to daylight could be documented by a glass surface without shadowing effect equivalent to minimum 10 percent of the relevant floor area,
- 300 lux rule: Sufficient daylight can be alternatively documented by spatial daylight autonomy (sDA_{300,50}), where 300 lux (minimum) is required for minimum 50 % of working area for minimum half of the daylight hours,
- Working area is defined as ‘the relevant floor area where workplaces are located’.

Based on the aforementioned building code requirements, Spatial Daylight Autonomy (sDA_{300,50}) was chosen to be the investigated output parameter from the daylight simulations. According to Mohsenin and Hu [72], sDA quantifies the sufficiency of daylight illuminance by defining the percentage of the floor area meeting certain illuminance levels for a specified amount of annual hours. Only daylight hours were considered while performing simulations. The operational profiles of the building were disregarded in the calculations.

3.3.2 Thermal comfort

Thermal comfort of building occupants is affected by a range of different factors including mean radiant temperature, relative airspeed, humidity and most importantly air temperature. Moreover, personal factors such as clothing level and metabolic rate influence the thermal comfort perception of the building users [73]. According to InnoBYG guideline for the thermal comfort [74], there are three quantification categories for the thermal comfort calculations in the commercial buildings, minimum, standard and ambitious. Each category requirements were adjusted to fit into the Danish climate context. Thermal comfort in the current project was assessed by the determination of the number of hours when the operative temperature exceeded 26 °C in the occupied spaces. According to the Building Regulations 2018 [1] following requirements have to be fulfilled for thermal comfort investigations.

- Satisfactory thermal comfort has to be ensured in the rooms with extended occupancy times (including activities in the rooms),
- Thermal comfort calculations have to be based on critical room conditions and design reference year DRY 2013,
- Calculation of the maximum number of occupational hours per year where room operative temperature exceeds 26 °C and 27 °C. For office building types maximum 100 hours over 26 °C and 25 hours over 27 °C are acceptable.

According to InnoBYG guideline [74], three evaluation periods are used for the thermal comfort calculations:

- summer period: May-August
- winter period: November-March
- ‘transition period’: April and October

Table 12 presents the maximum tolerance levels for the number of overheating hours based on different calculational periods.

Table 12. Tolerance level for different calculational periods.

	5 days working week	7 days working week
Summer and transition period	Max 100 hours	Max 140 hours
Winter period	Max 50 hours	Max 70 hours

For the current project case, limitation of five days working week is used, following BR18 regulations [1] for the maximum amount of overheating hours in the period from April to October. The room categories that were tested included office rooms (265), open plan office rooms (18), lounge (1), auditorium (3), restaurant (3), reception (2), meeting rooms (64),

circulation (31), kitchen (30) and changing rooms (20). The number in parenthesis indicates the number of rooms belonging to each category.

3.3.3 Energy

Danish Building Regulations [1] specify requirements for commercial buildings energy performance framework. Total supply energy demand is the sum of energy for heating, ventilation, cooling, domestic hot water and lighting per square meter heated floor area as shown in Equation 1 [54]:

$$\text{Total energy demand per year} \leq 41,0 + \frac{1000}{\text{heated floor area}} \text{ kWh/m}^2 \text{ per year} \quad (1)$$

Nevertheless, a different methodology not compliant with BR18 [1] was used for the final evaluation. Total energy output generated in IES did not account for domestic hot water but instead included equipment gains. Each sample in the project was evaluated for outputs including total energy consumption, space heating demand, and space cooling demand. The ranking of parameters presents the influence on each category, leading the designers towards improved strategies for decreasing the total energy demand of the investigated building.

3.4 Generation of samples:

The schematic process of sample generation is illustrated in Figure 4.

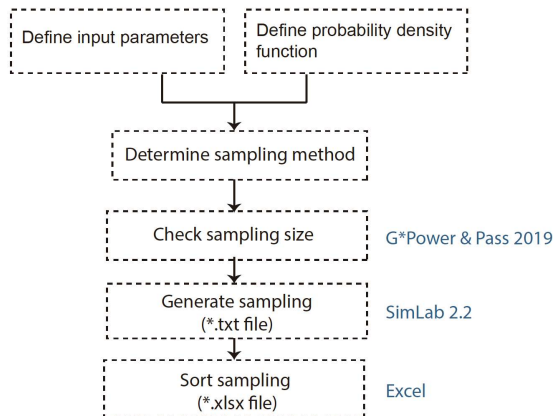


Figure 4. Process of sample generation.

The inputs and probability density functions (PDF) for each of the input parameters are presented in Table 9 in Section 3.2. The literature review regarding types of PDF was presented in Section 2.2.4.2. The PDFs were determined to be either uniform or discrete based on the possibilities and limitations of VEScript in IES, discussed in Section 3.6. Referring to Section 2.2.4.1, Latin Hypercube sampling method was chosen for this study, since it provides more evenly distributed sampling comparing to Monte-Carlo method. The sample size was determined based on the results from software G*Power and Pass 2019 and compared for the explicitness of the data, between the two software. Detailed information is provided in Figure 4. SimLab 2.2 was used for production of the samples data, since it is easy to use, and it

includes sampling methods according to the most common sensitivity analysis methods. The text file generated from SimLab 2.2 was converted to excel file, which could be read by the python code when automating the simulations. G*Power Analysis allowed determining the size of the sample based on the pre-determined effect of confidence in the results [75]. Power Analysis is based on the following four quantities:

- Size of the sample,
- Effect size,
- Level of significance (Type I error): the probability of finding an effect that is not there,
- Type II error: the probability of finding an effect that it is there.

Based on any three pre-determined variables, there is a possibility of calculating the fourth one, which in the project case was the size of the sample. Several options were tested with the following settings:

- Test family: exact,
- Statistical test: Correlation, bivariate normal mode,
- Type of power analysis: priori,
- Cohen's effect sizes: small 0.1, medium 0.3, large 0.5,
- $\alpha = 0.05$.

As a further test, sample results from G*Power were verified in software Pass 2019 (using PEAR formula for calculating the samples number) and the minimum recommended sample size was chosen (Table 13).

In Table 13, N is the number of samples, power is the probability of rejecting a false null hypothesis (between 0 and 1; usually 0.8, 0.95, 0.99), alpha is the probability of type I error, usually 0.05, Beta is the probability of type II error, ρ_0 (Baseline Correlation) is the value of correlation set at null hypothesis or the value of 0; ρ_1 (Alternative Correlation) is the value of correlation at alternative hypothesis. The null hypothesis is accepted at $\rho_0 = \rho_1$.

Table 13. Determination of the minimum sample size based on different accuracy levels.

Power	N	Alpha	Beta	ρ_0	ρ_1
0.95043	234	0.15	0.04957	0	0.2
0.95125	102	0.15	0.04875	0	0.3
0.95024	55	0.15	0.04976	0	0.4
0.95267	34	0.15	0.04733	0	0.5
0.80000	193	0.05	0.20000	0	0.2
0.80018	782	0.05	0.19982	0	0.1
0.85007	894	0.05	0.14993	0	0.1
0.90007	1046	0.05	0.09993	0	0.1
0.80008	193	0.05	0.19992	0	0.2
0.8509	221	0.05	0.14910	0	0.2
0.90038	258	0.05	0.09962	0	0.2

Values of the power, alpha and ρ_0 were estimated based on the recommended values obtained from the literature review [49, 50, 76, 77] and software tutorials for setting up PEARS sampling. As a result, the minimum number of samples was calculated to be 258 for $\rho_1 = 0.2$ and 1046 for $\rho_1 = 0.1$. However, due to the time limitations, running 1046 simulations was not possible, therefore an intermediate value of 400 samples was chosen. This value exceeds the minimum 258 samples recommendation for 90 % power with $\rho_1 = 0.2$ (higher accuracy with increased sample number).

3.5 Daylight analysis

3.5.1 General workflow

Workflow for the sensitivity and uncertainty analysis of building parameters affecting daylight (Figure 5) consisted of the following main steps.

- 1) Data creation: according to the workflow described in Section 3.4.
- 2) Model setup: Detailed description of taken steps is presented in the following Section.
- 3) Simulation: Dynamic simulations in DIVA were carried to assess the effect of the different parameters on the base case model. Two tests with different quality setting were performed for each sample. The difference in results (point-in-time-illuminance) between the two simulations settings was compared and verified before further processing.
- 4) Collection of the data: Excel VBA script and queries were used for the data extraction. Creation of the queries was time-saving in comparison to the usage of VBA script.
- 5) Results evaluation: Statistical interpretation of the data comparing results for Pearson's / Spearman's (appropriate method was selected) and the SRRC method was followed by the creation of the parallel coordinate plots.

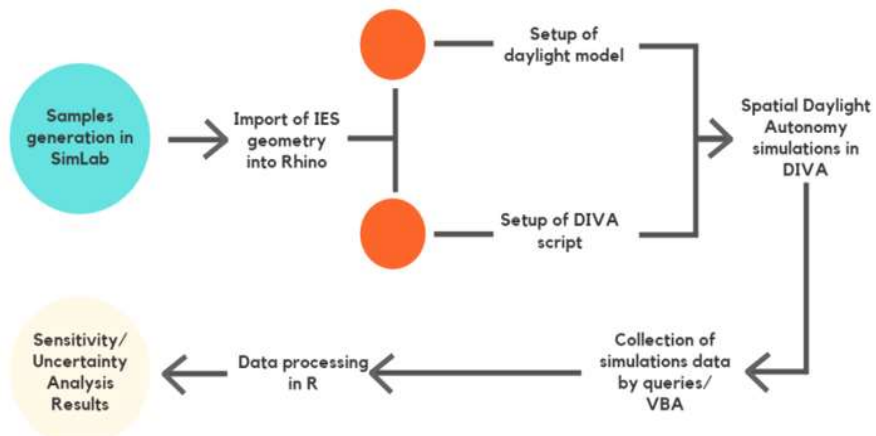


Figure 5. Daylight simulations workflow.

3.5.2 Assumptions

- For the daylight simulations, all floor plans were modelled without any internal objects / furniture.
- Simulations were performed based on the weather file with annual climate data from Copenhagen, Denmark.
- Different quality settings were tested prior to the final simulation runs.
- No neighboring buildings or plants were modelled in the base case surroundings.
- Only the top floor was simulated.

3.5.3 Detailed workflow

Setting daylight model:

Geometry for the daylight model was imported from the software IES (export as DXF -> polyline with openings -> save), directly into the Rhino model and further cleared up for any geometrical inconsistencies. Each surface type was distributed into different layers (floor, external wall, internal wall, etc.), which were further used for assigning surface properties in DIVA. The direction of each surface in Rhino model was controlled, for example, to ensure that the window surfaces were pointing towards outside while the internal surfaces were pointing towards inside. The purple marked geometries, illustrated in Figure 6, were used for daylight analysis. Figure 7 shows the top floor plan. The results only focused on meeting rooms, office rooms, and reception.

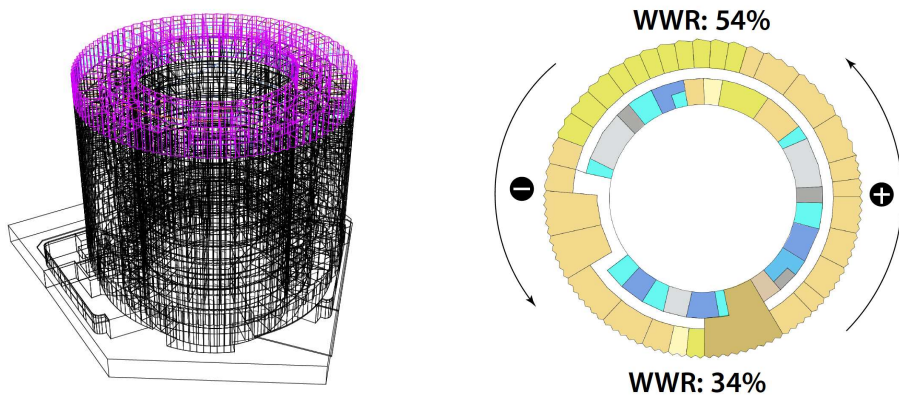


Figure 6. Daylight simulation model (left) glazing ratio variation on the top floor (right).

For the daylight simulations, top floor (presented in Figure 7) was chosen for assessment of the sDA in the working rooms (meetings, offices, reception). The assessment was performed according to the regulations discussed in Section 3.3.1. It is worth noting that windows varied in size alongside the façade, between 54 % on the north to 34 % on the south as illustrated in Figure 6 (right).

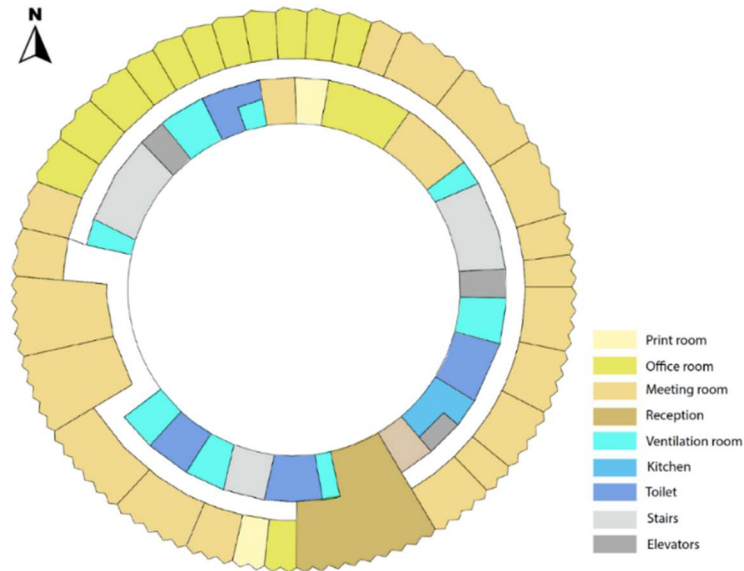


Figure 7. Floor plan for sDA simulations.

Customizing shading schedule:

In order to keep consistency between the two models (daylight and energy / thermal comfort) shading operation profiles had to be imported from initial IES model into DIVA for Grasshopper. However, exporting the shading profile from IES was not possible, therefore a different strategy had to be applied to secure the integrity of both models. Consequently, the following methodology was applied for ensuring consistency in the project:

- 1) Extraction of solar gains data for each room on the investigated floor (IES) with condition ‘internal shadings-on’,
- 2) Extraction of solar gains data with condition ‘internal shadings -off’,
- 3) Conversion of solar gains into ‘1’, ‘0’ shading operation profiles (where ‘1’ meant the shading was lowered down and ‘0’ meant shading was raised), based on the difference of the solar gains between two states,
- 4) Importing 8760 hours yearly ‘0’ / ‘1’ schedule to DIVA for Grasshopper.

It should be noted that each room on the top floor had different shading operational profiles, which as a consequence made the daylight simulation time significantly longer.

Specification of window properties:

As the next step in the development of the daylight parametric study, accuracy of window and surfaces data inputs was assured. Opaque components were simulated as ‘PLASTIC’ type of material, with roughness and specularity set to 0, whereas for windows, ‘GLASS’ was used as the set radiance material type. Radiance materials library requires conversion of the window visual transmittance (T_n) into the visual transmissivity (t_n), by application of following Equation [78]:

$$t_n = \frac{(\text{sqrt.}(0.8402528435 + 0.0072522239 * T_n * T_n) - 0.9166530661)}{0.0036261119} T_n \quad (2)$$

Automatic conversion of transmittance to transmissivity is possible by Honeybee_Radiance Glass material (Honeybee required) or excel converter. Corrected values were plugged directly into the DIVA Window component. Following transmissivity values (Table 14) were used for sDA_{300,50} simulations.

Table 14. Transmissivity values used for DIVA simulations.

Window type	Transmissivity value
1	0.784440
2	0.750665
3	0.570898
4	0.654789
5	0.664595

Due to the discrete distribution of the parameters (refer to Section 2.2.4.2) affecting daylight, 400 main samples were sorted out for repetitive patterns which as a consequence, reduced the number of samples for daylight simulations.

Grid size:

One of the most important steps in the preparation of the daylight simulations was to set the proper grid size according to the requirements of the project. Grid-size determines how many sensor points are used in the simulation. The smaller the distance between grid points (finer grid), the more accurate are the results. Result data is given at sensor points, which are defined on an analysis grid build on the horizontal plane. Placement of the grid (height) is defined by the user, corresponding to the task that is performed at the specific room. In the project case, the grid was placed 0.75 m above the floor in the investigated rooms. The specified grid displayed results of spatial daylight autonomy for dynamic simulations. The grid size was set to 1.5 m × 1.5 m, in order to obtain relatively accurate results without extensively long waiting time for high-quality simulations.

Raytrace quality setting parameters:

Radiance is based on the backward ray-tracing algorithms, which in essence means that the rays of light are traced back from the measurement point (or view) to the light source [79]. Radiance is able to process diffuse inter-reflections between the objects. Ambient calculations are used to describe the calculation of the inter reflected light [72, 80]. A large part of the daylight arriving at the sensor points (especially the points deeper in the rooms) was calculated by the indirect part of the Radiance algorithm. Therefore, the most crucial ambient parameters were investigated prior to selecting inputs, to ensure a good trade-off between accuracy and simulation time.

- **ab:** The number of ambient bounces characterizes the maximum number of diffuse bounces computed by the indirect calculation [81]. This parameter is set based on the number of reflections needed by the light to reach the task plus addition of interspace reflections. The optimization of the parameter is attributed to the type of analysed building. Setting the *ab* value to 0 indicates no indirect calculation, which as a result mean that the contribution of the indirect light from into the room will not be included since only direct sun / skylight patches are accounted for [80].

- **ar**: Ambient resolution determines the maximum density of interpolated ambient values [82, 83]. The maximum ambient value density is calculated as the ambient accuracy multiplied by the scene size, divided by the ambient resolution.

- **aa**: Ambient accuracy describes maximum error permitted in the indirect radiance interpolation. The lower the setting, the better the accuracy is achieved. When *aa* is set to 0, no interpolation is performed, however, simulation time will be significantly extended [80-82].

- **ad**: Ambient divisions regulate a number of rays sampled over the hemisphere centred above each evaluated point in the scene. Increasing the parameter results in a higher number of rays for testing and according to the literature [83, 84] increases the simulation time. By doubling ambient divisions, over four times of the initial simulation time is required.

- **as**: Parameter represents the number of extra rays applied to the areas with high variance. *As* applies only to the ambient divisions showing an indicative difference [84].

Rendering quality setting affects not only the accuracy of the simulations but can also significantly prolong the time needed to complete simulations. Therefore, careful choice and adjustment of settings were required to assure a satisfactory level of detail with optimized processing time. Radiance parameters for low-quality and high-quality settings are listed in Table 15.

Table 15. Raytrace quality settings; Source: [85].

Abbreviation	Parameter	low-quality settings	high-quality settings
-aa	Ambient accuracy	0.15	0.1
-ab	Ambient bounces	2	6
-ad	Ambient divisions	512	1024
-ar	Ambient resolution	256	256
-as	Ambient super-samples	128	256
-dr	Direct relays	2	2
-ds	Source substructuring	0.2	0.2
-lr	Limit reflection	6	6
-lw	Limit weight	0.004	0.000001
-dj	Source jitter	0	0
-lr	Limit reflection	6	6
-sj	Specular jitter	1	1
-st	Specular threshold	0.15	0.15

According to [72], doubling the ambient bounces parameter can double up the rendering time. Similarly, the increase of ambient divisions can double the simulation time. After an initial test of high-quality settings (default inputs), simulation time for 1 sample reached over 22 hours, therefore adjustments were implemented.

Increasing ambient bounces to 6 and ambient divisions to 1024 significantly increased simulation time to 5 hours 29 min per investigated sample in comparison to low-quality

simulations (55 min per one sample), however, decreased the simulation time in comparison to high-quality run.

Point-in-time illuminance simulations:

Point-in-time illuminance results for fall equinox (12:00) from low-quality and high-quality simulations, were compared for each sensor on the grid. Difference between the results yielded a maximum difference of 2384 lux between two consecutive runs (4.6 % difference). Therefore, it was concluded that low quality was not sufficient and sensitivity analysis / uncertainty analysis should be performed on data simulated with ‘high quality’ parameter settings.

3.6 Development of script in VEScript Python Editor

The VE Python application programming interface allows users to interact with the VE Model and Vista Results File, through the implementation of individually written Python code. Currently, there are no existing templates for writing the code and available learning sources are very limited. This application is still in the development phase, therefore import of individual packages adding functionality was not possible. Python programming language automatically transferred data between Excel file to / from IES, thus allowing to automatically run simulations, with changes in parameters based on the assigned function from the code. Creation of own customized script automatized the parametric studies and therefore reduced time spent on optimization of the buildings. Currently IES includes a tool which allows parametric studies. However, limitations do not allow to change several parameters at the same time. On contrary, unlimited changes to the model (except software own limitations, described further) were possibly by running simulations with Python code.

3.6.1 Steps in coding the VEScripts

The first step in the python code development was importing the package named ‘xlrd’ which enabled to read data in python from excel. Each variable created in SimLab 2.2 (see Section 3.4) was imported and read by the specified code function. Figure 8 presents the data allocation code based on the sample used in the project. Following code has to be adjusted accordingly for each new project (in case of additional variables).

```

aps_sample_name=sheet.cell(i,0).value #aps.name
wallinsul=sheet.cell(i,1).value # wall insulation thickness
roofinsul=sheet.cell(i,2).value # roof insulation thickness
groundinsul=sheet.cell(i,3).value #ground insulation thickness
infil=sheet.cell(i,4).value # infiltration index
auxi=sheet.cell(i,5).value # auxiliary ventilation index
hpt=sheet.cell(i,6).value # heatingsetpoint
cpt=sheet.cell(i,7).value # coolingsetpoint
occupancy=sheet.cell(i,8).value #occupancy rate index
light=sheet.cell(i,9).value #light gain index
equipment=sheet.cell(i,10).value #equipment gain index
glz=sheet.cell(i,11).value #glazing type
office_profile=sheet.cell(i,12).value #occupancy profile
inlet_profile=sheet.cell(i,13).value #supply air Temperature
hsb=sheet.cell(i,17).value #heatingsetback
csb=sheet.cell(i,18).value #coolingsetback

```

Figure 8. Python code for reading Excel data.

Changing the insulation thickness for the opaque construction:

In order to specify the construction types which users want to edit, the index of each construction type had to be identified. Each index ID corresponds to a specific construction type which was assigned in the initial building model. The code from Figure 9 describes the process to identify the index in the database by knowing its ID (Example: ID nr 20130014 for the external wall) which can be known from ‘IES construction database’. After knowing the index for each construction, user can call the “project.get_construction” function to get the specific construction by inputting the index (e.g. ids[1]). This methodology can also be applied to get a specific window construction.

```

import iesve
veproject = iesve.VEProject.get_current_project()
db = iesve.VECdbDatabase.get_current_database()
projects = db.get_projects()
project_list = projects[0]
project = project_list[0]
c_class = iesve.construction_class.opaque
ids = project.get_construction_ids(c_class)
index_1=ids.index('20130014') #externalwall
index_2=ids.index('20130017') #externalwall
index_3=ids.index('20130020') #externalwall
index_4=ids.index('20130007') #roof
index_5=ids.index('20130005') #ground
print(index_1,index_2,index_3,index_4,index_5) # found the index is 12,14,15,7,5)
wall_1_construction = project.get_construction(ids[12], c_class)
wall_2_construction = project.get_construction(ids[14],c_class)
wall_3_construction = project.get_construction(ids[15],c_class)
roof_1_construction = project.get_construction(ids[7],c_class)
ground_1_construction = project.get_construction(ids[5],c_class)

```

Figure 9. Python code for getting opaque constructions.

Figure 10 represents the workflow for setting the thickness of insulation for a specific construction. The layer of the insulation has to be specified according to the project

requirement. As an example, in the project base, the insulation layer is on the third place, therefore 2 was used as the index. Important: In python coding, the index starts from 0 and not from 1.

```
if wall_1_construction.is_editable:
    wall_layers_1 = wall_1_construction.get_layers()
    insulation_layer_1=wall_layers_1[2]
    insulation_layer_1.set_properties({'thickness': wallinsul})
```

Figure 10. Python code setting properties for constructions.

According to the VE Python functionality, it is possible to overwrite the following properties of the model:

- Layer level: surface emissivity, surface resistance and solar absorptance
- Material level: specific heat capacity, conductivity, density, vapour resistivity can be changed in the material level.

However, when the material properties have to be changed, the command ‘layer.get_material’ is required.

Changing the properties of the window constructions:

Using the same methodology of finding index as employed in ‘opaque construction’, the ‘external glazing construction’ indexes in the ‘construction database’ were read as 0, 4, 5, and 6. Since all the external glazing constructions should be changed at the same time for each investigated sample, the list ‘d’ was used to store the indexes as shown in Figure 11. Then, the code of ‘for i in d’ was used for looping 4 indexes in the list of d. In addition, the window type numbers 1 to 5 were pre-defined in the sample data, therefore, the transmittance and reflectance should be stored in the lists before extracting the window type. The outer pane was edited, and therefore 0 was used as the index.

```
#change outpane glazing properties
veproject = iesve.VEProject.get_current_project()
db = iesve.VECdbDatabase.get_current_database()
projects = db.get_projects()
project_list = projects[0]
project = project_list[0]
c_class_1 = iesve.construction_class.glazed
ids_1 = project.get_construction_ids(c_class_1)
transmittance=[0,0.871,0.710,0.30,0.470,0.350]
outside_reflectance=[0,0.078,0.2,0.6,0.38,0.4]
inside_reflectance=[0,0.078,0.2,0.6,0.38,0.4]
d=[0,4,5,6]
for i in d:
    base= project.get_construction(ids_1[i], c_class_1)
    if base.is_editable:
        layers= base.get_layers()
        outlayer=layers[0]
        material = outlayer.get_material(True)
        material.set_properties({'transmittance':transmittance[int(glz)],'outside_reflectance':outside
```

Figure 11. Python code for changing window properties.

It shall be noted that when the function ‘get_material’ is followed by ‘(True)’, the code will only apply changes to the material in the selected construction. If it is followed by ‘(False)’,

the changes will apply to all the constructions which have this material included. Nevertheless, if different constructions are using completely different materials from the database, then 'True' and 'False' will work the same.

Changing the occupancy profile and inlet temperature profile:

When testing different office occupancy profiles, canteen occupancy profiles and heating setpoint profiles should also be changed correspondingly. Correlation should be kept between the schedules in the whole building. For example, if the occupancy profile for the working area had one or two-hour lunch break, then the canteen profile should be adjusted accordingly. As it can be seen in Figure 12, the daily profiles were determined by their corresponding profile ID, which can be found in the profile database from the user interface.

```
project = iesve.VEProject.get_current_project()
office_daily_profile = project.daily_profile("DAY_0003")
canteen_daily_profile= project.daily_profile('DAY_0077')
inlet_temperature_daily_profile=project.daily_profile('DAY_0079')
heating_operation_daily_profile=project.daily_profile('SYS_0207')
cooling_operation_daily_profile=project.daily_profile('DAY_0087')
```

Figure 12. Python code for getting a daily profile from the database.

The different types of profiles should be stored in different lists, prior to extracting the data based on the type number. The code in Figure 13 shows an example of how the information corresponding to the profiles should be stored. The Python code overwrites the 24 h value for each profile. This is based on the user-defined profile variations. The term 'hsb' represents the heating setback value while 'hpt' corresponds to the heating setpoint value (specified in Excel). For example, [0, hsb, '-'] means that the temperature profile at 12 am is equal to the specified heating setback value.

```
heating_operation_list=[0,
[[0, hsb, '-'], [6, hsb, '-'], [6, hpt, '-'], [17, hpt, '-'], [17, hsb, '-'],[24, hsb, '-']],
[[0, hsb, '-'], [6, hsb, '-'], [6, hpt, '-'], [17, hpt, '-'], [17, hsb, '-'],[24, hsb, '-']],
[[0, hsb, '-'], [6, hsb, '-'], [6, hpt, '-'], [17, hpt, '-'], [17, hsb, '-'],[24, hsb, '-']],
[[0, hsb, '-'], [7, hsb, '-'], [7, hpt, '-'], [18, hpt, '-'], [18, hsb, '-'],[24, hsb, '-']],
[[0, hsb, '-'], [7, hsb, '-'], [7, hpt, '-'], [18, hpt, '-'], [18, hsb, '-'],[24, hsb, '-']],
[[0, hsb, '-'], [7, hsb, '-'], [7, hpt, '-'], [18, hpt, '-'], [18, hsb, '-'],[24, hsb, '-']],
[[0, hsb, '-'], [7.5, hsb, '-'], [7.5, hpt, '-'], [18.5, hpt, '-'], [18.5, hsb, '-'],[24, hsb, '-']],
[[0, hsb, '-'], [7.5, hsb, '-'], [7.5, hpt, '-'], [18.5, hpt, '-'], [18.5, hsb, '-'],[24, hsb, '-']],
[[0, hsb, '-'], [7.5, hsb, '-'], [7.5, hpt, '-'], [18.5, hpt, '-'], [18.5, hsb, '-'],[24, hsb, '-']]
```

Figure 13. Python code for storing information of daily profile.

Figure 14 demonstrates command which extracts the specific profile data from the list based on the profile type number, and followingly assign the new data to the existing profile.

```
heating_operation_daily_profile_data= heating_operation_list[int(office_profile)]
heating_operation_daily_profile.set_data(heating_operation_daily_profile_data)
```

Figure 14. Python code for overwriting daily profile.

One should carefully check if the setpoint is specified by a constant value, setpoint / setback setting or through the profile including daily variations (refer to apache settings for each thermal template). If the setpoint temperature is assigned by the profile, then it is flexible to

control which hour in the day when the desired setbacks or setpoints start. If the heating and cooling are assigned by a constant value, then system working hours will be based on the operational profile. However, if the setpoint temperature is set by constant values, they can be overwritten by the code command presented in Figure 15.

```

templates_iter = templates.values()
for template in templates_iter:
    if template.standard != iesve.VEThermalTemplate_standard.generic:
        continue
    room_settings = {'cooling_setpoint':cpt,'heating_setpoint':hpt}
    sys_settings={'HVAC_methodology':iesve.hvac_methodology.apache_system}
    template.set(room_settings,sys_settings)
    template.apply_changes()

```

Figure 15. Python code for changing set points.

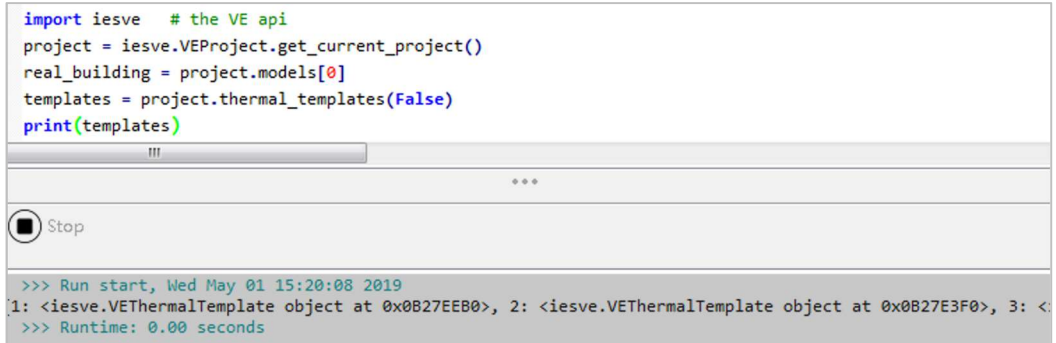
Changing the internal gains and air exchanges for the chosen templates:

Change of the data inputs in the thermal templates is based on the individual index for each template. Python code presented in Figure 16 allows extracting the template sequence in the database.

```

import iesve # the VE api
project = iesve.VEProject.get_current_project()
real_building = project.models[0]
templates = project.thermal_templates(False)
print(templates)

```



```

>>> Run start, Wed May 01 15:20:08 2019
1: <iesve.VEThermalTemplate object at 0x0B27EEB0>, 2: <iesve.VEThermalTemplate object at 0x0B27E3F0>, 3: <
>>> Runtime: 0.00 seconds

```

Figure 16. Python code for getting templates database.

The second step of the process is the determination of the number representing the specific template, which will be altered in the parametric study (Figure 17). The “get_bodies (True)” function returns the rooms which are selected in the user interface, while “get_bodies (False)” returns all the rooms in the model. Following process is required to extract the number for each template:

- Select one room belonging to each template,
- Run the script (Figure 17) for the selected rooms,
- Record the number followed by ‘general_template’ and name followed by ‘general_template_name’ accordingly into the table.

```

import iesve
import pprint
project = iesve.VEProject.get_current_project()
real_building = project.models[0]
bodies = real_building.get_bodies(True)
for body in bodies:
    if body.type != iesve.VEBody_type.room:
        continue
    room_data = body.get_room_data(0)
    pp = pprint.PrettyPrinter(indent=4)
    print("General Data:\n")

```

Run start, Wed May 01 15:29:55 2019

```

General Data:
{
  'circ_perc': 0,
  'circ_perc_from_template': True,
  'floor_area': 11.230937787550033,
  'general_template': 1,
  'general_template_name': 'default',
  'id': 'AIM25040',

```

Figure 17. Python code for getting template number.

Template numbers and indexes extracted for the base case model are presented in Table 16.

Table 16. Template number and index assigned in the base case model.

	Number	Index	Infiltration	Auxiliary Ventilation
Atrium	7	6	✓	
Auditorium	17	9	✓	✓
Garderober	24	14	✓	✓
Canteen	18	10	✓	✓
Heated rooms	8	7	✓	
Meeting rooms	19	11	✓	✓
Not heated rooms	10	8	✓	
Office	20	12	✓	✓
Sky lounge	21	13	✓	✓
Print room	25	15	✓	✓

The next step in this process is to add the additional internal gains and air exchanges into the database. This can be done as shown in Figure 18. Each element should have a unique name, referenced in the section ‘Gain Reference’. Naming conventions will be used to indicate the indexes of newly added gains and air exchanges.

Type	Gain Reference	Maximum Sensible	Maximum Latent G	Occupancy	Max Power C	Radiant Fractio	Meter	Variation	Dimming	Add To Terr
People	People-add2-index55	100.000 W/person	43.000 W/person	2.500 m2/per	-	-	-	REDocc	-	-
People	People-add3-index56	100.000 W/person	43.000 W/person	4.500 m2/per	-	-	-	REDocc	-	-
People	People-add4-index57	100.000 W/person	43.000 W/person	6.500 m2/per	-	-	-	REDocc	-	-
People	People-add5-index58	100.000 W/person	43.000 W/person	8.500 m2/per	-	-	-	REDocc	-	-
Miscellaneous	equip-add1-index59	0.000 W/m2	0.000 W/m2	-	0.000 W/m2	0.22	Electricity: Metr	REDocc	-	-
Miscellaneous	equip-add2-index60	2.500 W/m2	0.000 W/m2	-	2.500 W/m2	0.22	Electricity: Metr	REDocc	-	-
Miscellaneous	equip-add3-index61	5.000 W/m2	0.000 W/m2	-	5.000 W/m2	0.22	Electricity: Metr	REDocc	-	-
Miscellaneous	equip-add4-index62	7.500 W/m2	0.000 W/m2	-	7.500 W/m2	0.22	Electricity: Metr	REDocc	-	-
Miscellaneous	equip-add5-index63	10.000 W/m2	0.000 W/m2	-	10.000 W/m2	0.22	Electricity: Metr	REDocc	-	-

Figure 18. Internal gains database.

The script shown in Figure 19 describes how to access the database of internal gains and air exchanges. When referring to the “Gain Reference” names, the index of each gain or air exchange will be determined. The database length should be checked in advance to know the number of total internal gains. Since the added gains or air exchanges would normally be at the end of the database, counting backward would be suggested. For example, in project case, the total number of internal gains was 64 and the index of last gain was 63.

```

import iesve
project = iesve.VEProject.get_current_project()
casual_gains = project.casual_gains()
air_exchanges = project.air_exchanges()
print(casual_gains)
print(air_exchanges)
print(len(casual_gains))
print(len(air_exchanges))

!!!

***

[Stop]

>>> Run start, Wed May 01 15:07:49 2019
[LightingGain object at address 1314F818 for: Fluorescent Lighting, PeopleGain
[AirExchange object at address 1314F3E8 for: Infiltration, AirExchange object
64
19

```

Figure 19. Python code for getting internal gains and air exchanges database.

The code in Figure 20 shows the process of adding gains and air exchanges to the chosen templates. The occupancy, equipment and lighting gains have only been assigned to the office, while infiltration was added to all the templates. Auxiliary ventilation can only be assigned to the templates which had it assigned in the base case. Command of “template.apply.changes” was added at the end of the script to implement the pre-assigned changes.

```

casual_gains = project.casual_gains()
templates = project.thermal_templates(False)
templates_iter = templates.values()
alltemplates=list(templates.values())
# then only change the templates called office, office is index 12 template
alltemplates[12].add_gain(casual_gains[int(occupancy)]) # data from sample excel
alltemplates[12].add_gain(casual_gains[int(light)]) # data from sample excel
alltemplates[12].add_gain(casual_gains[int(equipment)]) # data from sample excel
alltemplates[12].apply_changes()
# now add infiltration rate, loop each template
air_exchanges = project.air_exchanges()
for template in templates_iter:
    template.add_air_exchange(air_exchanges[int(infil)])# data from sample excel
    template.apply_changes()
# now add ventilation rate, loop determinated templates, index 9,10,11,12,13,14
c=[9,10,11,12,13,14]
newarray = [alltemplates[int(i)] for i in c ]
for template in newarray:
    template.add_air_exchange(air_exchanges[int(auxi)])# data from sample excel

```

Figure 20. Python code for adding gains and air exchanges.

Removing gains and air exchanges before the next simulation run:

Modified gains and air changes have to be removed before overwriting data for the next simulation run. Figure 21 illustrates the steps needed to remove gains and air exchanges.

```

project = iesve.VEProject.get_current_project()
casual_gains = project.casual_gains()
templates = project.thermal_templates(False)
templates_iter = templates.values()
alltemplates=list(templates.values())
alltemplates[12].remove_gain(casual_gains[int(occupancy)]) # data from sample excel
alltemplates[12].remove_gain(casual_gains[int(light)]) # data from sample excel
alltemplates[12].remove_gain(casual_gains[int(equipment)]) # data from sample excel
alltemplates[12].apply_changes()
air_exchanges = project.air_exchanges()
for template in templates_iter:
    template.remove_air_exchange(air_exchanges[int(infil)])# data from sample excel
    template.apply_changes()
c=[9,10,11,12,13,14]
newarray = [alltemplates[int(i)] for i in c ]
for template in newarray:
    template.remove_air_exchange(air_exchanges[int(auxi)])# data from sample excel
    template.apply_changes()

```

Figure 21. Python code for removing gains and air exchanges.

Reading data of *.aps result file in Python:

Required results from simulated “*.aps” file can be directly written down to Excel, using the Python script. In the case of a large number of simulated samples, running python code significantly reduces the amount of time spent on the extraction of results data. In the project case the result categories that were extracted included heating and cooling demand, lighting demand, equipment demands, and total energy. However, when different types of results have to be extracted, additional “read_variable” functions can be added. The example shown in Figure 22 aimed to extract various variables. Results category in vista pro (where user can

read detailed results in general or detailed breakdown) have to be verified, prior to data extraction.

```

def read_variable_1(result_reader, result_variable):
.....

with iesve.ResultsReader.open('//Mac/Home/Desktop/Finaltian/vista/'+str(i)+'.aps') as results_
    assert results_file_reader is not None, "Error opening results file"

    aps_variables = results_file_reader.get_variables()
    aps_units = results_file_reader.get_units()

    read_variable(results_file_reader, find_variable('Total energy', 'e'))
    read_variable_1(results_file_reader, find_variable('Boilers energy', 'e'))
    read_variable_2(results_file_reader, find_variable('Chillers energy', 'e'))
    read_variable_3(results_file_reader, find_variable('Lights electricity', 'e'))
    read_variable_4(results_file_reader, find_variable('Equip electricity', 'e'))

```

Figure 22. Python code for extraction of the results.

3.6.2 Limitations in the VEScript Python Editor

Since the Python module in IES VE is still in the development phase, there are several limitations to functions which can be implemented by the python code. Unfortunately, this affected the initial choice of parameters for sensitivity and uncertainty analysis, which needed to be re-defined based on the software constraints. At the initial stage of the project, the test model was defined as a simple room with 1 window. Python code implementing changes in the test model was developed for a simple box before proceeding with adjustments to code designed for the more complex building. Following limitations were discovered in a ‘trial-error’ process of defining the possibility of parameter change:

- WWR: It is not possible to change the window-to-wall ratio in the case of having pre-defined window geometries. Change of the window to wall ratio is possible if windows geometries were defined by ‘add by percentage component’ in IES VE. One of the solutions proposed for parametric studies, where a change of WWR is required, is the development of different VE models containing different window geometries generated by Dynamo in Revit. Parametric studies with python code can be performed for scenarios with different models. Currently solution to problem with change of WWR is in development phase by IES technical department.
- Change of window construction: Only existing layers of assigned window type can be overwritten, without the possibility of changing construction type from the windows added to the database. Unfortunately, this limited the testing options of different window types in the current project. For example, if the existing window construction has triple pane windows, the double pane windows cannot be tested by ‘overwrite’ function. The faulty function was given in Figure 23. Currently, IES VE function for overwriting windows is in the development stage.

```

for id, body in bodies.items():
    if body.type != iesve.VEBody_type.room:
        # we only want to process thermal rooms here, so filter by type
        continue
    surfaces = body.get_surfaces()
    print(surfaces)
    for surface in surfaces:
        if surface.type == iesve.VESurface_type.ext_glazing:
            construction = project.get_construction(ids[0], c_class)# can also put glazing construct
            body.assign_construction(construction, surface)
            openings = surface.get_openings()
            for opening in openings:
                op_props = opening.get_properties()
                body.assign_opening_type(surface.index, opening.get_macroflo_id(), op_props["aps_har

```

Figure 23. Example of faulty function in the VEScript Python Editor.

- Gas-filled windows: The gas filling in the window construction cannot be changed by using the python code, which makes it impossible to test windows with large-span of U-values. Moreover, the VEScript can only change the outside emissivity of the outer pane and the inside emissivity of the inner pane. The inside emissivity of outer pane and outside emissivity of the inner pane are fixed. This limits the possibility of testing different coatings applied to surfaces. Therefore, the U-value can be fixed, by inputting the resistance in the air cavity, and only the windows with different glazing types for the outer pane were tested.
- Internal Gains and air exchanges: The only way to modify gains and air exchanges is by adding the value to the database, instead of overwriting the current value. Therefore, test options have been limited to discrete values excluding the possibility of testing ranges with uniform distributions. This negatively affected the results of the uncertainty analysis. Additionally, supplementary work of removing the internal gains and air exchanges is required, before running the next sample.
- Thermal templates: Quality assurance of changes implemented by each function of the developed code was checked in a series of ‘test runs. Unfortunately, error with changes in thermal templates was detected: once internal gains or air exchanges were added through the Python script, the assigned templates were reset and the whole building was distributed with the default template. To solve this error, the code of assigning templates to the whole building was added at the end of the whole python code. After running the code in Figure 24, the room id’s of each template was inserted to the different room lists and then each list was assigned with the corresponding template as shown in Figure 25.

```
import iesve
currentroom_list=[]
project=iesve.VEProject.get_current_project()
models=project.models
model=models[0]
bodies=model.get_bodies_and_ids(True)
for id,body in bodies.items():
    currentroom_list.append(body.id)
print(currentroom_list)
```

Figure 24. Python code for reading room ids.

```
office_id_list = ['AIM50770', 'AIM23400', 'AIM39070', 'AIM75380', 'L0000018', 'AIM53640', 'AIM57610', 'AIM50450', 'AIM48520', 'AIM42260', 'L0000023', 'AIM53910', 'AIM32460']
heated_id_list = ['AIM53910', 'AIM32460']
noheated_id_list=['AIM84890', 'AIM50600', 'AIM63820', 'AIM81550', 'AIM14150', 'AIM66080', 'AIM61260', 'AIM87660', 'AIM83450', 'AIM10590', 'skylounge_id_list=['L1000003']
auditorium_id_list=['AIM07690', 'AIM06330', 'AIM09370']
canteen_id_list=['AIM19380', 'AIM36310', 'AIM29560', 'AIM17210', 'AIM17940', 'AIM12370', 'AIM18440', 'AIM17560', 'AIM20390', 'AIM17250', 'AIM14870', 'L0000023', 'AIM03440', 'L0000026', 'RM000000', 'L0000024', 'L0000025', 'RM000002', 'RM000001']
atrium_id_list=['L0000023', 'AIM03440', 'L0000026', 'RM000000', 'L0000024', 'L0000025', 'RM000002', 'RM000001']
meeting_id_list=['AIM52250', 'AIM54560', 'AIM52220', 'AIM34900', 'AIM78900', 'AIM54500', 'AIM57240', 'AIM56270', 'AIM56020', 'AIM56480', 'AIM14870', 'AIM15660', 'AIM15210', 'AIM15020', 'AIM15850', 'AIM20680', 'AIM15700', 'AIM14380', 'AIM13960', 'AIM14870', 'AIM14870', 'AIM14870']
auditorium_gardarobe_id_list=['AIM15660', 'AIM15210', 'AIM15020', 'AIM15850', 'AIM20680', 'AIM15700', 'AIM14380', 'AIM13960', 'AIM14870', 'AIM14870', 'AIM14870']
print_id_list=['AIM83200', 'AIM58520', 'AIM57550', 'AIM59080', 'AIM57120', 'AIM57860', 'AIM79500', 'AIM57920', 'AIM57880', 'AIM57300', 'AIM52250']

real_building.assign_thermal_template_to_rooms(alltemplates[12], office_id_list)
real_building.assign_thermal_template_to_rooms(alltemplates[7], heated_id_list)
real_building.assign_thermal_template_to_rooms(alltemplates[13], skylounge_id_list)
real_building.assign_thermal_template_to_rooms(alltemplates[9], auditorium_id_list)
real_building.assign_thermal_template_to_rooms(alltemplates[10], canteen_id_list)
real_building.assign_thermal_template_to_rooms(alltemplates[6], atrium_id_list)
real_building.assign_thermal_template_to_rooms(alltemplates[11], meeting_id_list)
```

Figure 25. Python code for assigning templates to rooms.

- Application limitations: Some errors can only be fixed by IESVE technical support. For example, overwriting the construction will not be reflected in the model properly, unless manually saved after altering each template. This further disabled the possibilities of running the apache simulation directly from the Python script. The approach to solving the ‘overwriting’ problem was to open a construction type from the database and click “save changes” before closing the windows. The solution for the second problem would be to save the project in the user interface and then set the apache simulation in either the user interface or Python script. However, if IES development team can fix these two errors for VESript Python Editor, then the Python script could loop all the samples to run the simulations without any manual work.
- Data filtering: One more limitation is that Python cannot filter the required data when reading the “*.aps.” file. It is possible to limit the start and end day for hourly evaluation; however, it is not possible to exclude weekends / holidays / nighttime. The approach to solving this problem would be to extract all the operative temperature hourly values for each room and automatically write them to columns by using the code shown in Figure 26. Further data sorting in excel would be required for the purpose of excluding undesired days / times used in the overheating evaluation. To continue, the code showing the procedure to evaluate the number of overheating hours for the listed rooms (if 24 h and 7 days are considered) is presented in Figure 27. The code is able to extract the ids of the rooms which have overheating problems, as well as the number of overheating hours for each room.

```

global a
a=0
for room_id in room_id_list:

    aps_data_1= result_reader.get_room_results(room_id, result_variable['aps_varname'], result_variable[

    for row_ind, row_value in enumerate(zip(aps_data_1)):
        for col_ind, col_value in enumerate(row_value):
            worksheet.write(row_ind, a, col_value)

    a=a+1

```

Figure 26. Python code for writing data to Excel.

```

room_id_list=['AIM22780']
overheat_room=[]
numberover=[]

for room_id in room_id_list:
    aps_data_1= result_reader.get_room_results(room_id, result_variable['aps_varname'], result_variable[
    tem=aps_data_1
    overheat=sorted(i for i in tem if i>26)
    numberofhours=len(overheat)
    if numberofhours > 80:
        overheat_room.append(room_id)
        numberover.append(len(overheat_room))
        print(len(overheat))
print(overheat_room)
print(numberover)

```

Figure 27. Python code for checking the number of overheating hours in the problematic rooms.

3.7 Data processing in R

Choice of the right statistical method is highly dependent on the generated data sets as well as the type of function that is represented by the data plots. Correlation measures the strength of the association between the independent and dependent variable, while regression analysis is commonly used to predict the result based on the specific values of all the parameters [86]. Spearman's method is distribution-free, meaning non-parametric ranking, while Pearson's method requires fulfillment of specific assumptions [87-89]. Spearman's method is suitable for monotonic function (calculations based on ranks), whereas PEARS is computed based on true values, therefore requires linearity of the data [89]. Since Spearman's rho is not a measure for linear relationship between variables, it can be used for variables at the ordinal level which makes it a good fit for data sets with various distributions [87]. For Pearson's correlation following rules should be met [87, 89]:

- All variables should have a normal distribution,
- The linearity of the function: straight line between variables,
- Homoscedasticity: data should be equally distributed alongside the regression line,
- Outliers can negatively affect linearity.

If even one of the pre-requisites is not fulfilled, Pearson's method cannot be used. In contrast to Pearson's method, the Spearman's rank correlation does not require any prior assumptions about the data distribution. However as previously mentioned, data must be monotonically related [50, 77, 87, 89]. In order to best define the suitability of the method for data evaluation, both PEARS and SPEAR were plotted in 'R' software (scatter plots) and correlation / determination rank was calculated. Following steps were required for the calculations:

- 1) Adjustment of data to comply with the format required for data import in 'R': rows / columns headings, naming conventions, data format (*.txt or *.csv),
- 2) Setting the right directory for data import,
- 3) Standardization of the data prior to the statistical analysis,
- 4) Computation of correlation matrix,
- 5) Graphical interpretation: Scatter Plots,
- 6) Determination of model linearity / none-linearity.

The initial assumption of the suitability of Pearson's method was verified by testing models linearity. In case of proven linearity, parameters' distributions, outliers, and homoscedasticity were tested. However, in case of nonlinearity of model, Pearson's method was excluded, and statistical analysis proceeded based on Spearman's Rank Correlation Coefficient. The linearity of the model was tested based on the coefficient of determination (R^2), describing models performance for R^2 below 0.5 as unsatisfactory [90], and R^2 values over 0.5 validate the chosen method.

The value of the correlation coefficient and significance level (p) for each independent variable (vs output parameter) was calculated and analyzed. The value of the correlation coefficient has to be placed in an interval between -1 to 1, where 0 means no correlation [91]. When the correlation coefficient is positive, it means y (dependent variable) will be increased when x (independent variable) increases, meanwhile when the correlation coefficient is negative, y will be decreasing. Strength of correlation can be described by following level of association [92], listed in Table 17:

Table 17. Evaluation of correlation strength.

Value of coefficient of correlation (R) (+ and -)	Level of association
0	None
0.1 to 0.3	Weak
0.4 to 0.6	Moderate
0.7 to 0.9	Strong
1	Perfect

Additionally, in order to confirm or reject the null hypothesis of the method, significance level (p) of the results needed to be evaluated. The ' p ' value describes the probability of a null hypothesis being correct, therefore the value of below 5 % ($p < 0.05$) is considered statistically significant [87] as presented in Table 18.

Table 18. Evaluation of significance level.

Significance level ' p '	Description of the results
< 0.05	Statistically significant
≥ 0.05	Statistically non-significant

The p -value of 0.05 indicates that, if there is no correlation between the variables, there is a possibility of obtaining the observed difference in 5 % of the statistical studies due to the random sampling error. Ranking of the parameters is based both on the calculated correlation and the verification of the significance level of the investigated population. For cross-validation of the outcomes between different sensitivity analysis methods, variables from chosen correlation method were compared to the ranking from the Standardized Regression Rank Coefficient.

3.8 Overall results in Design Explorer

The approach of data-processing mentioned above might be complicated and time-consuming. Therefore, this thesis also explored the feasibilities of using an online tool named Design Explorer. Design Explorer can generate parallel coordinate plots which illustrate multi-disciplinary results instantly by importing the inputs and outputs of all the samples. Also, it can add filtration to the results according to user requirements. This leads to quicker filtering the best-performing samples and yielding the favorable ranges for building parameters. As a result, this might provide quick suggestions to facilitate the decision for the consultants.

To test the applicability of Design Explorer, the same filtering process used by the uncertainty study were applied. Then, the best performing ranges yielded by Design Explorer were compared with the results of the uncertainty study to verify the validation of using the software.

4 Results

This chapter presents the final outcomes of the sensitivity and uncertainty analysis of the building parameters affecting daylight, thermal comfort, and energy consumption of the considered case. The workflow is shown in Figure 28. All simulated data is presented in the form of histograms, parallel coordinate plots and scatter plots. In the following sections, detailed analysis of the data is presented and discussed for each investigated category.

Results Interpretation:

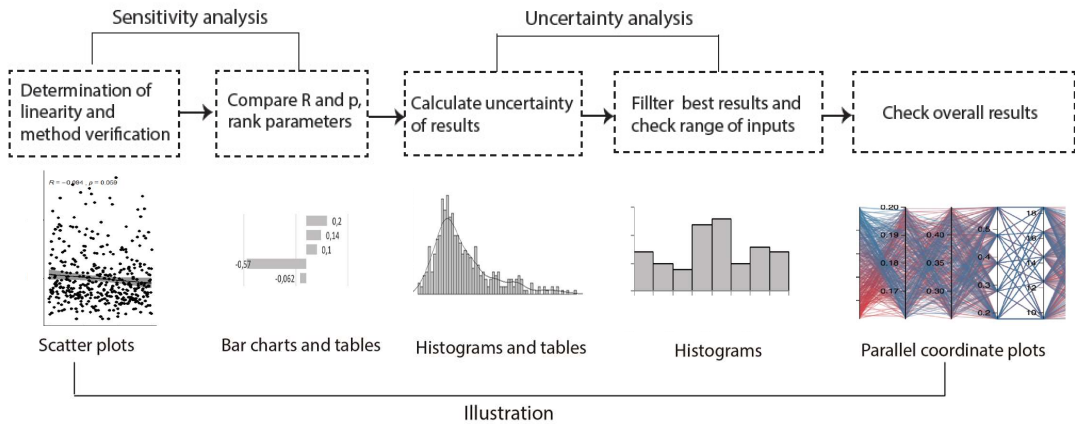


Figure 28. Flow chart for interpretation of the results.

4.1 Sensitivity analysis

Sensitivity analysis results are highly dependent on the type of the function (linear, non-linear, and monotonic) represented by the simulated data sets. As a first step, Pearson's determination coefficient (R^2) was calculated to validate the suitability of the analysis method against the requirements specified in Section 3.7. The results of calculated coefficients (R^2) are presented in Table 19. As all coefficients are below 0.5, suggesting unsatisfactory performance of the current statistical model, Pearson's method was unsuitable for the studied case. [90]. The calculated coefficients revealed the significant non-linear effect of the simulated data [29]. Consequently, Spearman's method was chosen as the final sensitivity analysis method for the interpretation of the results.

Table 19. Pearson's determination coefficient.

Parameters	Total energy consumption	Heating demand	Cooling demand	Thermal comfort
Wall insulation thickness	0.000079	0.018380	0.005502	0.000371
Roof insulation thickness	0.003597	0.003048	0.000092	0.000673
Floor insulation thickness	0.004646	0.000169	0.002004	0.001126
Inlet air temperature	0.052470	0.133033	0.118067	0.019309
Infiltration rate	0.012642	0.307623	0.027720	0.051624
Auxiliary ventilation rate	0.093048	0.060617	0.000674	0.055767
Heating setpoint	0.005231	0.265877	0.010801	0.006952
Heating setback	0.004523	0.011011	0.005071	0.001923
Cooling setpoint	0.008934	0.000013	0.039702	0.273984
Cooling setback	0.000938	0.000931	0.003306	0.000149
Occupancy profile type	0.003214	0.000331	0.000812	0.000522
Occupancy rate	0.389619	0.006263	0.345372	0.002133
Window g-value	0.002051	0.025760	0.062276	0.301542
Lighting gains	0.008217	0.001143	0.000028	0.006271
Equipment gains	0.022699	0.000471	0.000372	0.000020

For each independent variable defined in Section 3.2, the distribution of the results data is presented as scatter plots. The coefficient R describes the level of correlation between the input and output variable. The p -value represents the significance level of the correlation. If $p < 0.05$, it means that the rejection of the null hypothesis is achieved, and therefore it validates the existence of the correlation.

4.1.1 Energy & Thermal comfort

Firstly, the correlation between building parameters and energy results is presented. Figure 29 shows the correlation between wall insulation thickness and the total energy consumption, and heating and cooling demand. It indicates that the increasing thickness of the wall insulation positively contributes to the reduction of the heating demand. However, the level of correlation between the wall insulation thickness and heating demand can be described as negative, weak (see Section 3.7). The correlation and significance level of the wall insulation thickness towards cooling demand, suggest a positive, weak correlation. This implies that increasing the insulation thickness will lead to higher cooling loads. Nevertheless p -value over 0.05, neglects the significance of the correlation between the cooling demand and wall insulation thickness. Followingly, significance level p of the correlation results between wall insulation thickness and the total energy consumption equals to 0.41. Therefore, the initial hypothesis that there is no correlation between the thickness of wall insulation and the total energy demand, fails to be rejected. In the studied case wall insulation thickness does not have high importance in reducing the total energy consumption.

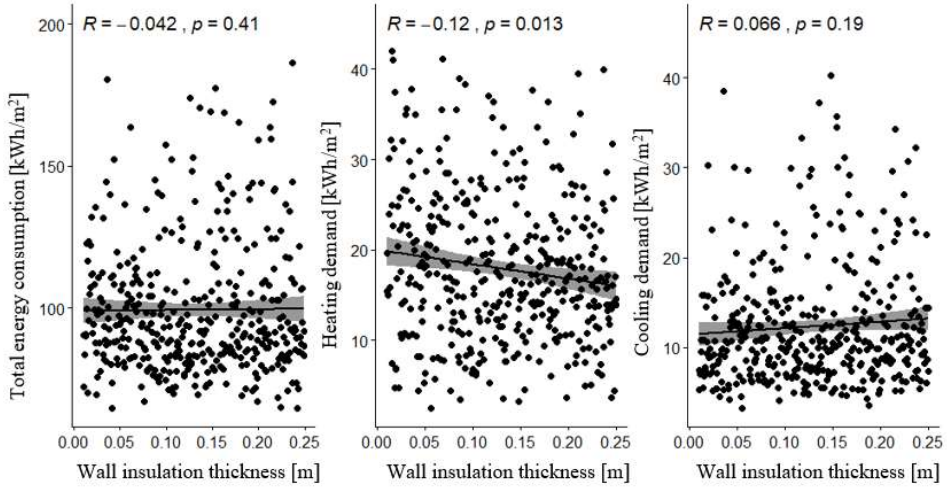


Figure 29. Scatter plots showing correlation level between wall insulation thickness and total energy consumption, and heating and cooling demand.

Figure 30 shows the correlation level between roof insulation thickness and total energy consumption, and heating and cooling demand. Roof insulation thickness has a weak correlation level with total energy consumption, with p equal to 0.13. The p -value is equivalent to 13 % error margin, due to random sampling error, as described in Section 3.7. The significance level of the correlation results between the heating demand, cooling demand and roof insulation thickness are over 0.05. Therefore, there is no proven statistical correlation between roof insulation thickness and cooling and heating demands for the studied range. In the case building, roof insulation thickness will not be prioritized in the optimization process.

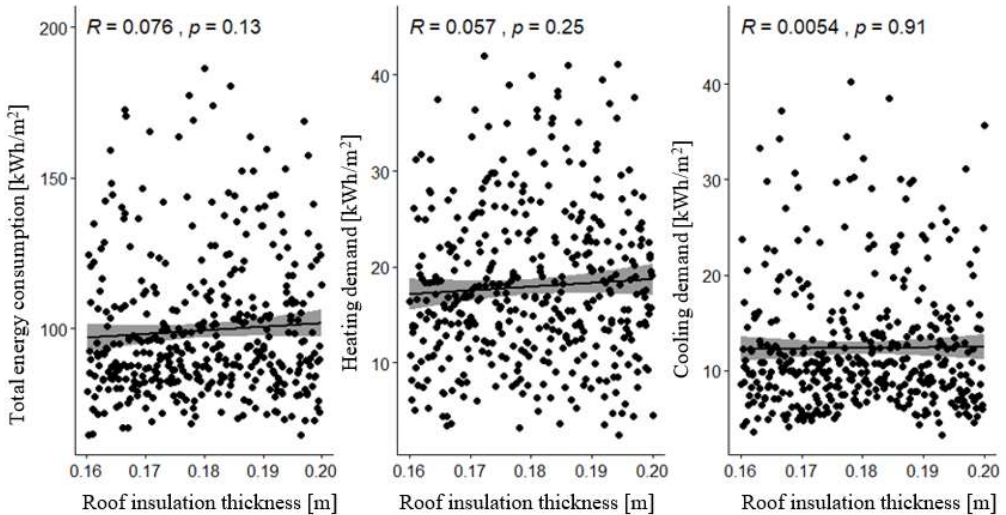


Figure 30. Scatter plots showing correlation level between roof insulation thickness and total energy consumption, and heating and cooling demand.

Figure 31 presents the correlation level between floor insulation thickness and total energy consumption, and heating and cooling demand. The scatter plot for floor insulation thickness presented in Figure 31 clearly indicates how increasing the ground floor insulation contributes to decreasing the total energy consumption. Despite this positive effect, the high p -value of 0.15 and very low R -value of -0.072 indicate no correlation between the floor insulation thickness and the total energy consumption. This is due to the statistical insignificance of the datasets. Similarly, the p -value of correlation results between the floor insulation thickness and the heating and cooling demands is over 0.05, therefore there is no proven correlation between variables in the studied building case.

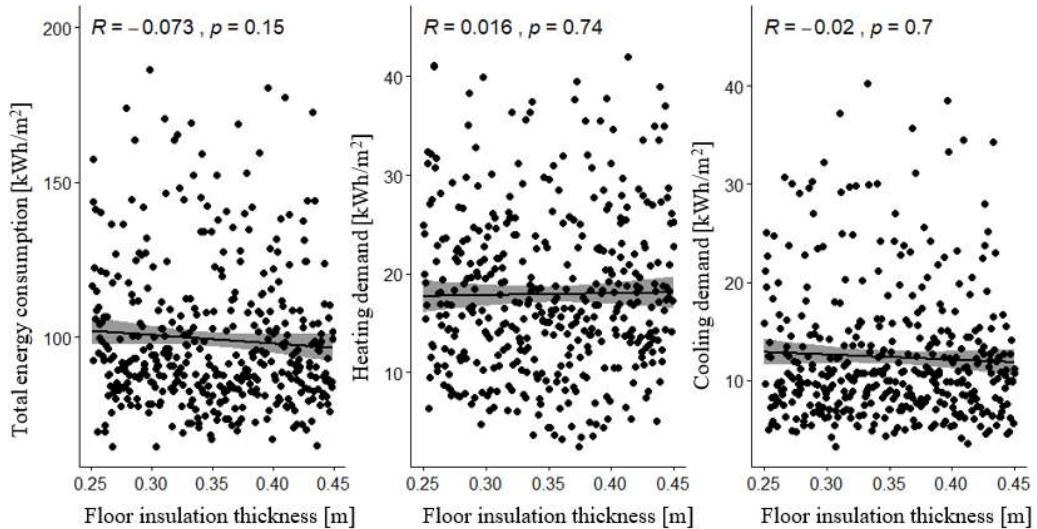


Figure 31. Scatter plots showing the correlation between floor insulation thickness and total energy consumption, and heating and cooling demand.

Figure 32 presents the correlation level between inlet air temperature and the total energy consumption, and heating and cooling demand. Figure 32 shows that increasing the inlet air temperature significantly decreases both the heating demand and cooling demand. This is represented by moderate, negative correlation with a high significance level of the results. The explanation for the decreased cooling demand is that higher inlet temperature air increases the use of free cooling through the ambient air thus decreases the cooling demand. The correlation between total energy consumption and the inlet air temperature can be described as weak, negative. Nevertheless, thermal comfort assessment should be performed, to ensure an acceptable level of air temperature in the occupied rooms.

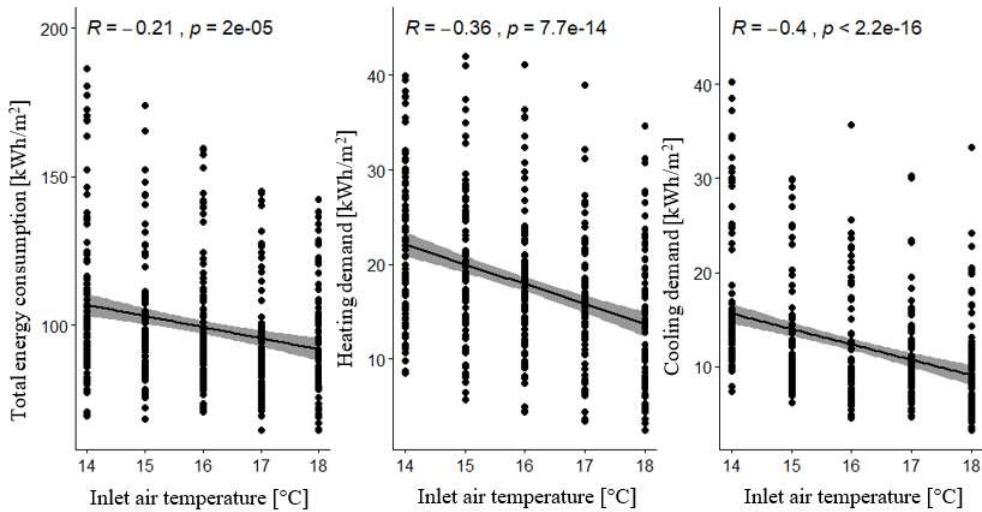


Figure 32. Scatter plots showing the correlation between inlet air temperature and total energy consumption, and heating and cooling demand.

Figure 33 shows the correlation level between the infiltration rate and the total energy consumption, and heating and cooling demand. As can be seen from Figure 33, the higher infiltration is another factor significantly contributing to the increase of the heating energy demand. High significance level confirms correlation between the infiltration and the heating demand. Therefore, the airtightness of the building has to be carefully examined. Moreover, infiltration rate has a negative correlation with the cooling energy demand. Higher air change rates result in lower cooling energy values. Nonetheless level of association is weak. Looking at the overall results for correlation between total energy consumption and the infiltration, it can be implied that increased level of infiltration results in a slight increase in the total energy consumption.

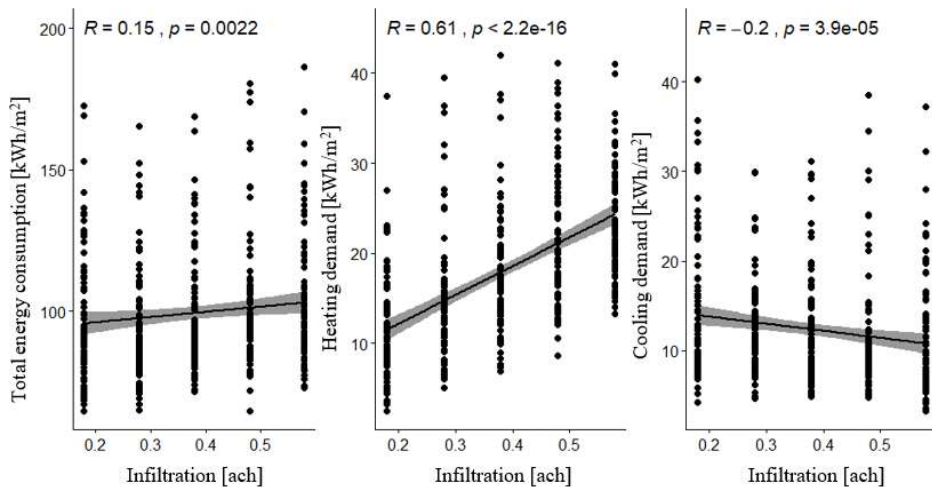


Figure 33. Scatter plots showing the correlation between infiltration and total energy consumption, and heating and cooling demand.

Figure 34 presents the correlation level between the auxiliary ventilation airflow rate and the total energy consumption, and heating and cooling demand. As seen from Figure 34, there is a weak, statistically significant correlation between the infiltration and the total energy consumption. Auxiliary ventilation airflows contribute to increasing of the total energy consumption. Therefore, while designing HVAC system, it is very important to adequately define ventilation rate per person. Increased auxiliary ventilation airflows result in the minimal decrease of cooling demand in investigated population. At the same time, higher ventilation rates contribute to increased heating demand. However, while assessing the realistic effect of the auxiliary ventilation airflow rate on the heating demand, ventilation flow rate and the inlet air temperature should also be accounted for. In order to do that, statistical method, accounting for interactions between the input variables, should be used. However, the multivariable interactions were not tested in this thesis.

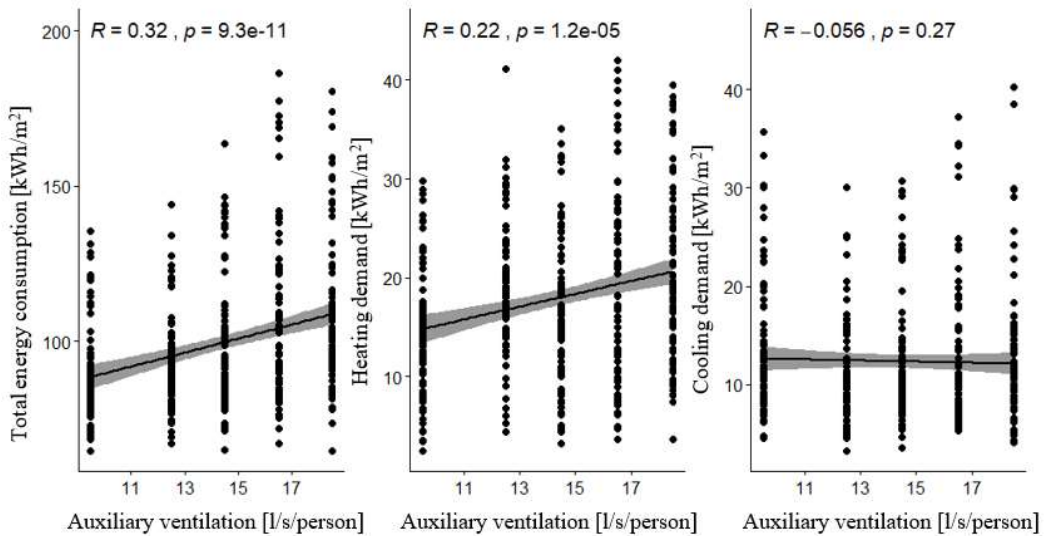


Figure 34. Scatter plots showing the correlation between auxiliary ventilation and total energy consumption, and heating and cooling demand.

Figure 35 and Figure 36 show the correlation level between the heating setback and setpoint temperature and total energy consumption, and heating and cooling demand. The comparison of the figures indicates that heating setpoint temperature plays more important role in the heating demand and total energy consumption. As expected, heating setpoint temperature is moderately, positively correlated with the heating demand. Higher heating setpoint results in higher heating demand. Furthermore, the heating setpoint temperature was negatively correlated with the cooling demand. A possible explanation can be that the heating and cooling occur simultaneously during the summertime. The heating setback temperature does not have a statistically proven correlation with the cooling demand.

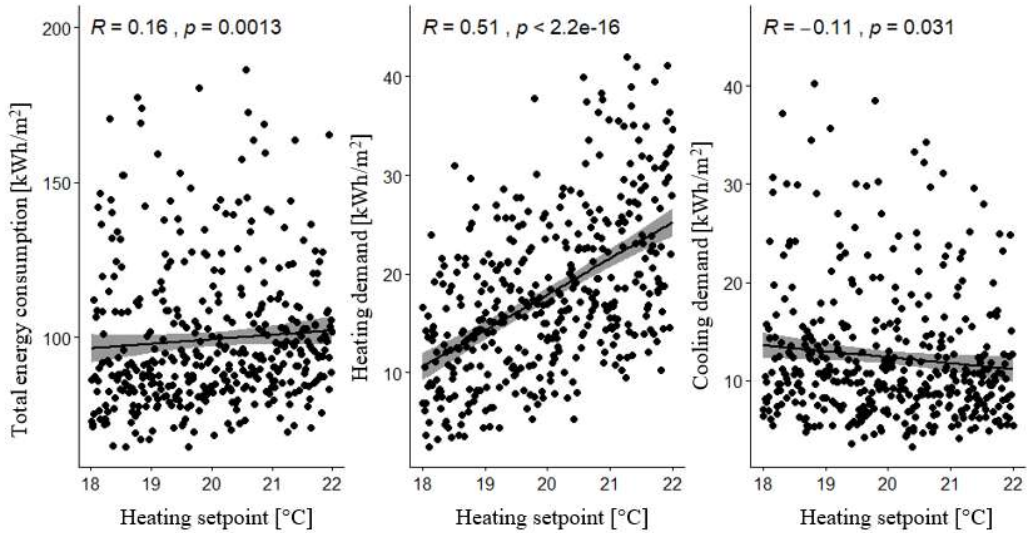


Figure 35. Scatter plots showing the correlation between heating setpoint and total energy consumption, and heating and cooling demand.

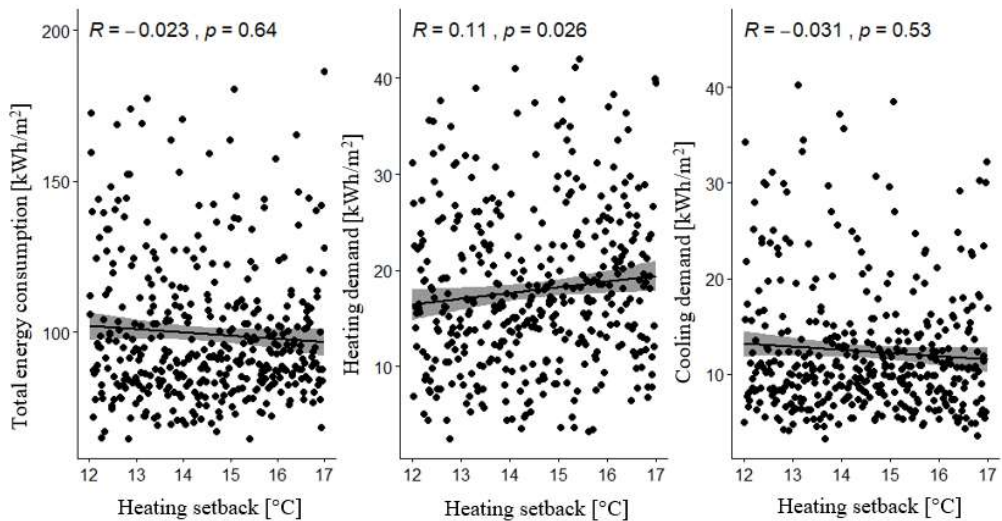


Figure 36. Scatter plots showing the correlation between heating setback and total energy consumption, and heating and cooling demand.

Figure 37 and Figure 38 present correlation level between the cooling setpoint and setback temperature and the total energy consumption, and heating and cooling demand. The figures show that the cooling setpoint temperature has a larger influence on the cooling demand than the cooling setback. The correlation level between cooling setpoint temperature and cooling demand is negative, weak. On contrary, there is no statistically proven correlation between cooling setback temperature and cooling demand for the studied case. Moreover, none of these two parameters have a significant effect on the total energy consumption, since p -value in both cases exceeds 0.05. Heating demand is correlated neither with cooling setpoint temperature nor with cooling setback temperature. Results of the studied building indicate that when specifying the space conditions, it is important to dedicate most attention to the

heating setpoint temperature in comparison to cooling setpoint temperature and heating / cooling setback temperature.

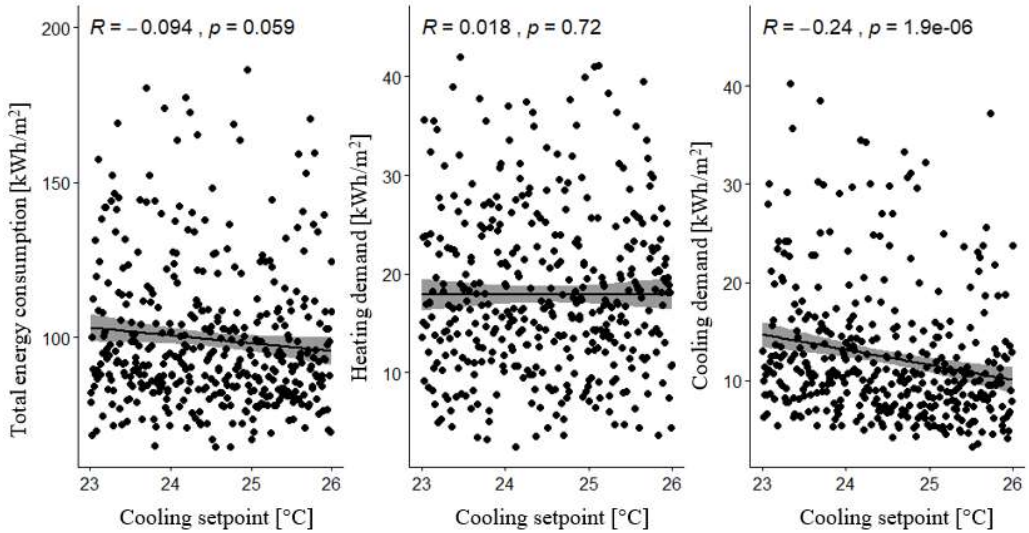


Figure 37. Scatter plots showing the correlation between cooling setpoint and total energy consumption, and heating and cooling demand.

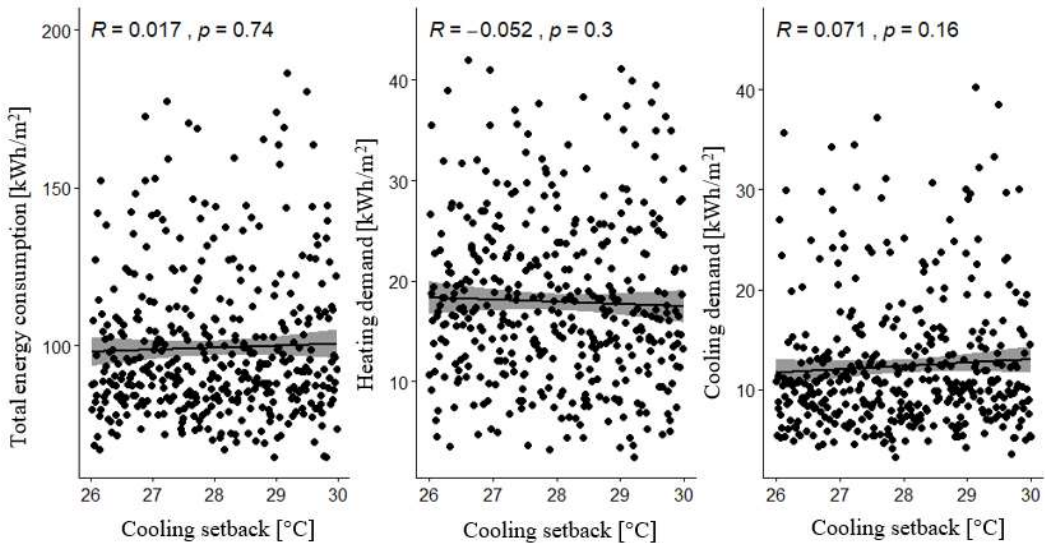


Figure 38. Scatter plots showing the correlation between cooling setback and total energy consumption, and heating and cooling demand.

Figure 39 presents the correlation level between the type of occupancy profile and the total energy consumption, and heating and cooling demand. Figure 39 below shows that there is no significant correlation between the occupancy profile type and the total energy consumption since p -value is equal to 0.22. Similarly, there is no correlation between the occupancy profile type and the heating and cooling demand. All the profiles had equal length of working hours and the only difference between them was the starting hour and the length of the lunch break.

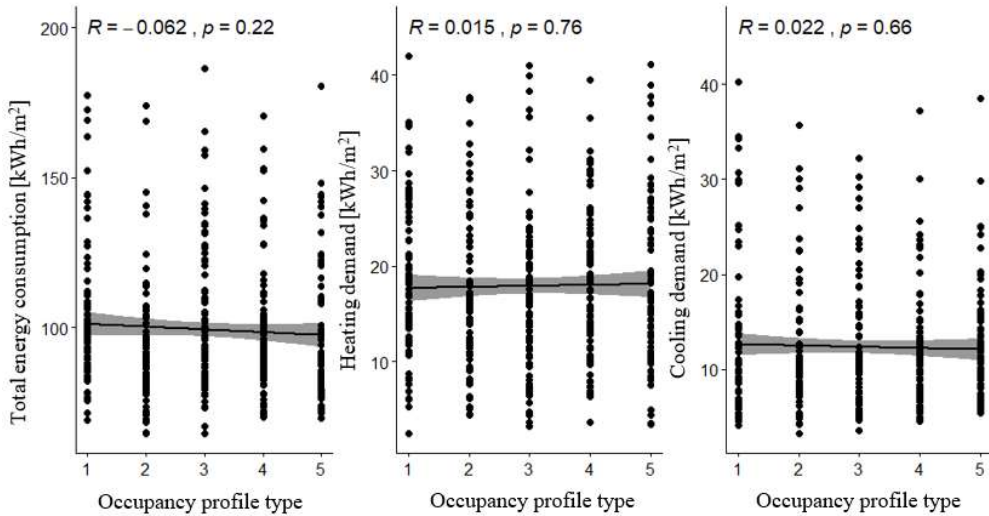


Figure 39. Scatter plots showing the correlation between the type of occupancy profile and total energy consumption, and heating and cooling demand.

Figure 40 shows the correlation between occupancy rate and the total energy consumption, and heating and cooling demand. The results show that the occupancy rate has more influence on the cooling demand in comparison to the heating demand. The significance of the correlation results between the occupancy rate and the heating demand is not statistically proven since p -value is equal to 0.086. Considering the total energy consumption, there is a moderate, negative correlation between the variables indicating that higher occupancy rate results in lower total energy consumption. Decrease of total energy is connected to the way in which occupancy rate was defined. In this thesis, occupancy rate is defined in term of m²/person. Hence, an increase in occupancy rate means lesser number of people in the building. Nevertheless, in a real case scenario, the occupancy rate is not a factor that can be controlled by the building design.

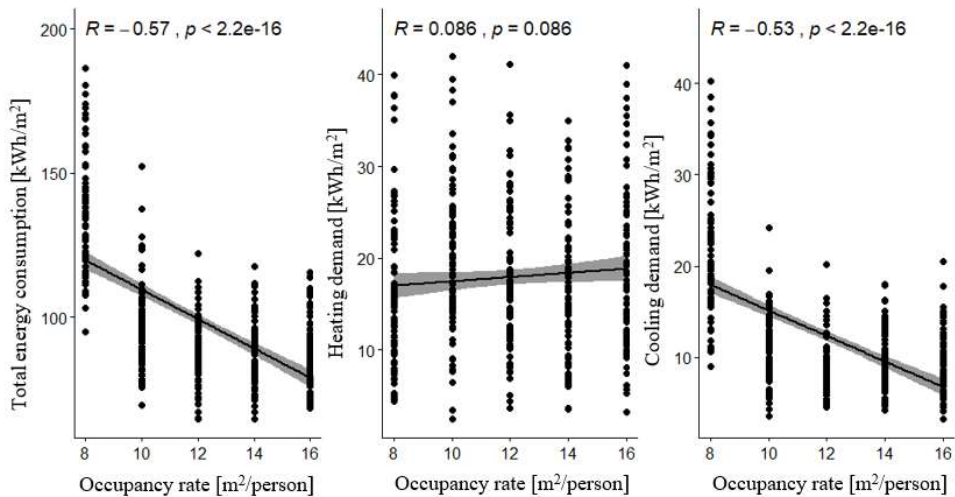


Figure 40. Scatter plots showing the correlation between occupancy rate and total energy consumption, and heating and cooling demand.

Figure 41 shows the correlation between the g -value of the window and the total energy consumption, and heating and cooling demand. Based on the figure, it can be concluded that g -value is positively correlated with cooling demand. This indicates that higher solar gains result in enhanced cooling demand of the building. The g -value is directly connected with the type of windowpane. Therefore, glazing should be chosen considering both energy consumption and daylighting. Due to the moderate level of correlation, g -value of window is considered one of the crucial factors affecting cooling demand. In terms of heating demand, higher g -value is beneficial in cooler climate (represented by the building case study), since higher solar gains positively contribute to the reduction of heating demand. In investigated in thesis building, g -value of the window had weak, positive correlation with the total energy consumption, represented by R equal to 0.1

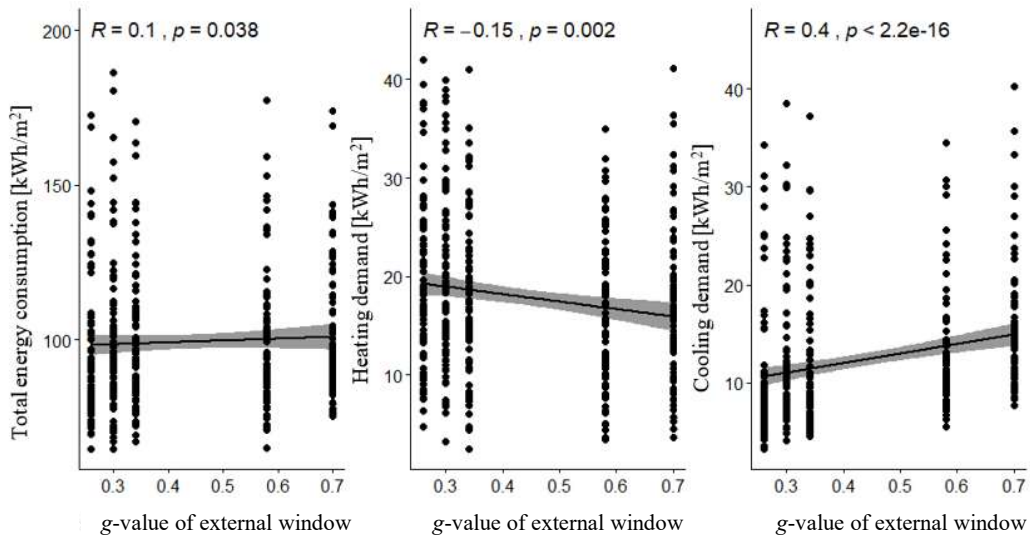


Figure 41. Scatter plots showing the correlation between g -value of window and total energy consumption, and heating and cooling demand.

Figure 42 presents the correlation between lighting gains and total energy consumption, and heating and cooling demand. Based on the figure, higher lighting gains lead to an increase in total energy consumption. Correlation between the total energy consumption and the lighting gains can be described as weak. Even though higher lighting gains contribute to lower heating demand in winter (minimal, negative correlation), less efficient lighting leads to higher electricity consumption in the building. Therefore, usage of the energy-efficient luminaries is recommended. There is no proven correlation between cooling demand and lighting gains in this case study since p -value is equal to 0.38.

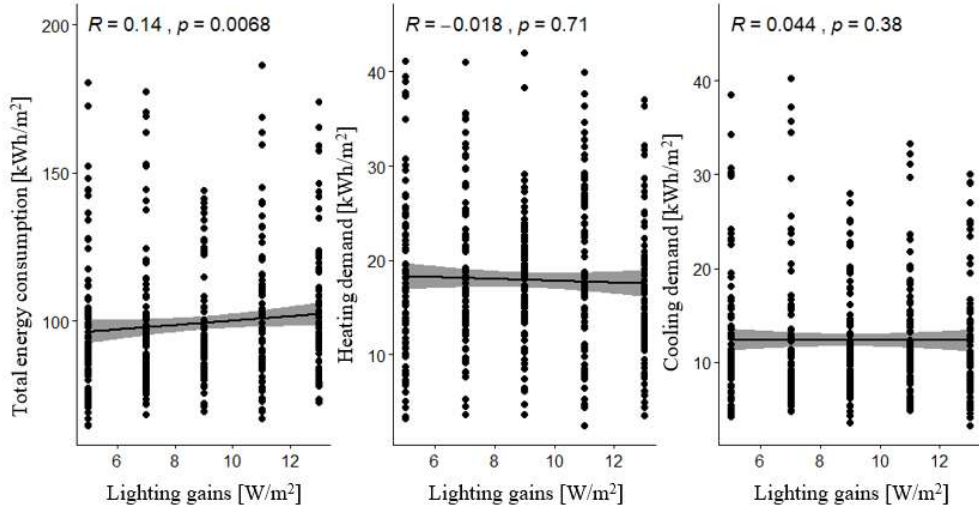


Figure 42. Scatter plots showing the correlation between lighting gains and total energy consumption, and heating and cooling demand.

Figure 43 shows the correlation between equipment gains and total energy consumption, and heating, and cooling demand. The figure presents that increase of equipment gains do not have a correlation with the cooling demand (85 % error margin on the rejection of null hypothesis, referring to Section 3.7). On contrary, there is weak, positive correlation between equipment gains and total energy consumption. The coefficient of the correlation between those two factors is equal to 0.2. Higher equipment heat gains lead to increased total energy consumption. There is no statistically proven correlation between heating demand and equipment gains.

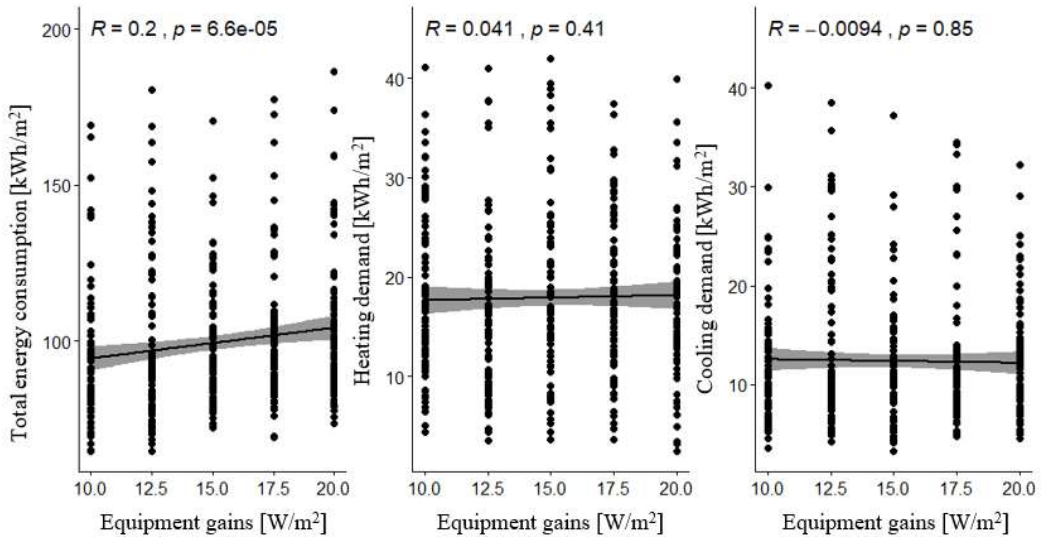


Figure 43. Scatter plots showing the correlation between equipment gains and total energy consumption, and heating and cooling demand.

In the following paragraphs, correlation results between building parameters and thermal comfort are presented and discussed. Thermal comfort in the building was evaluated in terms of the number of rooms complying with the requirements set in Section 3.3.2, including calculation of the maximum number of occupational hours per year where room operative temperature exceeds 26 °C and 27 °C. For office building types maximum 100 hours over 26 °C and 25 hours over 27 °C are acceptable. The scatter plots showing correlation between different independent parameters and number of complied rooms are presented in the following paragraphs.

Figure 44 presented below shows that the thickness of the insulation layers of opaque elements including the wall, roof, and floor, does not have a significant influence on the thermal comfort, due to the p -value over 0.05 in each studied case. Spearman's coefficient of correlation between the insulation thickness of each element and thermal comfort is close to 0, therefore there is no proven connection between the parameters.

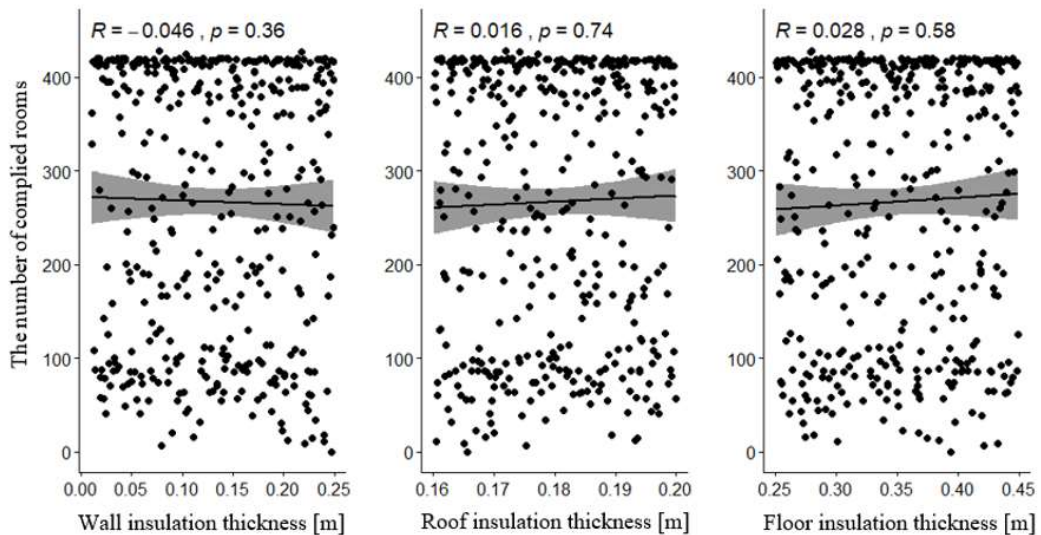


Figure 44. Scatter plots showing the correlation between the thickness of building envelope materials and thermal comfort.

Figure 45 shows the correlation between inlet air temperature, infiltration rate, auxiliary ventilation and the number of rooms complied with the thermal comfort standard set in Section 3.3.2. The figure shows that higher infiltration and auxiliary ventilation rates dramatically increase the number of rooms which are compliant with regulations, while higher inlet air temperature negatively impacts the number of rooms fulfilling set requirements. All the correlation results are statistically proven ($p < 0.05$) resulting in rejection of null hypothesis.

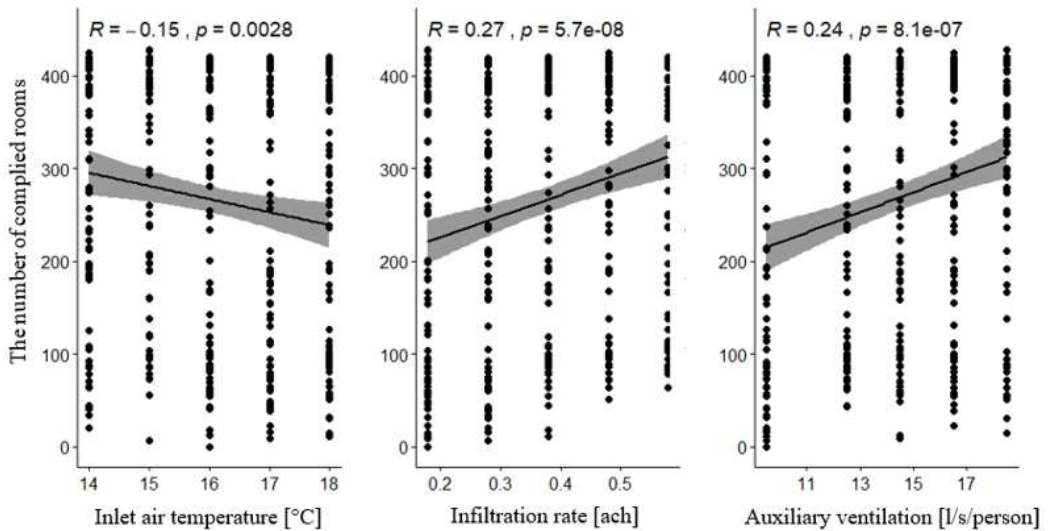


Figure 45. Scatter plots showing the correlation between inlet air properties and thermal comfort.

Figure 46 shows the correlation between heating and cooling setback / setpoint temperature and thermal comfort, described as number of rooms which are in compliance to standard from Section 3.3.2. Figure 46 figure demonstrates that the cooling setpoint temperature significantly affects the thermal comfort indices. The coefficient of correlation equal to -0.53 indicates moderate, negative correlation with thermal comfort. Based on the high correlation level between thermal comfort and cooling setpoint temperature, it can be argued that decreasing cooling setpoint temperature would significantly increase the number of rooms which are in compliance to standard from Section 3.3.2. There is no proven correlation (p -value over 0.05) between cooling and heating setback temperature and number of rooms complying with the thermal comfort requirements. Higher heating set point temperature results in minimal negative effect ($R = -0.077$) on the thermal comfort parameter. Nevertheless, significance of the correlation results between the heating setpoint temperature and thermal comfort is not statistically proven.

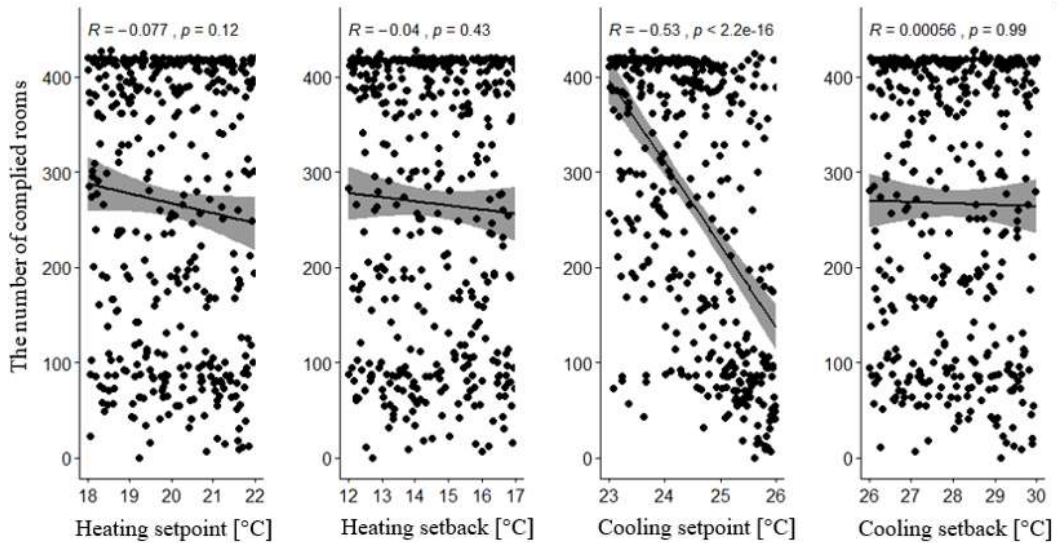


Figure 46. Scatter plots showing the correlation between setback / setpoints temperature and thermal comfort.

Figure 47 presents correlation occupancy profile type, occupancy rate, and thermal comfort, described as number of rooms which are in compliance with standard from Section 3.3.2. The figure below shows that the considered occupancy profile types and occupancy rates do not significantly influence on the number of rooms fulfilling the thermal comfort requirements. Very low correlation coefficient (R), followed by high margin of statistical error (significance level p over 0.05 for both cases), indicates that there is no correlation between the investigated parameters and thermal comfort.

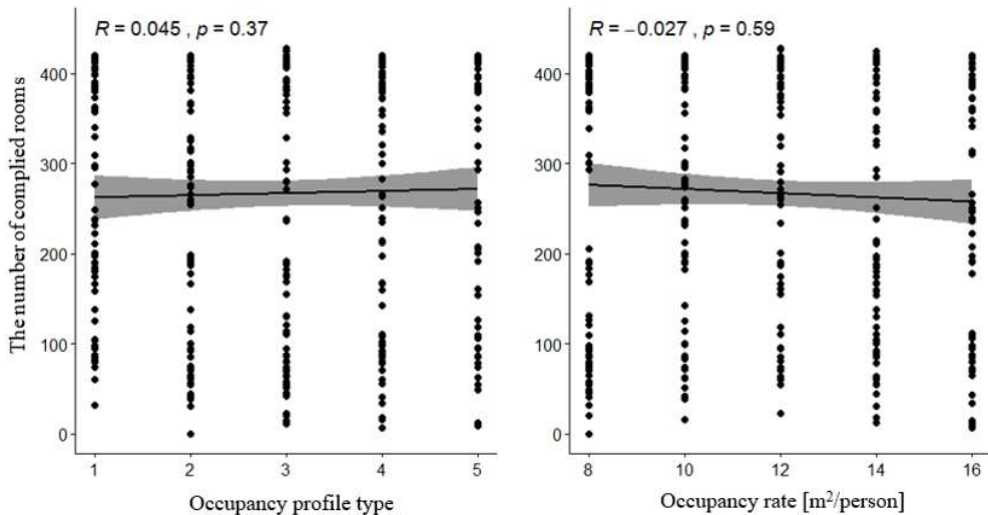


Figure 47. Scatter plots showing the correlation between type of occupancy profile / occupancy rate and thermal comfort.

Figure 48 presents the correlation between lighting gains, equipment gains, g -value of external windows and the number of rooms complied with the thermal comfort requirements from Section 3.3.2. The g -value of the window is highly correlated with thermal comfort. The lower the g -value, the lower solar gains are, which effectively leads to a higher number of rooms complying with thermal comfort requirements. On contrary, there is no statistically proven correlation between lighting / equipment gains and the thermal comfort, due to the p -value over 0.05 for both cases.

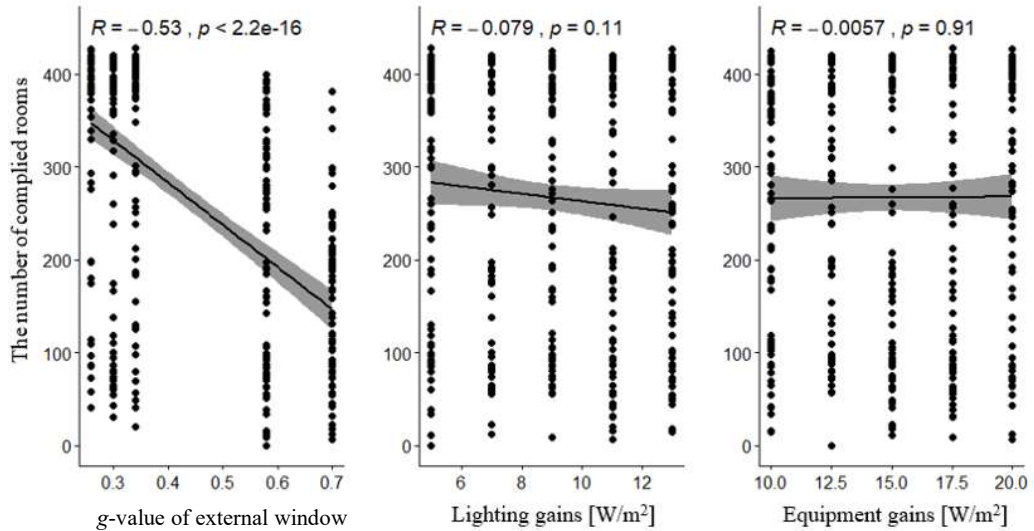


Figure 48. Scatter plots showing the correlation between window g -value, lighting gains, equipment gains, and thermal comfort.

Final evaluation of input parameters importance is based on calculated Spearman's correlation coefficient (R), summarized in Figure 49, Figure 50, Figure 51, and Figure 52. These figures provide an overview of different input parameters and total energy consumption, thermal comfort, heating demand, and cooling demand, respectively. The figures also show if the input variables are positively or negatively correlated. Based on the differences between the variables, ranking of the most important parameters in Table 20, clearly indicates which parameters should be prioritized in the optimization process of studied building. The first five most important input parameters for each output indicator have been shaded, to indicate the similarities and differences between different result indicators. Moreover, the cross method verification with standardized regression coefficient (SRRC) method provides the reliability of the results from the Spearman's method.

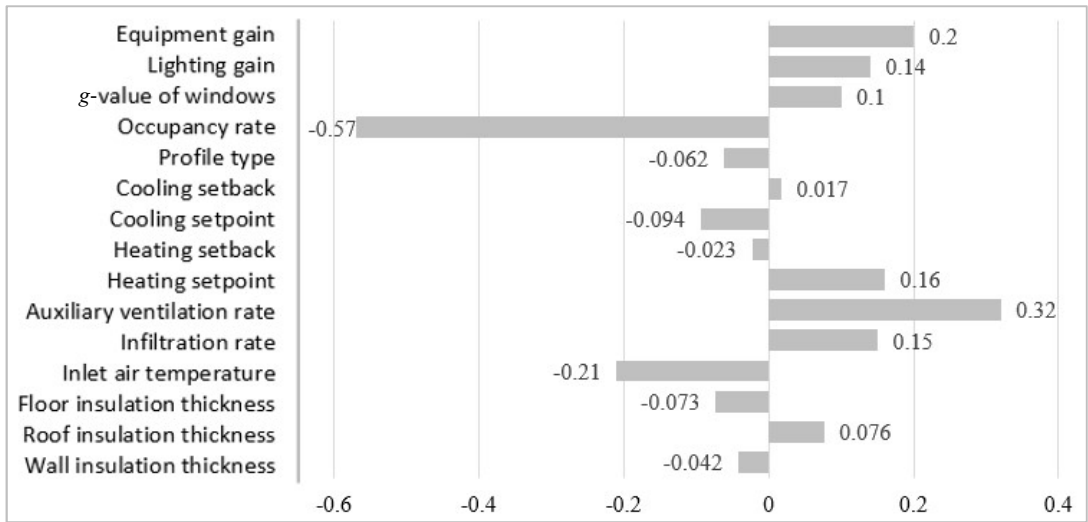


Figure 49. Spearman's coefficient of different input parameters for total energy consumption.

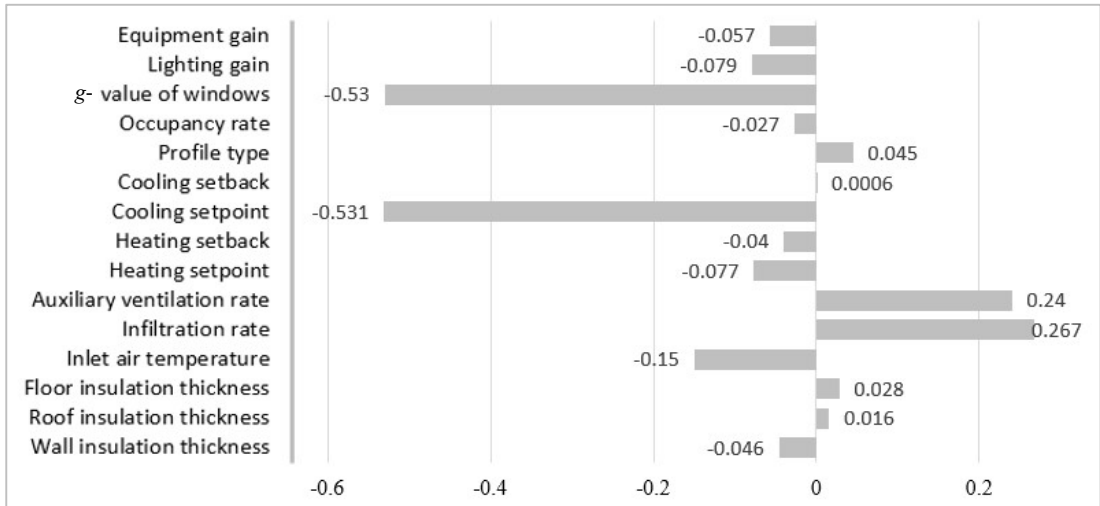


Figure 50. Spearman's coefficient of different input parameters for thermal comfort.

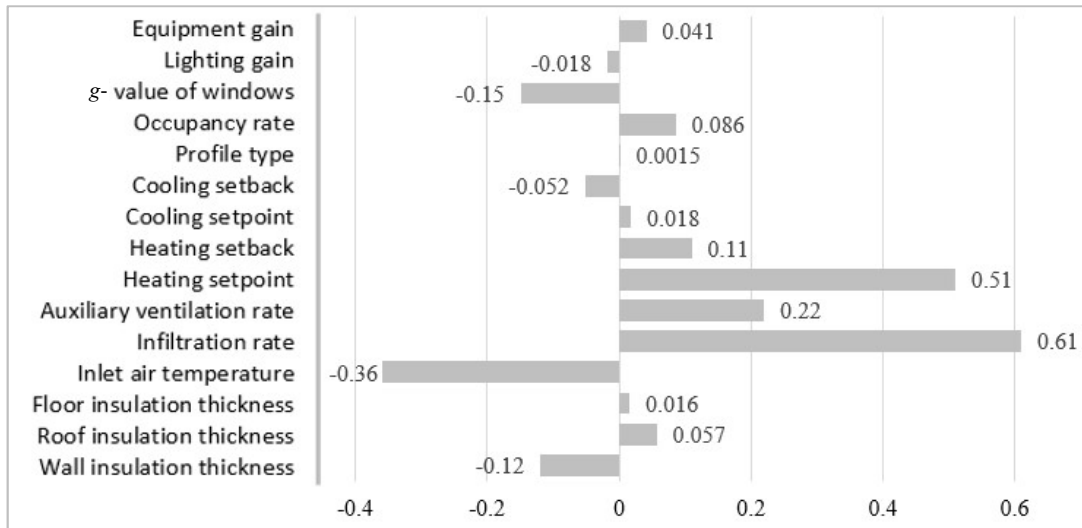


Figure 51. Spearman's coefficient of different input parameters for heating demand.

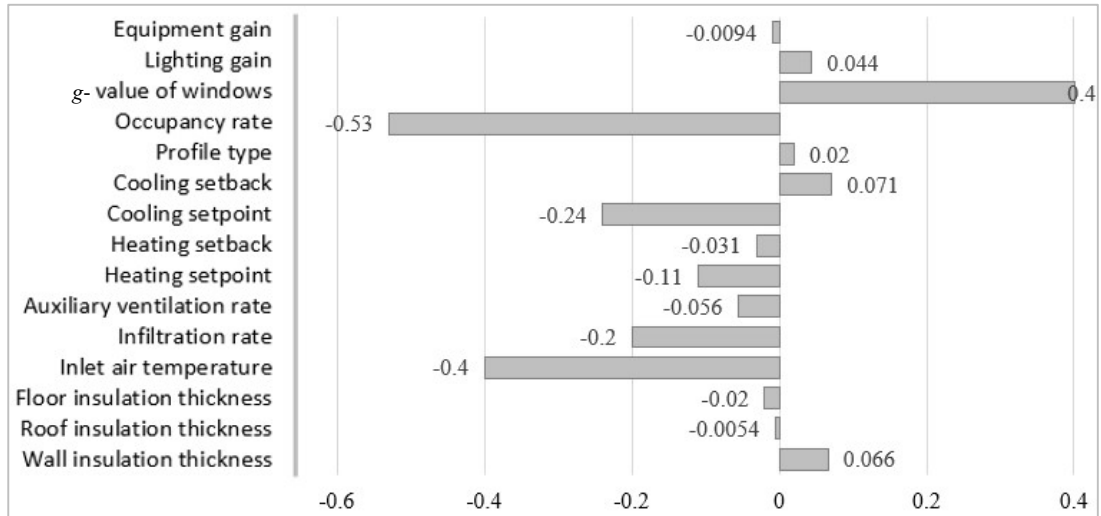


Figure 52. Spearman's coefficient of different input parameters for cooling demand.

Table 20 presents the ranking of the most important parameters in the optimization process of the initial design. The results from Table 20 show that input parameters affect the output indicators differently, especially between total energy consumption and thermal comfort criteria. For example, occupancy rate is strongly correlated to the total energy consumption, while it has relatively insignificant effect regarding the thermal comfort and heating demand. Window g-value and cooling setpoint appear to be the most important parameters with the strongest correlation to thermal comfort. These parameters also have high importance due to strong correlation with the cooling demand, whereas they are ranked in the middle among all the other input parameters affecting total energy consumption. Infiltration rate is important for summer thermal comfort evaluations in the studied building. On the contrary, it does not have high importance considering total energy consumption due to the weak correlation with the output parameter. Equipment gains have a high correlation level with the total energy

consumption, meanwhile considering heating demand, cooling demand and thermal comfort as separate indicators, importance of the parameter is disregarded. Lighting gains do not have an optimization priority in the studied building due to low correlation. Setback temperature show weak correlation with total energy consumption and thermal comfort, therefore, place towards the bottom of the importance ranking of those parameters. Profile type and insulation thickness of opaque construction show low to no correlation towards different result indicators, therefore, can be considered as less important parameters. Inlet air temperature has high importance for cooling energy demand. Variation in the total energy consumption results is mostly driven by occupancy rate, auxiliary ventilation rate, inlet air temperature, equipment gains, and heating setpoints. Therefore, they can be considered a priority for further optimization. Even though SRRC results are not fully consistent with Spearman's method, the first five most important parameters are common for both methods. Nevertheless, cooling setpoint, window *g*-value, and infiltration rate are of high importance towards the thermal comfort assessment, therefore should not be disregarded in the optimization process.

Table 20. Ranking of the most important parameters in the building optimization process.

Parameters / Ranking	Total energy consumption	Total energy consumption (SRRC)	Heating demand	Cooling demand	Thermal comfort
Occupancy rate	1	1	8	1	13
Auxiliary ventilation	2	2	4	9	4
Inlet air temperature	3	4	3	2	5
Equipment gains	4	5	11	14	8
Heating setpoint	5	3	2	6	7
Infiltration rate	6	6	1	5	3
Lighting gains	7	8	12	10	6
<i>g</i> -value of windows	8	7	5	2	2
Cooling setpoint	9	9	12	4	1
Roof insulation thickness	10	11	9	15	14
Floor insulation thickness	11	14	14	12	12
Occupancy profile type	12	12	15	12	10
Wall insulation thickness	13	10	6	8	9
Heating setback	14	15	7	11	11
Cooling setback	15	13	10	7	15

4.1.2 Daylight

This section presents the sensitivity analysis results of the parameters affecting daylight in the base case building. In order to determine type of function obtained from simulation results, scatter plots for Pearson method were plotted. Unfortunately, due to the nature of the data, graphical interpretation alone was not enough to determine the type of model represented by the samples. Therefore, Pearson's coefficient of determination (R^2) as presented in Table 21 was calculated. All the results presented in this chapter are based on the data from high-quality settings simulations.

Table 21. Comparison of Spearman's and Pearson's coefficients.

Parameter / value	Pearson			Spearman	
	p	R	R^2	p	R
Wall Reflectance	3.73e-16	0.380	0.144	2.2e-16	0.560
T_{vis}	2.2e-16	0.680	0.462	2.2e-16	0.690
Floor Reflectance	0.032	0.160	0.025	0.400	0.063
Ceiling Reflectance	0.520	0.047	0.002	0.028	0.160

The calculated Pearson's coefficient of determination (R^2) for different parameters was presented in Table 20. As $R^2 < 0.5$, it was deduced that datasets do not represent linear behavior, due to the unsatisfactory performance of the investigated model. Hence, Spearman's rank correlation method was used for final evaluation of the data.

Figure 53 and 54 present the correlation between reflectance's of different surfaces, T_{vis} and $sDA_{300,50}$. It can be seen that visible transmittance (representing different window types), wall and ceiling reflectance's results were statistically significant. For T_{vis} and wall reflectance p is below 1 %, indicating that there is a strong or moderate correlation between the parameter and $sDA_{300,50}$ results. Ceiling reflectance results have 97.2 % significance with $p = 0.0028$, the low R -value means a very weak level of correlation.

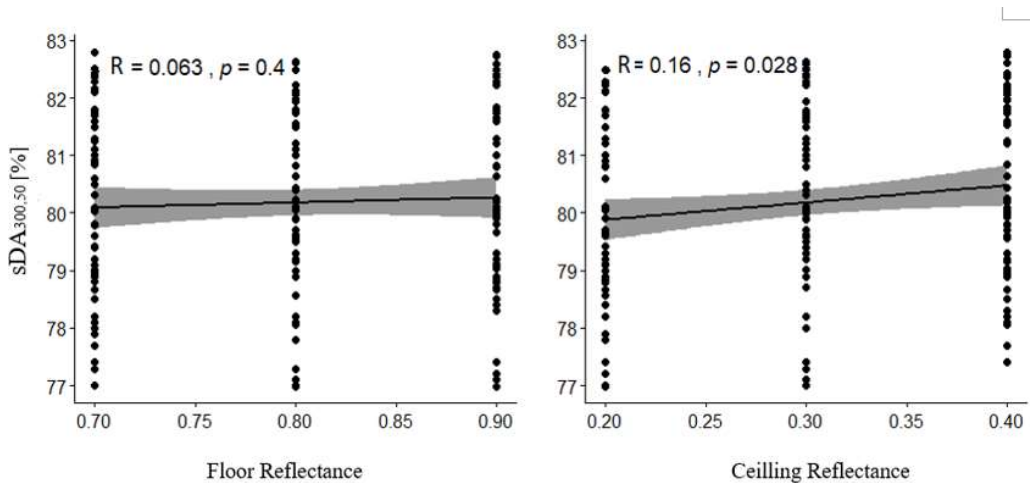


Figure 53. Scatterplot showing the correlation between floor reflectance, ceiling reflectance, and spatial daylight autonomy.

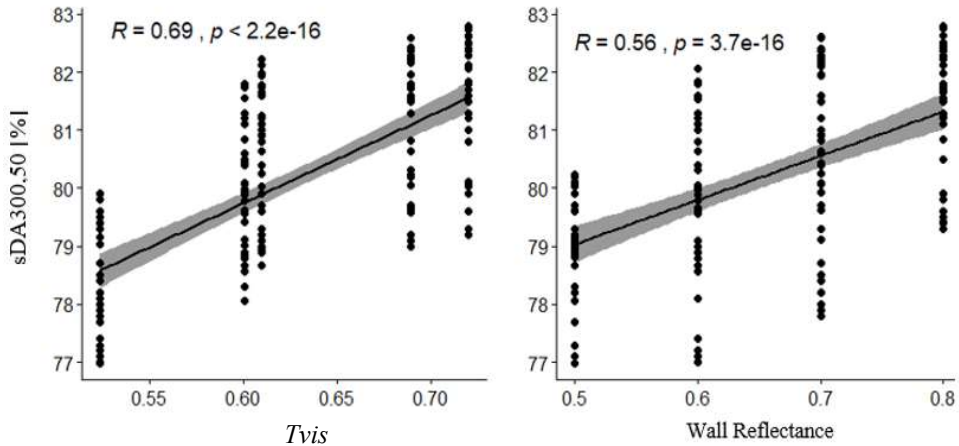


Figure 54. Scatterplot showing the correlation between reflectance of wall and T_{vis} of different window types and spatial daylight autonomy.

Table 22 presents the ranking of investigated independent variables based on calculated Spearman's rank calculation coefficient and standardized rank regression coefficient (SRRC). Based on the parameters ranking shown in Table 22, it can be deduced that the window type effectively increases the $sDA_{300,50}$, whereas reflectance of floor does not have any impact on the results. The reflectance of the wall plays a role in the distribution of light in the investigated space since increase of the reflectance value results in the increase of $sDA_{300,50}$. The wall reflectance has positive correlation with $sDA_{300,50}$, however level of association can be described as moderate. Ceiling reflectance has a weak correlation with the $sDA_{300,50}$. Based on the analysis of SRRC and Spearman's method, it is deduced that type of the window should be the priority in the early design stage, whereas wall reflectance can have moderate importance for the results.

Table 22. Ranking of coefficients affecting daylight.

Parameters	Significance level (represented by p)	Ranking Spearman's method	Level of association (represented by R)	Ranking according to SRRC method
T_{vis}	Strong- null hypothesis rejected	1	Strong, positive correlation	1
Wall Reflectance	Strong- null hypothesis rejected	2	Moderate, positive correlation	2
Ceiling Reflectance	Strong- null hypothesis rejected	3	Weak, positive correlation	3
Floor Reflectance	Failed to reject null hypothesis	4	Negligible, no association	4

4.2 Uncertainty analysis

4.2.1 Energy & Thermal comfort

One of the key problems when simulating building energy consumption is the lack of reliable information regarding the building envelope, detailed system design and users' behaviour. The uncertainty of total energy consumption results, heating demand results, and cooling demand results were plotted in form of histograms in Figure 55, 56 and 57, respectively. The figures represent the density of result occurrences over investigated population. The summary of uncertainty analysis is presented in Table 23.

Table 23. Summary of the data.

Output parameter	Median	Mean	Standard deviation	Minimum	Maximum
Total energy consumption [kWh/m ²]	92.7	99.4	23.1	64.9	186.4
Heating demand [kWh/m ²]	16.9	17.9	8.2	2.5	41.9
Cooling demand [kWh/m ²]	10.6	12.3	6.7	3.3	40.3
Thermal comfort (Number of rooms complied)	301.5	267.1	143.6	0	429

The density plots help to visualize the distribution of data over the whole range of the results. Based on the results of the whole design space presented in Figure 55 - 57 and Table 23, the results of total energy consumption, heating demand, and cooling demand are concentrated between 99 ± 23 kWh/m², 18 ± 8 kWh/m², and 12 ± 7 kWh/m², respectively. The density of sub-ranges regarding energy demand is normally distributed as there is only one obvious peak in the trendlines. The normal distribution also implies that the median values will be close to the mean values.

The number of rooms which complied with the thermal comfort standard have bimodal distribution (2 peaks). The median value is far from the mean, which indicates that the mean, median, and standard deviation values can be misleading when predicting the concentration. Figure 58 shows that density columns vary between 0 - 429 rooms. However, it has a peak between 410 - 420 rooms. This means that some specific building parameters in certain ranges affect thermal comfort.

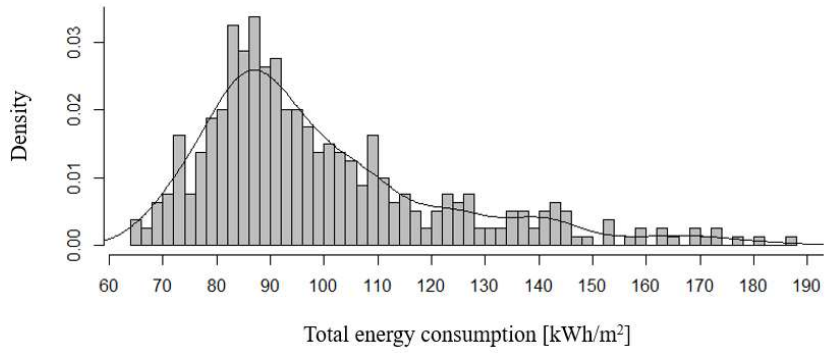


Figure 55. Density plot for total energy consumption results based on 400 simulated samples.

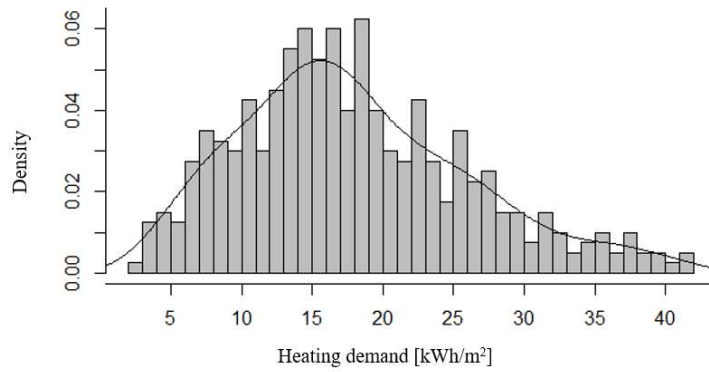


Figure 56. Density plot for heating demand results based on 400 simulated samples.

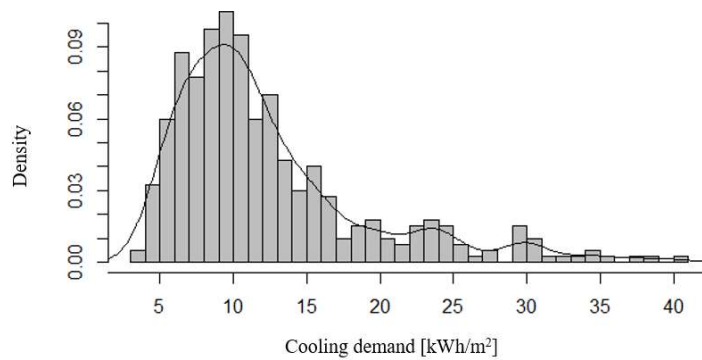


Figure 57. Density plot for cooling demand results based on 400 simulated samples.

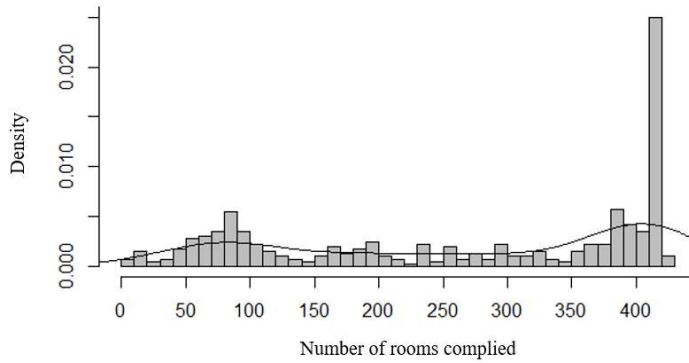


Figure 58. Density plot of results representing the number of rooms complying with requirements set in thermal comfort section (Less than 100 hr in period from April to October, with operative temperature exceeding 26 °C).

The following paragraphs present favourable ranges of input under different filters. The most favourable ranges of input were identified using a three-step procedure. Firstly, 117 samples corresponding to total energy below 85 kWh/m² were taken. Then the density of each sub-ranges was plotted in form of the histograms. Secondly, 118 samples corresponding to over 400 rooms complied with thermal comfort standards were selected. Then histograms were made to present the density of each subrange. In the end, applying both filters at the same time, resulted in identification of the 8 % best performing results (31 samples). In these figures, the input values with higher densities yield the favourable ranges of input, and therefore it can provide the suggestions for the latter design stage.

Figure 59 shows that there is no obvious pattern of favorable input ranges when considering total energy consumption or thermal comfort separately. However, wall insulation thickness between 0.10 - 0.15 m yields better performance when considering both thermal comfort and energy savings.

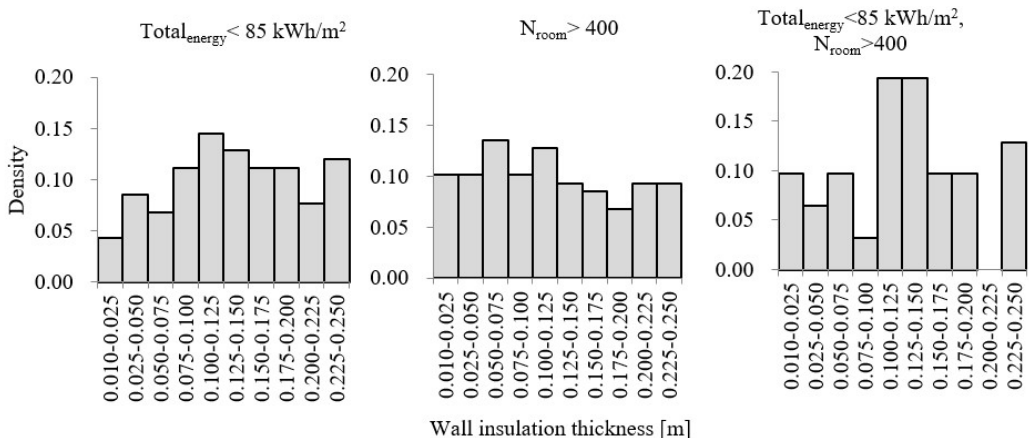


Figure 59. Favorable input ranges for wall insulation thickness in 117, 118, and 31 samples.

In Figure 60, no obvious pattern of favorable input ranges was observed when total energy consumption and thermal comfort criteria were applied separately. Nevertheless, roof insulation thickness between 0.160 - 0.165 m; 0.170 - 0.175 m and 0.195 - 0.200 m had the

highest density of occurrence when the criteria for thermal comfort and total energy consumption were applied simultaneously.

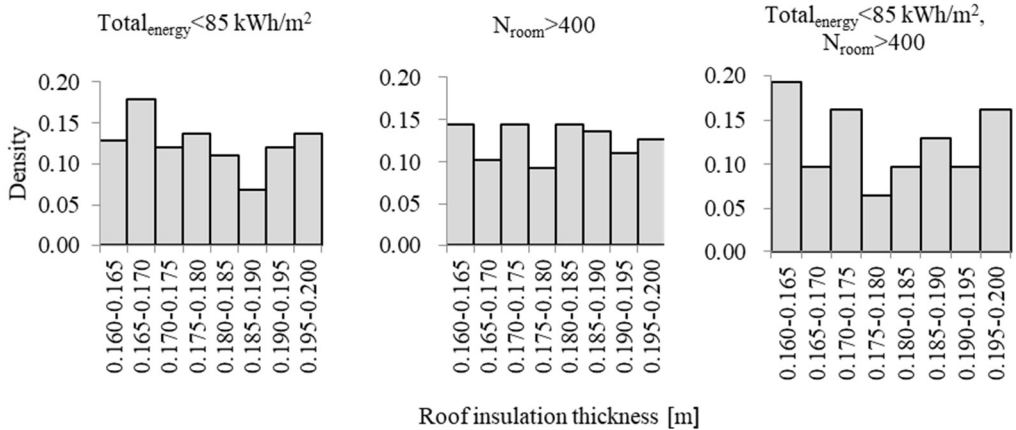


Figure 60. Favorable input range for roof insulation thickness in 117, 118, and 31 samples.

Figure 61 shows that it can be concluded that thicker insulation will be preferred regarding lower energy consumption, while thinner insulation could bring the benefit of having more rooms complied with BR18 [1]. However, floor insulation thickness between 0.350 - 0.375 m had the highest density of occurrence when the criteria for thermal comfort and total energy consumption were applied together.

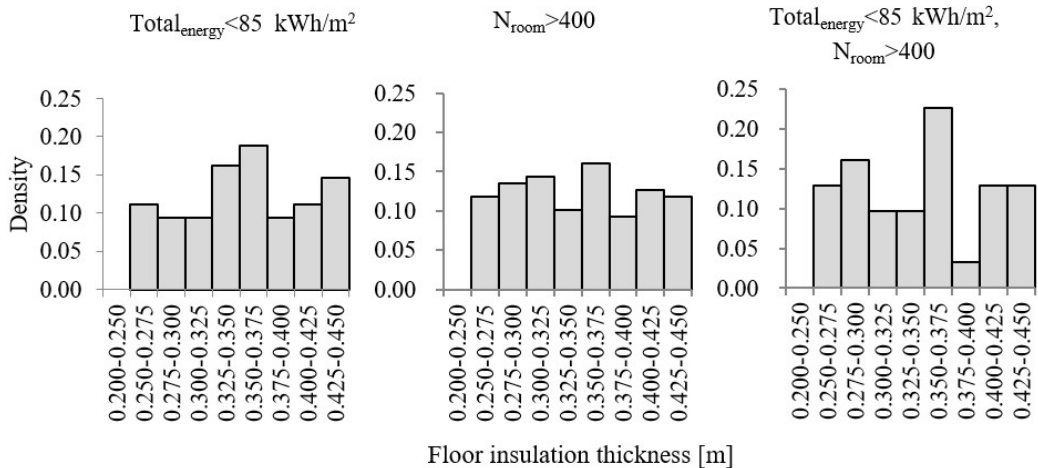


Figure 61. Favorable input range for floor insulation thickness in 117, 118, and 31 samples.

Patterns from Figure 62 below show that higher inlet air temperature is preferable for lower total energy consumption, while it is undesirable for avoiding the overheating issues. The inlet temperature of 16 °C and 18 °C have the highest occurrence when both criteria were applied together. However, since this model had generic HVAC system, detailed HVAC design is required for further verification of the favourable input ranges.

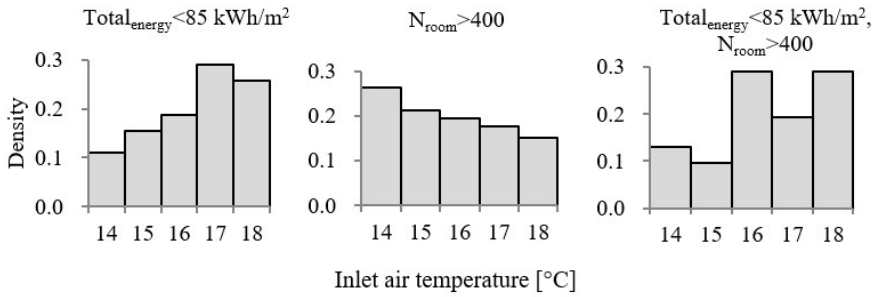


Figure 62. Favorable input range for inlet air temperature in 117, 118, and 31 samples.

Figure 63 shows the overall patterns are contradictory when the two criteria for total energy consumption and thermal comfort were applied separately. However, the distribution of density becomes uniform when two criteria were applied together. In this study, thermal comfort was analysed only between April to October. Therefore, if winter thermal comfort is concerned, low infiltration rate should be targeted. This is due to that higher infiltration rate will lead to winter discomfort [57]. This always requires a higher quality of construction and implementation of impermeable materials.

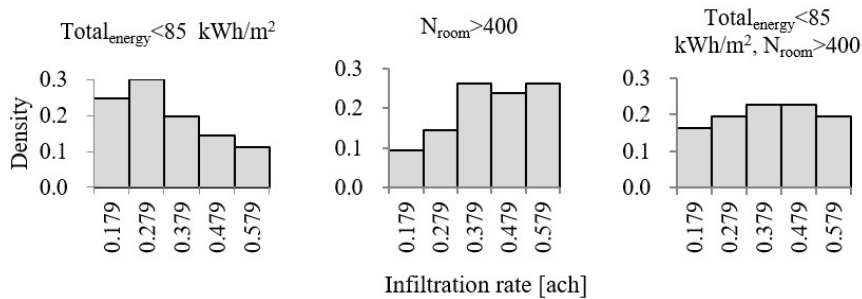


Figure 63. Favorable input range for infiltration rate in 117, 118, and 31 samples.

Similar to air inlet temperature and infiltration rate, favourable ranges for auxiliary ventilation rate is opposite when two criteria of energy consumption and thermal comfort are applied separately, which is illustrated in Figure 64. However, auxiliary ventilation of 9.5 l/s/person gives the highest probability of low energy consumption and reduced overheating problem in the studied case. The decision process of optimizing auxiliary ventilation rate should take account ventilation system standards, purpose of the building and client's wishes.

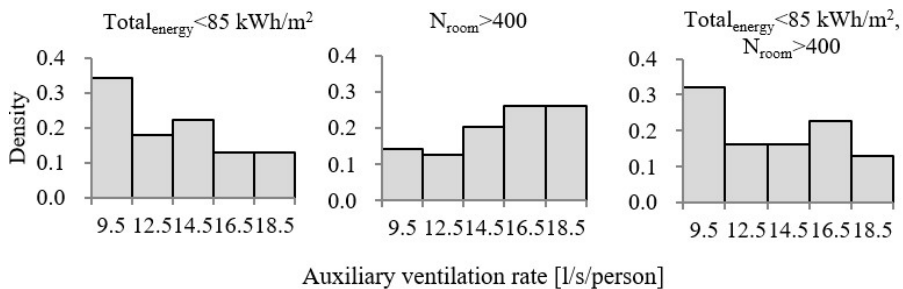


Figure 64. Favorable input range for auxiliary ventilation rate in 117, 118, and 31 samples.

Figure 65 suggests that a lower heating setpoint temperature is preferable for lower total energy consumption, whereas there is no obvious pattern regarding thermal comfort. Concluding general data pattern, it is recommended to lean towards the lower range of investigated setpoints in comparison to higher values. Nevertheless, heating setpoint temperature between 19.5 - 20 °C provide best overall performance when both criteria are considered together.

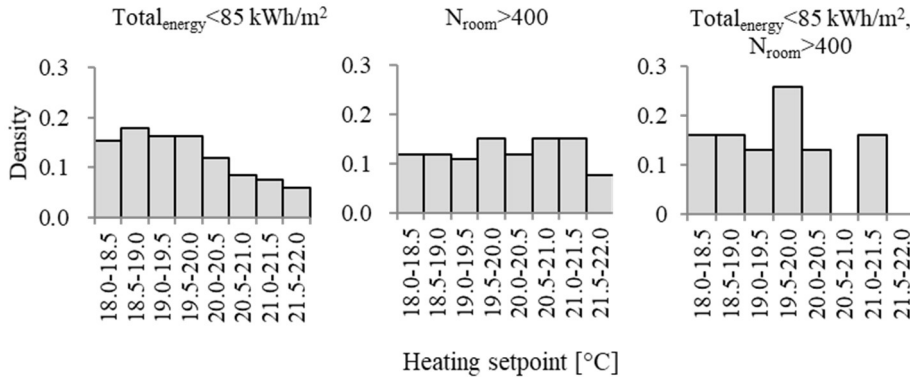


Figure 65. Favorable input range for heating setpoint in 117, 118, and 31 samples.

It can be seen from Figure 66 that heating setback temperature in the range of 14 - 15 °C is most suitable when both criteria are considered. However, sensitivity analysis indicated that the heating setback temperature had a relatively low Spearman's coefficient. Therefore, this parameter should not be a design priority.

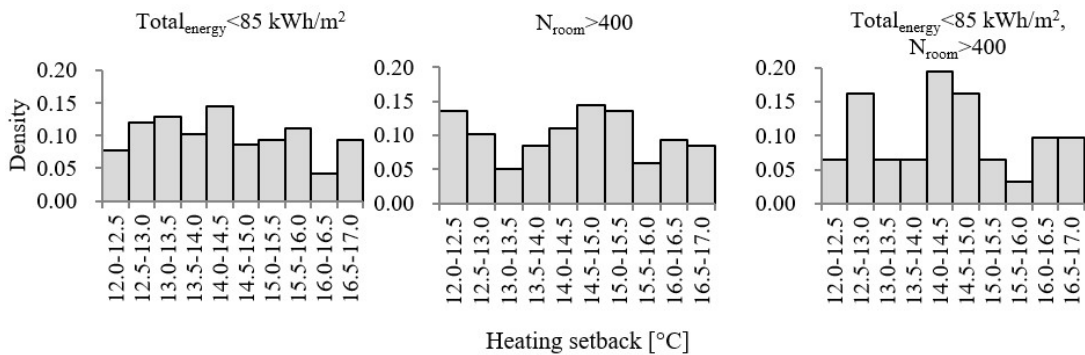


Figure 66. Favorable input range for the heating setback in 117, 118, and 31 samples.

Figure 67 indicates that lower cooling setpoint significantly reduces the number of rooms with overheating problem. However, there is no distinctive range of favourable cooling setpoints affecting total energy consumption. After applying filters for both categories, cooling setpoint temperature between 23 - 24 °C is formed to be the most favorable range.

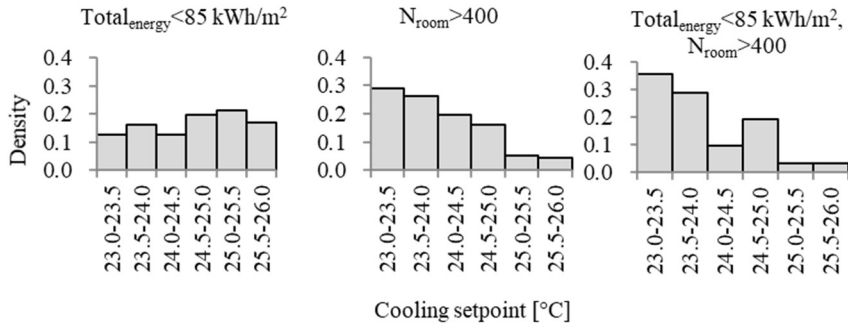


Figure 67. Favorable input range for cooling setpoint in 117, 118, and 31 samples.

As can be seen from Figure 68, thermal comfort is not affected by any particular range of cooling setback temperature. However, cooling setback temperature ranges of 26 - 26.5 °C and 27.5 - 28 °C are most suitable for total energy. Nevertheless, after applying both filters of energy consumption and thermal comfort, a cooling setback temperature of 27.5 - 28 °C turns out to be the most optimal range.

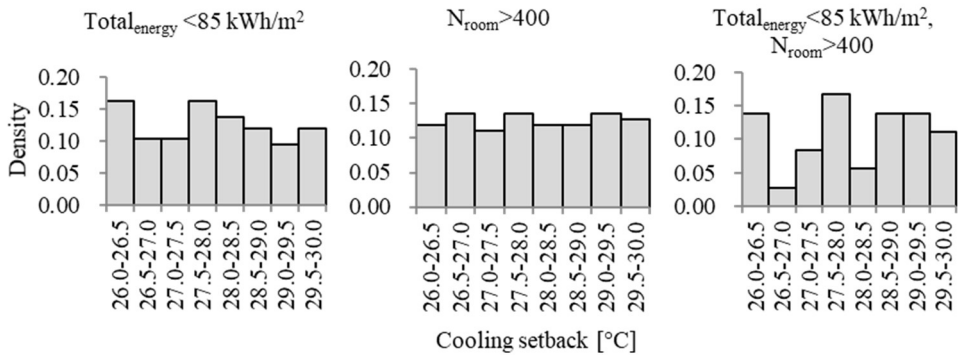


Figure 68. Favorable input range for cooling setback in 117, 118, and 31 samples.

As shown in Figure 69 occupancy profile number 5, corresponding to working hours starting from 8:30 with a two-hour lunch break, provides the most optimal solutions. Nevertheless, detailed investigation of profile type connected with electrical lighting consumption is recommended.

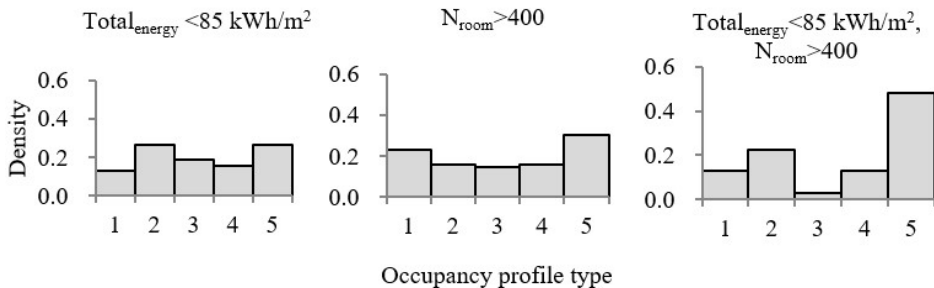


Figure 69. Favorable input range for occupancy profile type in 117, 118, and 31 samples.

As initially expected, higher occupancy rate is directly linked to the lower total energy consumption in the building (Figure 70). Nevertheless, buildings are designed for fixed amount of people. Modification in occupancy rate would be valuable when analyzing different alterations of building layouts.

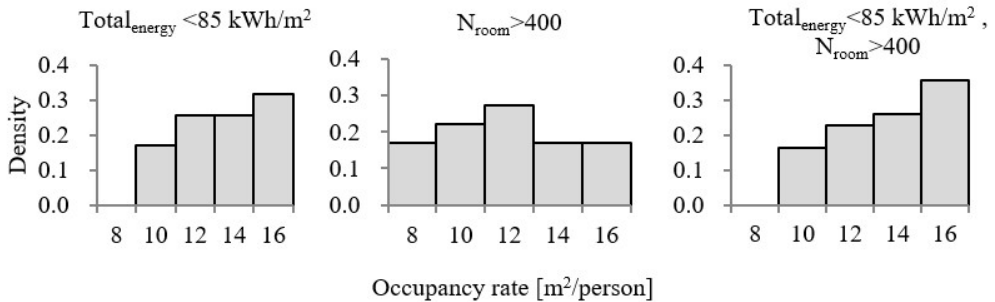


Figure 70. Favorable input range for occupancy rate in 117, 118, and 31 samples.

According to Figure 71, in order to avoid overheating issues, higher g -values such as 0.58 and 0.7 are not favourable. Window g -value does not have a big difference in density regarding total energy consumption. This implies that lower g -values are recommended when considering both total energy consumption and thermal comfort. Window with g -value of 0.26 performed the best in terms of energy and thermal comfort. However, before the final selection of the window, daylight performance of pre-specified types should be investigated.

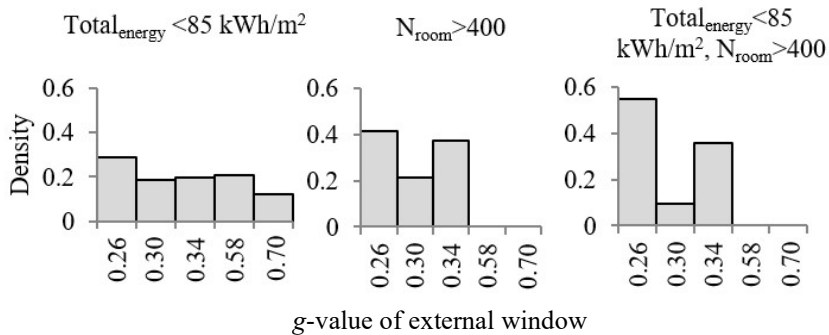


Figure 71. Favorable input range for g -value of the window in 117, 118, and 31 samples.

Figure 72 shows that lighting gains of 7 W/m² occur the most in the population of samples when two criteria are added together. Even though the correlation between lighting gains and total energy places the variable in the middle of the ranking, energy-efficient lighting is recommended.

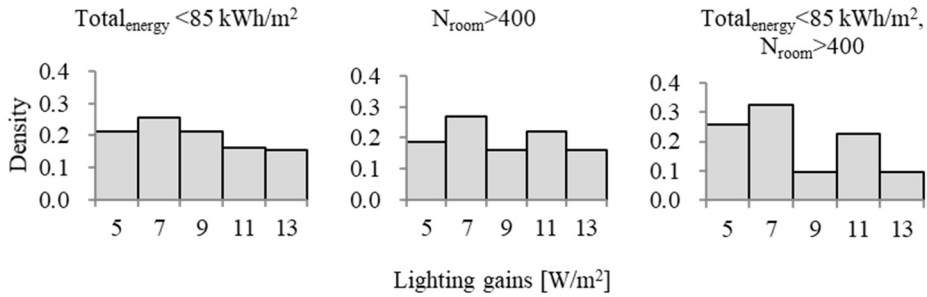


Figure 72. Favorable input range for lighting gains in 117, 118, and 31 samples.

Figure 73 indicates that different equipment gains result in almost the same number of samples when the criterion of thermal comfort is applied. On the other hand, lower lighting gains result in the largest number of samples meeting the criterion of energy consumption below 85 kWh/m². Based on the density of occurrence, equipment gains of 12.5 W/m² result in the highest number of samples meeting both criteria.

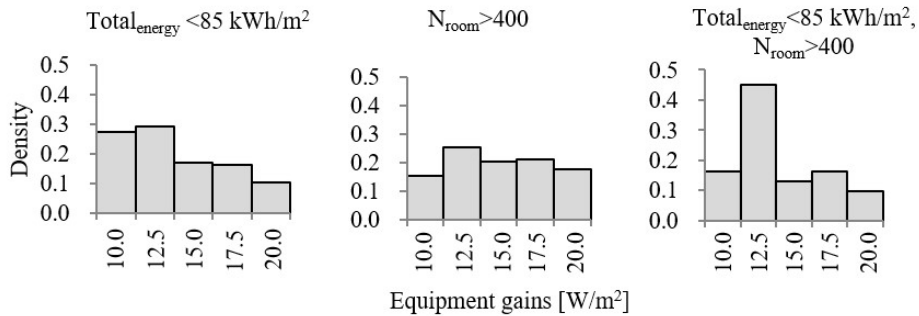


Figure 73. Favorable input range for equipment gains in 117, 118, and 31 samples.

To sum up, uncertainty analysis defined the predicted spans of total energy consumption based on the variations in the input parameters. Moreover, input ranges for each design variable, based on the density of occurrence in the filtered best 8 % of the total results have been analyzed. Before proceeding with the overall recommendations for the whole building, sensitivity and uncertainty analysis of daylight variables will be presented, followed by the final solution.

4.2.2 Daylight

Study of 400 samples representing different design solutions, included 180 variations of inputs affecting spatial daylight autonomy. The study was conducted to investigate the distribution of predicted values of sDA_{300,50}. The analysis was undertaken for all uncertain input parameters discussed in the methodology chapter.

Table 24 shows that all samples present satisfactory performance in terms of the spatial daylight autonomy. All samples fulfill the requirements set in Section 3.3.1. Worst case scenario resulted in 76.98 % of the area receiving light over 300 lux in 50 % of the working area for minimum half of the daylight hours. The low value of the standard deviation means that most of the simulated samples are close to the mean value of 80.17 %.

Table 24. Uncertainty Results parameters for sDA_{300,50} output.

Output parameter	Median	Mean	Standard deviation	Minimum	Maximum
sDA _{300,50} [%]	80.55	80.17	1.53	76.98	82.8

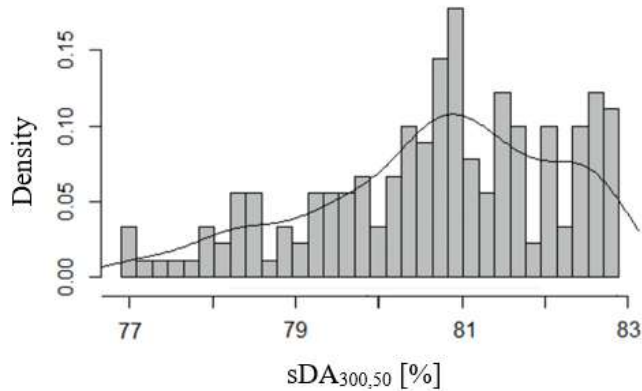


Figure 74. Density plot representing the distribution of Spatial Daylight Autonomy results in simulated population.

According to Figure 75 and Figure 76, higher reflectance of surfaces results in a greater number of samples meeting the criteria of 82.27 %. Ceiling reflectance of 0.9 and floor reflectance of 0.4 occurred most often in the population of samples. However, referring back to the sensitivity analysis results, it is important to understand the level of correlation between dependent and independent variable, therefore floor reflectance does not significantly affect daylight.

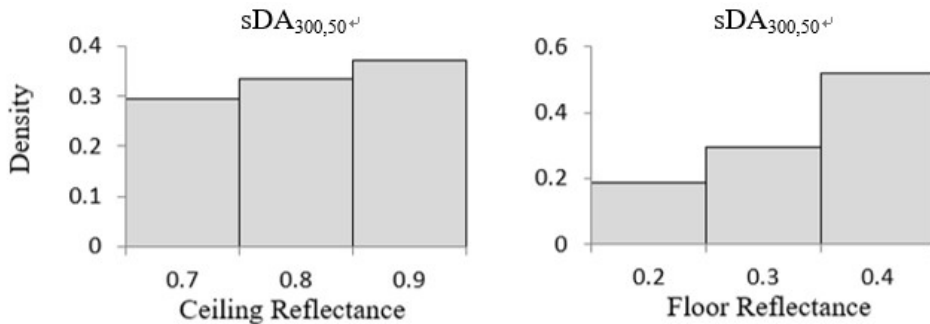


Figure 75. Favorable input ranges for ceiling and floor reflectance, meeting the criterion of sDA over 82.27 %.

Figure 76 shows that window type with visible transmittance of 0.72 performed the best in terms of daylight. Nevertheless, multi-variate assessment (especially for window type parameter) requires further analysis including both energy and thermal comfort performance. Concerning the wall reflectance, surfaces with the reflectance of 0.8 perform the best.

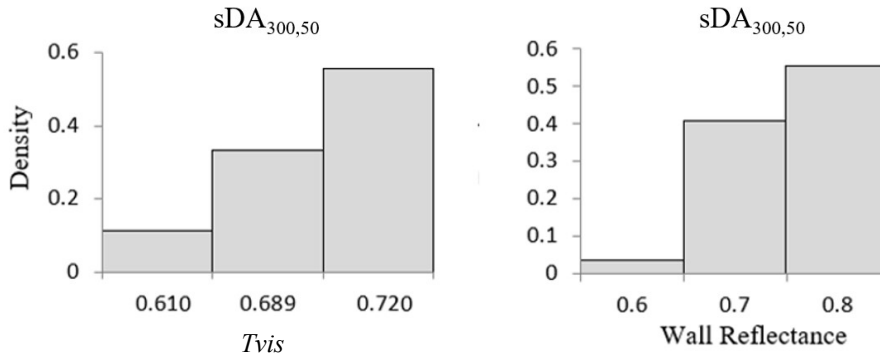


Figure 76. Favorable input ranges for wall reflectance and window T_{vis} , meeting the criterion of sDA over 82.27 %.

4.3 Overall Results

Five parallel coordinate plots (PCP) were generated in Design explorer by applying different filtering criteria. Figure 77 shows PCP for 400 samples. Figure 78 presents the best-performing samples generated by applying a filter of total energy consumption lower than 85kWh/m^2 . It can be seen that the distribution of remaining samples was concentrated around lower infiltration values, lower auxiliary ventilation rate, lower heating setpoint temperature and higher inlet air temperature. These findings verify the results of sensitivity and uncertainty analysis presented before. However, the preferred inputs for some building parameters, such as cooling setpoint temperature and window types, cannot be clearly seen.

Figure 79 presents the best-performing samples generated by applying the second filter representing number of rooms complied with standard from Section 3.3.2 ≥ 400 . In general, the revealed input spans are the same as the results derived from the uncertainty analysis. For example, the lower values within the span of the heating setpoint temperature and cooling setpoint temperature are preferable. Besides, the distributions of lower ventilation rate, higher infiltration rate, and higher cooling setback temperature results are denser. In addition, as seen from Figure 79, window type of 1 and 2 which had g -values of 0.58 and 0.70 should not be chosen. Besides, it can be also observed that occupancy profile 3 is not favourable.

Finally, samples with $sDA_{300,50}$ over 82.27 % were selected. Remaining samples presented in Figure 80, were coherent with the performed uncertainty and sensitivity analysis, suggesting higher reflectance of the surfaces especially for the ceiling and the wall. However, the clear pattern for the floor reflectance could not be observed. Figure 81 presents the final, optimized multivariate solution .

Therefore, to conclude, PCP can quickly illustrate the preferable input ranges and can rapidly exclude some design options, for example, window type 1 and 2 could be neglected. However, further analysis will be required when preferred input ranges can not be clearly identified. Density plots can be one solution. Nevertheless, generating parallel coordinate plots in Design Explorer is suggested for consultants, since it is an easy and quick way to give a sense of overall results.

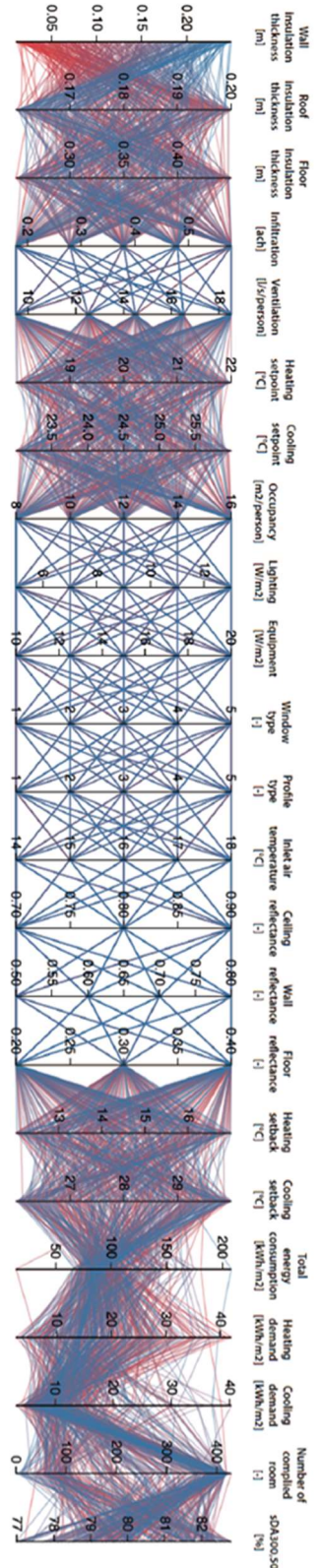


Figure 77. Parallel coordinate plot for 400 samples.

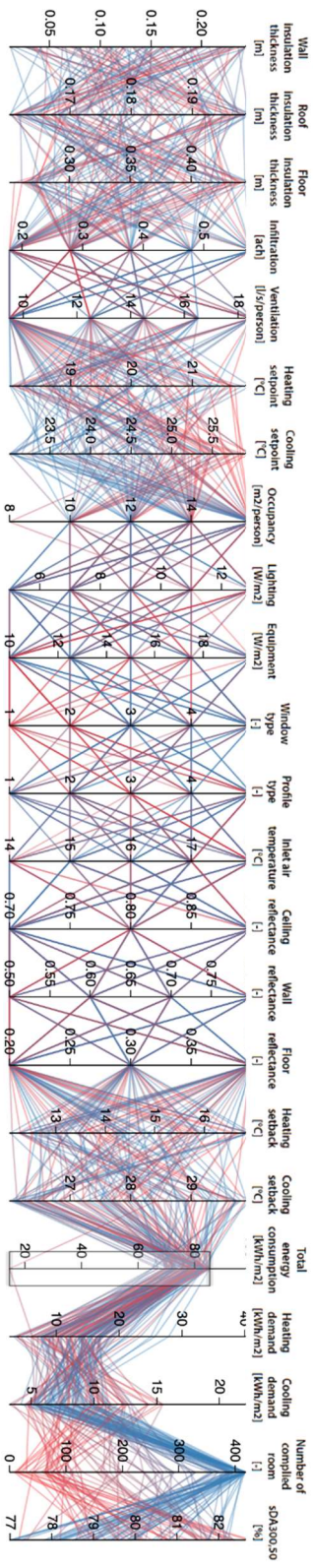


Figure 78. Parallel coordinate plot for remaining samples after adding the first filter.

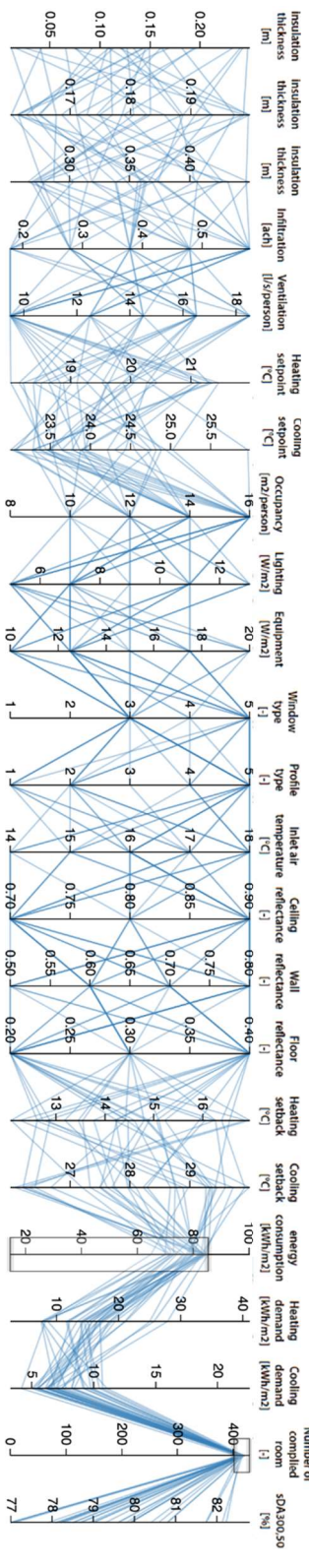


Figure 79. Parallel coordinate plot for remaining samples after adding the second filter.

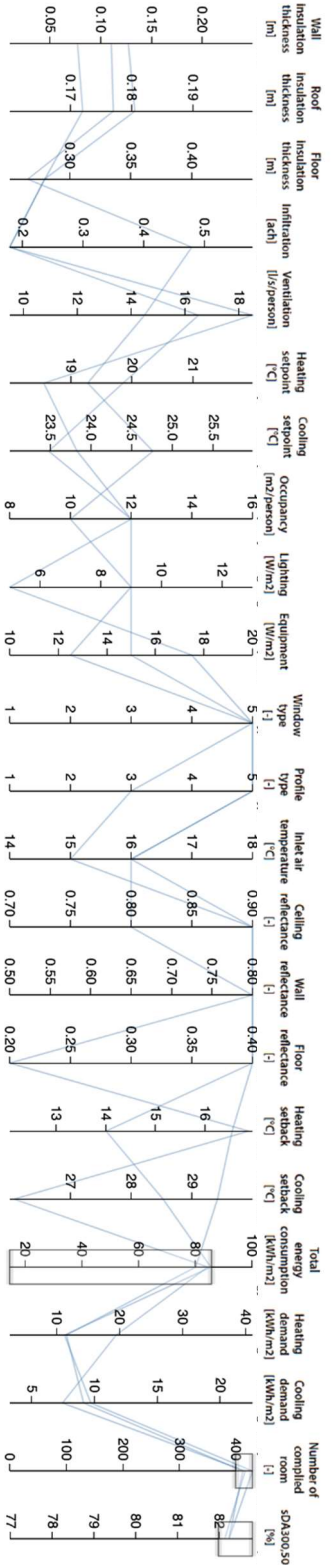


Figure 80. Parallel coordinate plot for remaining samples after adding the third filter.

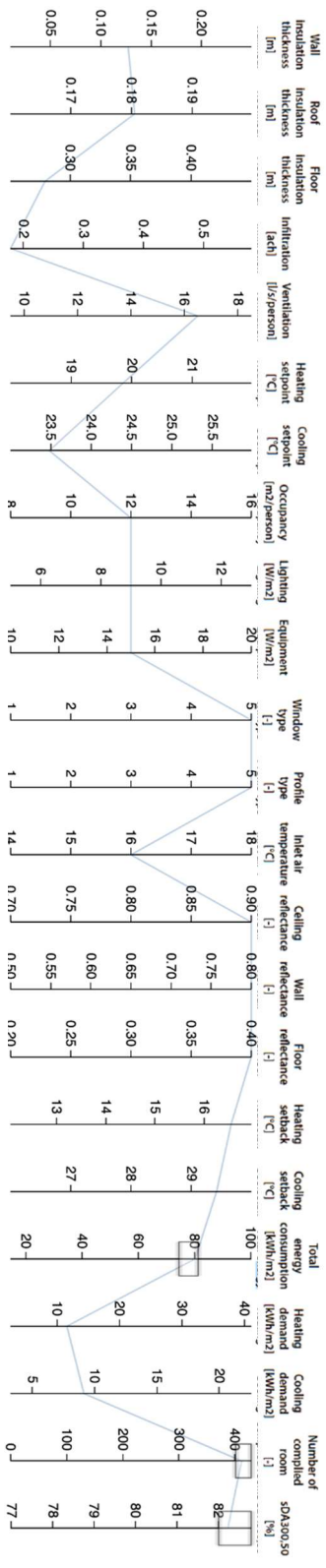


Figure 81. Parallel coordinate plot for the optimum approach.

5 Discussion

The main focus of the thesis was the development of methodology for performing multidisciplinary sensitivity and uncertainty analysis. Proof of the concept was based on the case study of an office building in Copenhagen, Denmark. The developed methodology included stepwise processes for performing sensitivity and uncertainty analysis, starting from the definition of input / output parameters to completing statistical analysis of simulated data for the specific building case. Feasibility of automating simulations in IES VE by utilizing python code was explored. The concept of integrating python script in IES VE for multidisciplinary studies is relatively new since the application is still in the development stage. Due to the limitations of the interface, selection of input parameters and the probability density functions was limited. Looking from the short-term perspective, current IES VE software limitations significantly decrease the feasibility of performing sensitivity analysis in the early design stages of the building projects. Nevertheless, if the studies would relate to automated geometrical modifications in other software (Dynamo or Rhino) or if the current VEScript-limitations would be eliminated, sensitivity and uncertainty analysis could have a huge potential of usability in early design stages of the building projects. Implementing sensitivity and uncertainty analysis studies could lead to better time-efficiency and gradual cost reduction by limiting the number of time-consuming parametric simulations by using the importance ranking of input parameters.

In this thesis, eighteen parameters related to façade design, construction quality, system design, internal heat gains and material surface optical were tested. Fourteen parameters influenced total energy consumption and thermal comfort, while three parameters affected daylight performance. The only parameter which had an influence on multidisciplinary results was window type. The ranges of input parameters were selected based upon building codes, indoor climate standards, and the literature review. The output parameters were determined according to Danish Building Regulations and available outputs from the chosen software. Four hundred simulations in IES VE and one hundred and eighty simulations in DIVA for grasshopper were carried out for this study. Based on the literature review, correlation method was chosen for the study and applied to the base case office building. Initially Pearson's correlation coefficient method was tested. Unfortunately, after validating simulated datasets, no linearity was found in the functions represented by the data plots. Since the coefficients of determination (R^2) for all tested variables, indicated a lack of satisfactory model performance in Pearson's correlation coefficient method, Spearman's rank-order correlation method was chosen as the suitable one for analysis. Although, different statistical analysis methods could be tested, more complex methods increase the time required for detailed analysis. Therefore, the choice of a suitable method based on the pre-defined time frame for project work is very important before proceeding with the sensitivity and uncertainty analysis. In this work, correlation method was chosen due to its simplicity and low computational cost in comparison to variance-based methods.

The results presented importance ranking of parameters based on the correlation level with the output indicator and statistical significance of the results. As initially expected, each input parameter performed differently depending on different result indicators. As an example, window types with low g -values performed better in terms of energy and thermal comfort, but worse in terms of daylight. Therefore, it is recommended to implement an approach based on the multi-disciplinary analysis of the results. In this thesis, multidisciplinary evaluation of

the results was achieved by gradually adding filters representing different result indicators. Additionally, parallel coordinate plots were presented for verifying the results. According to the literature review, weighting system and global objective can also be used to assess the overall performance. In this study, the number of rooms complied with BR 18 (number of hours in the period from April to October, when operative temperature exceeds $26\text{ }^{\circ}\text{C} < 100$) cannot be translated to thermal discomfort index, therefore it cannot be combined with the total energy, as a single global objective. However, if PMV or PPD were used as the results indicators, methodology of creating a single global results objective would be possible.

Based on the sensitivity analysis for the case building, it was found that insulation thickness of opaque constructions and occupancy type have very low correlation level with the energy consumption and thermal comfort. Inlet air temperature and auxiliary ventilation rate significantly influenced both energy consumption and thermal comfort. Higher inlet air temperature and lower auxiliary ventilation rate resulted in lower total energy consumption. On the contrary, lower inlet air temperature and higher auxiliary ventilation resulted in better thermal comfort. Based on the multi-disciplinary uncertainty analysis, airflow of minimum 9.5 l/s/person with air temperature between $16\text{ }^{\circ}\text{C}$ to $18\text{ }^{\circ}\text{C}$ is recommended.

Infiltration rate significantly affected both total energy consumption and thermal comfort. Lower infiltration rate contributed to the reduction of the total energy consumption but decreased the number of rooms complying with thermal conditions stated in BR18. As a final choice infiltration rate between 0.379 - 0.579 ach is recommended for the case building. Among setpoint and setback temperature, heating setpoint temperature plays the biggest role in affecting the total energy consumption, while cooling setpoint temperature has the strongest correlation with thermal comfort. Considering both energy consumption and thermal comfort, heating setpoint between $19.5 - 20\text{ }^{\circ}\text{C}$, and cooling setpoint between $23 - 24\text{ }^{\circ}\text{C}$ are suggested for the case building. It is interesting to notice that occupancy rate influences the total energy the most. However, the occupancy rate is not a factor that building design can control. Different ways of testing the occupancy rates would be recommended. For example, occupancy rates in rooms with different orientations can be altered simultaneously, which could help to determine more optimized building layout. Lighting and equipment internal gains had positive, weak correlation with the total energy consumption and no correlation with thermal comfort. The final recommendation for the investigated building is 7 W/m^2 for lighting gains and 12.5 W/m^2 equipment gains.

Window type had a significant impact on all the investigated categories, especially thermal comfort and daylight. Window type, translated into light transmittance value for daylight investigations, had the strongest correlation level with spatial daylight autonomy among the investigated parameters. Nevertheless, all simulated samples fulfilled conditions set for daylight in Danish Building Regulations. In terms of multivariate analysis, windows with lower g -values are recommended, since they performed better for both thermal comfort and total energy consumption. The lesser overheating problem occurred among the simulated samples, with the lower the g -values. Choice of the right window type is very crucial in the optimization of the buildings, especially in colder climate as proven by the sensitivity analysis results of the case building. Even though window to wall ratio could not be tested due to the existing VEScript limitations, manual testing of the parameter is recommended for the future research.

To conclude, the results of the sensitivity and uncertainty analysis presented in this thesis are only valid for the investigated building case. Nevertheless, the developed methodology is applicable for future building projects, after adjustments to the python code based on the alterations to input parameters. The list of inputs and output parameters is strictly dependent on the project requirements and client needs; therefore, changes can be applied. Moreover, the selection of probability density functions is relatively flexible, since ranges for testing are user-defined. Uniform distribution requires more computational time for testing but yield more accurate results in comparison to discrete distribution of values. Sensitivity and uncertainty analysis can also be applicable while working with different software' than IES VE and DIVA. Unfortunately, it is not guaranteed that utilization of created codes for analysis, will be possible in other software.

6 Conclusions and Future Work

The main conclusions based on the thesis work are stated below.

- VEScript python editor has facilitated partial automation of simulation process, drastically reducing time spent on the parametrical studies in IES VE. The functionality of VEScript is still under development, therefore, it limits possibilities for in-depth optimization of all the possible variations of parameters.
- Choice of the suitable sensitivity analysis method is very crucial for the success of analysis. In the current project, due to lack of model linearity, Pearson's correlation coefficient method could not be used, therefore final choice shifted towards Spearman's method. Unfortunately, the interaction effect between input variables is not included, thus meta-modeling, Morris or variance-based methods could be investigated in the future research.
- Sensitivity and uncertainty analysis provided enough information for prioritizing the most important variables affecting the final results. Parameters performed differently according to different result indicators. The result of total energy consumption was mostly influenced by occupancy rate, auxiliary ventilation rate, and inlet air temperature, whereas thermal comfort results were affected by cooling setpoint, g-value of window and infiltration rate. Even though further optimization is required, a range of uncorrelated parameters can be excluded from the design process, which as a result will be time-saving for the consultants.
- Results of sensitivity analysis and uncertainty analysis are highly dependent on the input ranges and their distributions. Therefore, the larger the input span the bigger the possibility of producing statistically accurate results regarding the optimization solution.

Regarding future work, the methodology proposed in this study can be further developed to increase the efficiency and accuracy of the analysis. Tests of other sensitivity analysis methods, such as Morris or variance-based methods would be recommended. Those methods investigate the interactions between parameters and account for nonlinearity. Nevertheless, more complex methods require a larger sample size, which will lead to higher computational needs and longer time for analysis. Furthermore, the VEScript application is still under development, which reduced the possibility of having more testable input parameters. Work could be continued to follow up on the progressive development of the application. As an example, the development of python code for overwriting input parameters in IES VE would be very beneficial for future usage. Moreover, implementation of the weighting system for multidisciplinary assessment between energy, thermal comfort, and daylight could be investigated. Different approaches concerning the method could be tested, leading to the formation of a global assessment objective. Finally, life-cycle cost and life-cycle assessment could also be incorporated when identifying the best performing samples.

Summary

The main focus of this thesis was multivariate, cross-disciplinary sensitivity and uncertainty analysis of the building parameters integrating thermal comfort, energy and daylight. The case study of a Danish office building was used for performing the simulations.

A literature review was conducted aiming to place the thesis in the broader context and sum up current research about sensitivity and uncertainty analysis of building parameters. The literature research indicated that majority of sensitivity and uncertainty analysis papers focused on only one or two output indices (thermal comfort being most popular), but very few implemented holistic approach including energy, thermal comfort, and daylight at the same time. There were no unified trends regarding input parameters and the choice of the method. Both factors are highly dependent on time-framework and resources for the project implementation.

Eighteen building parameters were tested, including window types, opaque constructions insulation thicknesses, infiltration rate, ventilation rate, setpoint and setback temperature, internal gains and surface optical properties. Total energy consumption, number of rooms compiled with Danish Building Regulations thermal comfort requirements and $sDA_{300,50}$, were used as the result indicators.

Spearman's rank-order correlation method was chosen for sensitivity analysis. Results of the thesis identified the most crucial parameters for the case building optimization. In addition, the uncertainty of the results due to uncertainties in design parameters was quantified in the project context. For the overall analysis, three type of filters were gradually applied to all the samples. As a result, input spans yielding the best holistic results in terms of daylight, thermal comfort and energy, were identified. In the case building result of total energy consumption was mostly influenced by occupancy rate, auxiliary ventilation rate, and inlet air temperature, whereas thermal comfort results were affected by cooling setpoint, window type, and infiltration rate. In terms of daylight performance, window type had higher correlation level with the spatial daylight autonomy results, than the optical properties of the surfaces.

For the investigated building, lower auxiliary ventilation rate, inlet air temperature between 16 - 18 °C, cooling setpoint between 23 - 24 °C, windows with lower g -value and infiltration rate between 0.379 - 0.579 ach yielded the best results considering multidisciplinary analysis, including energy, thermal comfort, and daylight at the same time. Nevertheless, the results are strongly case dependent, therefore careful selection of input parameters, ranges for testing and probability density functions is very crucial at the initial stage of performing sensitivity and uncertainty analysis.

Overall study proves the suitability of developed methodology for further usage in the early design stages of the building projects. Python code for multivariate analysis in IES VE, as well as DIVA script, can be further re-adjusted, based on the choice of parameters for sensitivity and uncertainty analysis in the future projects. Nevertheless, both can be used as a solid basis for further development.

References

- [1] “BR18.” [Online]. Available: <http://byggningsreglementet.dk/Tekniske-bestemmelser/18/Krav>. [Accessed: 04-May-2019].
- [2] S. Burhenne, “Monte Carlo Based Uncertainty and Sensitivity Analysis for Building Performance Simulation,” p. 208.
- [3] D. Garcia Sanchez, B. Lacarrière, M. Musy, and B. Bourges, “Application of sensitivity analysis in building energy simulations: Combining first- and second-order elementary effects methods,” *Energy and Buildings*, vol. 68, pp. 741–750, Jan. 2014.
- [4] A.-T. Nguyen and S. Reiter, “A performance comparison of sensitivity analysis methods for building energy models,” *Building Simulation*, vol. 8, no. 6, pp. 651–664, Dec. 2015.
- [5] G. Augenbroe, “Integrated building performance evaluation in the early design stages,” *Building and Environment*, vol. 27, no. 2, pp. 149–161, Apr. 1992.
- [6] T. Østergård, R. L. Jensen, and S. E. Maagaard, “Early Building Design: Informed decision-making by exploring multidimensional design space using sensitivity analysis,” *Energy and Buildings*, vol. 142, pp. 8–22, May 2017.
- [7] A. Capozzoli, A. Gorrino, and V. Corrado, “A building thermal bridges sensitivity analysis,” *Applied Energy*, vol. 107, pp. 229–243, Jul. 2013.
- [8] H. Li, S. Wang, and H. Cheung, “Sensitivity analysis of design parameters and optimal design for zero/low energy buildings in subtropical regions,” *Applied Energy*, vol. 228, pp. 1280–1291, Oct. 2018.
- [9] R. Gagnon, L. Gosselin, and S. Decker, “Sensitivity analysis of energy performance and thermal comfort throughout building design process,” *Energy and Buildings*, vol. 164, pp. 278–294, Apr. 2018.
- [10] I. Bournas, M. Abugabbara, A. Balcerzak, M.-C. Dubois, and S. Javed, “Energy renovation of an office building using a holistic design approach,” *J. Build. Eng.*, vol. 7, pp. 194–206, Sep. 2016.
- [11] S. de Wit and G. Augenbroe, “Analysis of uncertainty in building design evaluations and its implications,” *Energy and Buildings*, vol. 34, no. 9, pp. 951–958, Oct. 2002.
- [12] T. Østergård, R. L. Jensen, and S. E. Maagaard, “Building simulations supporting decision making in early design – A review,” *Renewable and Sustainable Energy Reviews*, vol. 61, pp. 187–201, Aug. 2016.
- [13] L. Van Gelder, H. Janssen, and S. Roels, “Probabilistic design and analysis of building performances: Methodology and application example,” *Energy and Buildings*, vol. 79, pp. 202–211, Aug. 2014.
- [14] K. J. Lomas and H. Eppel, “Sensitivity analysis techniques for building thermal simulation programs,” *Energy and Buildings*, vol. 19, no. 1, pp. 21–44, Jan. 1992.

- [15] W. Tian and P. de Wilde, "Uncertainty and sensitivity analysis of building performance using probabilistic climate projections: A UK case study," *Automation in Construction*, vol. 20, no. 8, pp. 1096–1109, Dec. 2011.
- [16] A. Ioannou and L. C. M. Itard, "Energy performance and comfort in residential buildings: Sensitivity for building parameters and occupancy," *Energy and Buildings*, vol. 92, pp. 216–233, Apr. 2015.
- [17] F. Bre, A. S. Silva, E. Ghisi, and V. D. Fachinotti, "Residential building design optimisation using sensitivity analysis and genetic algorithm," *Energy and Buildings*, vol. 133, pp. 853–866, Dec. 2016.
- [18] H. Li, S. Wang, and H. Cheung, "Sensitivity analysis of design parameters and optimal design for zero/low energy buildings in subtropical regions," *Applied Energy*, vol. 228, pp. 1280–1291, Oct. 2018.
- [19] R. Gagnon, L. Gosselin, and S. Decker, "Sensitivity analysis of energy performance and thermal comfort throughout building design process," *Energy and Buildings*, vol. 164, pp. 278–294, Apr. 2018.
- [20] H. Shen and A. Tzempelikos, "Sensitivity analysis on daylighting and energy performance of perimeter offices with automated shading," *Building and Environment*, vol. 59, pp. 303–314, Jan. 2013.
- [21] S. Yang, W. Tian, E. Cubi, Q. Meng, Y. Liu, and L. Wei, "Comparison of Sensitivity Analysis Methods in Building Energy Assessment," *Procedia Engineering*, vol. 146, pp. 174–181, 2016.
- [22] E. Brembilla, J. Mardaljevic, and C. J. Hopfe, "Sensitivity analysis studying the impact of reflectance values assigned in climate-based daylight modelling," 2015.
- [23] M. C. Kennedy and A. O'Hagan, "Bayesian Calibration of Computer Models," *Journal of the Royal Statistical Society. Series B (Statistical Methodology)*, vol. 63, no. 3, pp. 425–464, 2001.
- [24] C. J. Hopfe and J. L. M. Hensen, "Uncertainty analysis in building performance simulation for design support," *Energy and Buildings*, vol. 43, no. 10, pp. 2798–2805, Oct. 2011.
- [25] W. Tian *et al.*, "A review of uncertainty analysis in building energy assessment," *Renewable and Sustainable Energy Reviews*, vol. 93, pp. 285–301, Oct. 2018.
- [26] K. Menberg, Y. Heo, and R. Choudhary, "Sensitivity analysis methods for building energy models: Comparing computational costs and extractable information," *Energy and Buildings*, vol. 133, pp. 433–445, Dec. 2016.
- [27] A. Mokhtari and H. C. Frey, "Evaluation of Sampling-Based Methods for Sensitivity Analysis: Case Study for the *E. coli* Food Safety Process Risk Model," *Human and Ecological Risk Assessment: An International Journal*, vol. 12, no. 6, pp. 1128–1152, Dec. 2006.
- [28] P. Heiselberg, H. Brohus, A. Hesselholt, H. Rasmussen, E. Seinre, and S. Thomas, "Application of sensitivity analysis in design of sustainable buildings," *Renewable Energy*, vol. 34, no. 9, pp. 2030–2036, Sep. 2009.

- [29] D. M. Hamby, "A Comparison of Sensitivity Analysis Techniques:," *Health Physics*, vol. 68, no. 2, pp. 195–204, Feb. 1995.
- [30] W. Tian, "A review of sensitivity analysis methods in building energy analysis," *Renewable and Sustainable Energy Reviews*, vol. 20, pp. 411–419, Apr. 2013.
- [31] N. Delgarm, B. Sajadi, K. Azarbad, and S. Delgarm, "Sensitivity analysis of building energy performance: A simulation-based approach using OFAT and variance-based sensitivity analysis methods," *Journal of Building Engineering*, vol. 15, pp. 181–193, Jan. 2018.
- [32] B. Iooss and P. Lemaître, "A review on global sensitivity analysis methods," *arXiv:1404.2405 [math, stat]*, Apr. 2014.
- [33] K. Menberg, Y. Heo, and R. Choudhary, "Sensitivity analysis methods for building energy models: Comparing computational costs and extractable information," *Energy and Buildings*, vol. 133, pp. 433–445, Dec. 2016.
- [34] H. Breesch and A. Janssens, "Performance evaluation of passive cooling in office buildings based on uncertainty and sensitivity analysis," *Solar Energy*, vol. 84, no. 8, pp. 1453–1467, Aug. 2010.
- [35] T. Østergård, R. L. Jensen, and S. E. Maagaard, "Early Building Design: Informed decision-making by exploring multidimensional design space using sensitivity analysis," *Energy and Buildings*, vol. 142, pp. 8–22, May 2017.
- [36] M. H. Kristensen and S. Petersen, "Choosing the appropriate sensitivity analysis method for building energy model-based investigations," *Energy and Buildings*, vol. 130, pp. 166–176, Oct. 2016.
- [37] J. S. Hygh, J. F. DeCarolis, D. B. Hill, and S. Ranji Ranjithan, "Multivariate regression as an energy assessment tool in early building design," *Building and Environment*, vol. 57, pp. 165–175, Nov. 2012.
- [38] Y. Yildiz, K. Korkmaz, T. Göksal Özbalta, and Z. Durmus Arsan, "An approach for developing sensitive design parameter guidelines to reduce the energy requirements of low-rise apartment buildings," *Applied Energy*, vol. 93, pp. 337–347, May 2012.
- [39] F. Pianosi *et al.*, "Sensitivity analysis of environmental models: A systematic review with practical workflow," *Environmental Modelling & Software*, vol. 79, pp. 214–232, May 2016.
- [40] X. Chen, H. Yang, and K. Sun, "Developing a meta-model for sensitivity analyses and prediction of building performance for passively designed high-rise residential buildings," *Applied Energy*, vol. 194, pp. 422–439, May 2017.
- [41] M. H. Kristensen and S. Petersen, "Choosing the appropriate sensitivity analysis method for building energy model-based investigations," *Energy and Buildings*, vol. 130, pp. 166–176, Oct. 2016.
- [42] E. Patelli, "COSSAN: A Multidisciplinary Software Suite for Uncertainty Quantification and Risk Management," p. 70.

- [43] M. J. Sørensen, S. H. Myhre, K. K. Hansen, M. H. Silkjær, A. J. Marszal-Pomianowska, and L. Liu, “Integrated Building Energy Design of a Danish Office Building Based on Monte Carlo Simulation Method,” *Energy Procedia*, vol. 132, pp. 93–98, Oct. 2017.
- [44] G. Lovison, “A matrix-valued Bernoulli distribution,” *Journal of Multivariate Analysis*, vol. 97, no. 7, pp. 1573–1585, Aug. 2006.
- [45] Stephanie, “Bernoulli Distribution: Definition and Examples,” *Statistics How To*, 29-Jul-2016. [Online]. Available: <https://www.statisticshowto.datasciencecentral.com/bernoulli-distribution/>. [Accessed: 19-Mar-2019].
- [46] “Statistical Distributions and Climate Change | Elsevier Enhanced Reader.” [Online]. Available: <https://reader.elsevier.com/reader/sd/pii/S2210983815002473?token=45F35F9F91463D83FA2C2DDB66B0E63C53B055929026C931260332E54E5EE84ECDCFA80A819BF3AF01E4D555F722716E>. [Accessed: 19-Mar-2019].
- [47] M. H. Kristensen and S. Petersen, “Contrasting the Capabilities of Three Different Sensitivity Analysis Methods for Building Energy Model-based Investigations,” p. 7, Nov. 2018.
- [48] H. Eggebø, “Sensitivity analysis for investigating the energy performance of a retrofitted kindergarten under different weather scenarios,” p. 67, Jun. 2017.
- [49] G. P. Brooks and R. S. Barcikowski, “The PEAR Method for Sample Sizes in Multiple Linear Regression,” vol. 38, p. 16, 2012.
- [50] J. B. Hittner, “Effects of Population Distribution, Sample Size and Correlation Structure on Huberty’s Effect Size R,” 2009.
- [51] J. L. Loeppky, J. Sacks, and W. J. Welch, “Choosing the Sample Size of a Computer Experiment: A Practical Guide,” *Technometrics*, vol. 51, no. 4, pp. 366–376, Nov. 2009.
- [52] E. Vanuytrecht, D. Raes, and P. Willems, “Global sensitivity analysis of yield output from the water productivity model,” *Environmental Modelling & Software*, vol. 51, pp. 323–332, Jan. 2014.
- [53] W. Tian *et al.*, “Building Energy Assessment Based on a Sequential Sensitivity Analysis Approach,” *Procedia Engineering*, vol. 205, pp. 1042–1048, 2017.
- [54] “Sweden BBR,” *Sweden BBR*, 13-May-2019. [Online]. Available: <http://www.gbpn.org/databases-tools/bc-detail-pages/sweden#Values%20for%20New%20Buildings>.
- [55] H. Shen and A. Tzempelikos, “Sensitivity analysis on daylighting and energy performance of perimeter offices with automated shading,” *Building and Environment*, vol. 59, pp. 303–314, Jan. 2013.
- [56] F. Bre, A. S. Silva, E. Ghisi, and V. D. Fachinotti, “Residential building design optimisation using sensitivity analysis and genetic algorithm,” *Energy and Buildings*, vol. 133, pp. 853–866, Dec. 2016.
- [57] M. Sherman, “Building Airtightness: Research and Practice,” p. 47.

- [58] Y. Zou, "Classification of buildings with regard to airtightness," p. 100.
- [59] "CIBSE Guide A," *CIBSE Guide A: Environmental design*. [Online]. Available: <https://www.cibse.org/knowledge/knowledge-items/detail?id=a0q2000008I79JAAS>. [Accessed: 12-May-2019].
- [60] "ASHRAE handbook," *ASHRAE Handbook Fundamentals 2009*. [Online]. Available: <https://www.ashrae.org/technical-resources/ashrae-handbook>. [Accessed: 10-May-2019].
- [61] "DS 447 E_2013.pdf."
- [62] J.-M. Dussault and L. Gosselin, "Office buildings with electrochromic windows: A sensitivity analysis of design parameters on energy performance, and thermal and visual comfort," *Energy and Buildings*, vol. 153, pp. 50–62, Oct. 2017.
- [63] G. Wang and L. Song, "Air handling unit supply air temperature optimal control during economizer cycles," *Energy and Buildings*, vol. 49, pp. 310–316, Jun. 2012.
- [64] D. Johansson, "Optimal supply air temperature with respect to energy use in a constant air volume system," p. 11.
- [65] "City Switch case studies," *City Switch case studies :Indoor comfort and temperature set-points*. [Online]. Available: <https://cityswitch.net.au/Resources/CitySwitch-Resources/CitySwitch-case-studies/category/heating-and-cooling/indoor-comfort-and-temperature-set-points>. [Accessed: 12-May-2019].
- [66] "ASHRAE Standard 55," *ASHRAE Standard 55, Thermal Environmental Conditions for Human Occupancy*. [Online]. Available: <https://www.ashrae.org/technical-resources/bookstore/standard-55-thermal-environmental-conditions-for-human-occupancy>.
- [67] Building Research Established, "Internal heat gains." National Calculation Methodology, Unknown.
- [68] S. Ezzeldin and S. J. Rees, "The potential for office buildings with mixed-mode ventilation and low energy cooling systems in arid climates," *Energy and Buildings*, vol. 65, pp. 368–381, Oct. 2013.
- [69] R. Alastair and S. Stephen, "Tips for daylighting with windows." Environmental Energy Technologies Division, Oct-2013.
- [70] M. Wilson, "Lighting in museums: Lighting interventions during the European demonstration project 'Energy efficiency and sustainability in retrofitted and new museum buildings' (NNES-1999-20)," *International Journal of Sustainable Energy*, vol. 25, no. 3–4, pp. 153–169, 2006.
- [71] European Standard, "EN 12464-1: Light and lighting - Lighting of workplaces - Part 1: Indoor work places." European Standard, Nov-2002.
- [72] M. Mohsenin and J. Hu, "Assessing daylight performance in atrium buildings by using Climate Based Daylight Modeling," *Solar Energy*, vol. 119, pp. 553–560, Sep. 2015.

- [73] K. Butcher, B. Craig, and Chartered Institution of Building Services Engineers, Eds., *Environmental design: CIBSE guide A*, Eighth edition. London: Chartered Institution of Building Services Engineers, 2015.
- [74] “Branchevejledning for indeklimaberegninger opdateret version final web,” *Issuu*. [Online]. Available: https://issuu.com/www.innobyg.dk/docs/branchevejledning_for_indeklimabere_b91162768c9b79. [Accessed: 05-May-2019].
- [75] “Sample Size Software | Power Analysis Software | PASS | NCSS.com.” [Online]. Available: <https://www.ncss.com/software/pass/>. [Accessed: 25-Apr-2019].
- [76] F. Faul, E. Erdfelder, A. Buchner, and A.-G. Lang, “Statistical power analyses using G*Power 3.1: Tests for correlation and regression analyses,” *Behavior Research Methods*, vol. 41, no. 4, pp. 1149–1160, Nov. 2009.
- [77] C. Gatsonis and A. R. Sampson, “Multiple correlation: Exact power and sample size calculations,” *Psychological Bulletin*, vol. 106, no. 3, pp. 516–524, 1989.
- [78] “The RADIANCE 5.1 Synthetic Imaging System.” [Online]. Available: <https://floyd.lbl.gov/radiance/refer/ray.html#Materials>. [Accessed: 09-May-2019].
- [79] “Radiance tutorial.pdf.”
- [80] Ö. Erlendsson, “Daylight Optimization: A Parametric Study of Atrium Design,” p. 136.
- [81] “03_Radiance Primer.pdf.”
- [82] “Radiance Parameters - SPOT Pro v.5 - 5.0,” *SPOT Pro v.5*. [Online]. Available: <https://www.manula.com/manuals/zogers/spot-pro-v-5/1/en/topic/radiance-parameters>. [Accessed: 10-May-2019].
- [83] D. R. Compagnon, “a simulation tool for daylighting systems,” p. 60.
- [84] “Daylighting Calculation Options.” [Online]. Available: https://designbuilder.co.uk/helpv3.4/Content/Daylighting_Calculation_Options.htm#Ambient4. [Accessed: 10-May-2019].
- [85] “RTRACE.” [Online]. Available: https://floyd.lbl.gov/radiance/man_html/rtrace.1.html. [Accessed: 10-May-2019].
- [86] M. L. Gaddis and G. M. Gaddis, “Introduction to biostatistics: Part 6, correlation and regression,” *Annals of Emergency Medicine*, vol. 19, no. 12, pp. 1462–1468, Dec. 1990.
- [87] J. Hauke and T. Kossowski, “Comparison of Values of Pearson’s and Spearman’s Correlation Coefficients on the Same Sets of Data,” *Quaestiones Geographicae*, vol. 30, no. 2, pp. 87–93, Jun. 2011.
- [88] “A comparison of the Pearson and Spearman correlation methods.” [Online]. Available: <https://support.minitab.com/en-us/minitab-express/1/help-and-how-to/modeling-statistics/regression/supporting-topics/basics/a-comparison-of-the-pearson-and-spearman-correlation-methods/>. [Accessed: 12-May-2019].

- [89] “How to choose between Pearson and Spearman correlation?” *Cross Validated*. [Online]. Available: <https://stats.stackexchange.com/questions/8071/how-to-choose-between-pearson-and-spearman-correlation>. [Accessed: 12-May-2019].
- [90] S. A. Abou Rafee *et al.*, “Large-Scale Hydrological Modelling of the Upper Paraná River Basin,” *Water*, vol. 11, no. 5, p. 882, Apr. 2019.
- [91] “Sample Size for Bivariate Correlation, Pearson Correlation, and Pearson Product Moment Correlation,” *Statistics Solutions*, 30-Dec-2008.
- [92] H. Akoglu, “User’s guide to correlation coefficients,” *Turkish Journal of Emergency Medicine*, vol. 18, no. 3, pp. 91–93, Sep. 2018.
- [93] J. D. Herman, J. B. Kollat, P. M. Reed, and T. Wagener, “Technical Note: Method of Morris effectively reduces the computational demands of global sensitivity analysis for distributed watershed models,” *Hydrology and Earth System Sciences*, vol. 17, no. 7, pp. 2893–2903, Jul. 2013.
- [94] M. D. Morris, “Factorial Sampling Plans for Preliminary Computational Experiments,” *Technometrics*, vol. 33, no. 2, pp. 161–174, May 1991.
- [95] D. Wallach, D. Makowski, J. W. Jones, and F. Brun, “Uncertainty and Sensitivity Analysis,” in *Working with Dynamic Crop Models*, Elsevier, 2019, pp. 209–250.

Appendix

Appendix A: Literature review of other sensitivity analysis methods

1) Screening methods

Morris one-at-a-time-screening:

According to Herman [93], Morris method measures the global sensitivity by the usage of a set of the local derivatives taken at point sampled throughout the whole parameter design space. In the method both the variance and mean of the elementary effects are assessed. The method is suitable for applications with moderate computational cost in comparison to other global methods [2]. The method is aiming to identify the least influential parameters and as a result lead to ranking of all the inputs. Due to reduced computational time, method is widely used in the building performance simulation research, since it compromises time efficiency with the accuracy of datasets and it's suitable for an extensive dataset [2, 11, 25]. Factorial sampling in Morris method belongs to OAT category, previously mentioned in Section 2.2.3.1 [26]. According to Morris [94], method is based on approach of efficient parameter screening alongside the factorial sampling strategy, which directly leads to pointing out the fixed parameters not influencing the results. Parameter space is discretized by transforming the input parameters into the variables (dimensionless) which fall into (0;1) interval. Then each parameter is divided into a number of p levels, which are forming a grid in the unit length hypercube H^k [94]. Location of the sampling starting point in the design space is randomly chosen. Moreover, for each sample, only one coordinate is varied in relation to the previous sample [26].

2) Variance based methods

Sobol Sensitivity Indices:

Sobol' method for sensitivity analysis is a global, variance-based method which is very computationally demanding. It attributes the variance in the outputs to each set parameter and includes interactions between the parameters [93]. The method is described by the following Equation 3:

$$D(f) = \sum_i D_i + \sum_{i < j} D_{ij} + \sum_{i < j < k} D_{ijk} + D_{12..p}, \quad (3)$$

- $D(f)$: the total variance of the output metric f
- D_i : first-order variance contribution of the i -th parameter
- D_{ij} : second-order contribution of the interaction between parameters i and j
- $D_{12...p}$: contains all interactions higher than third-order, up to p total parameters [93].

In Sobol's method, two measures can be derived for each parameter: first-order index, which describes the contribution of the parameter to the variance in response and total effect index which is a total contribution including interactions of a parameter to the response variance.

Fourier amplitude sensitivity test:

FAST is a method which originally was designed for analyzing the sensitivity of chemical reactions to rate the coefficients, however further has been adapted for use in different scientific problems [95]. FAST method explores the space of the input variables with a periodic curve by using different variables frequencies. The classical FAST method does not account for the interaction between parameters (considers only non-linear effects) [21]. The extended FAST method leads to the computation of the higher-order effects. Capozzoli [7] describes the FAST method as based on the transformation that converts the Y variable variance (k-dimensional integral), to the single-dimensional integral with respect to a scalar variable s . This process is conducted by transformation of each input factor X_i into the form presented in Equation 4 [33]:

$$X_i = G_i(\sin(\omega_i s)) \quad (4)$$

3) Meta-model methods

Meta-model sensitivity method included two steps. The first step is to create meta-modelling (machine learning numerical model) based on results from thousands of simulation according to the global design space or building performance databases [35]. The second step is to conduct a variance-based sensitivity method such as Sobol' on this meta-modelling. Tian [30] has stated that meta-modelling is easier, cheaper and faster to get the predictive results and it is especially suitable when the simulation of building performance is complex and computationally intensive. It has been found by Tian [53] that the speed of getting convergent is faster in meta-modelling Sobol' method in comparison with SRC method.

Predictive validation of the meta-modelling will be judged if it has a high coefficient of determination (R^2) and a low Root-Mean-Square-Error (RMSE) [35]. However, it is only valid for the specific regions where the training data distributed within. Tian [30] has argued that the accuracy of sensitivity analysis will significantly depend on the meta-model. Nevertheless, meta-model not only can be implemented to perform quantitative sensitivity analysis but also be favorable for design space exploration and optimization [35]. For example, Østergård [35] used meta-model to solve what-if questions, answering how the output changes when the input has been changed by a specific value, and therefore benefits the informed decision-making.

Appendix B: Python script for IES VE

1) Overwrite values of input parameters

```

import xlrd
from xlrd import open_workbook
workbook=open_workbook('sampletorun0429.xlsx') #remember to put excel file in the same
folder of your ies model
sheet =workbook.sheet_by_index(0)# get sheet 1
import iesve
import pprint
import time
b=47
# manually to change number here to loop different columns of data
# select this to execute and then open database, double click one wall construction and close
it and save changes

for i in range(b,b+1):
    # get each cell value(every time the same row)
    aps_sample_name=sheet.cell(i,0).value #aps.name
    wallinsul=sheet.cell(i,1).value # wall insulation thickness
    roofinsul=sheet.cell(i,2).value # roof insulation thickness
    groundinsul=sheet.cell(i,3).value #ground insulation thickness
    infil=sheet.cell(i,4).value # infiltration index
    auxi=sheet.cell(i,5).value # auxiliary ventilation index
    hpt=sheet.cell(i,6).value # hpt is heating set point degree
    cpt=sheet.cell(i,7).value # cpt is cooling set point degree
    occupancy=sheet.cell(i,8).value #occupancy gain index, remember to remove it before next
simulation
    light=sheet.cell(i,9).value #light gain index, remember to remove it before next simulation
    equipment=sheet.cell(i,10).value #equipment gain index, remember to remove it before
next simulation
    glz=sheet.cell(i,11).value
    office_profile=sheet.cell(i,12).value
    inlet_profile=sheet.cell(i,13).value
    hsb=sheet.cell(i,17).value
    csb=sheet.cell(i,18).value

veproject = iesve.VEProject.get_current_project()
db = iesve.VECdbDatabase.get_current_database()
projects = db.get_projects()
project_list = projects[0]
project = project_list[0]
c_class = iesve.construction_class.opaque
ids = project.get_construction_ids(c_class)

# if we know construction id, 20130014-Uvalue0.699,20130017-Uvalue0.715,20130020-
Uvalue0.706

```

```

# we know the top roof id is 20130007, we know ground floor id is 20130005
# insulation layer index is 2 for 3 types of wall construction, index 1 for roof, index for
ground
# we get index now
# then we get index_1=12, index_2=14, index_3=15, index_4=7, index_5=5
wall_1_construction = project.get_construction(ids[12], c_class)
wall_2_construction = project.get_construction(ids[14],c_class)
wall_3_construction = project.get_construction(ids[15],c_class)
roof_1_construction = project.get_construction(ids[7],c_class)
ground_1_construction = project.get_construction(ids[5],c_class)

if wall_1_construction.is_editable:
    wall_layers_1 = wall_1_construction.get_layers()
    insulation_layer_1=wall_layers_1[2]
    insulation_layer_1.set_properties({'thickness': wallinsul})#mind here: the thickness
here is meter.

if wall_2_construction.is_editable:
    wall_layers_2 = wall_2_construction.get_layers()
    insulation_layer_2=wall_layers_2[2]
    insulation_layer_2.set_properties({'thickness': wallinsul})

if wall_3_construction.is_editable:
    wall_layers_3 = wall_3_construction.get_layers()
    insulation_layer_3=wall_layers_3[2]
    insulation_layer_3.set_properties({'thickness': wallinsul})

if roof_1_construction.is_editable:
    roof_layers_1 = roof_1_construction.get_layers()
    insulation_layer_roof=roof_layers_1[0]
    insulation_layer_roof.set_properties({'thickness': roofinsul})

if ground_1_construction.is_editable:
    ground_layers_1=ground_1_construction.get_layers()
    insulation_layer_ground=ground_layers_1[3]
    insulation_layer_ground.set_properties({'thickness': groundinsul})

#change outpane glazing properties
veproject = iesve.VEProject.get_current_project()
db = iesve.VECdbDatabase.get_current_database()
projects = db.get_projects()
project_list = projects[0]
project = project_list[0]
c_class_1 = iesve.construction_class.glazed
ids_1 = project.get_construction_ids(c_class_1)
transmittance=[0,0.871,0.710,0.30,0.470,0.350]
outside_reflectance=[0,0.078,0.2,0.6,0.38,0.4]
inside_reflectance=[0,0.078,0.2,0.6,0.38,0.4]

```

```

d=[0,4,5,6]
for i in d:
    base= project.get_construction(ids_1[i], c_class_1)
    if base.is_editable:
        layers= base.get_layers()
        outlayer=layers[0]
        material = outlayer.get_material(False)

material.set_properties({'transmittance':transmittance[int(glz)],'outside_reflectance':outside_
reflectance[int(glz)],'inside_reflectance':inside_reflectance[int(glz)]})

project = iesve.VEProject.get_current_project()
office_daily_profile = project.daily_profile("DAY_0003")
canteen_daily_profile= project.daily_profile('DAY_0077')
inlet_temperature_daily_profile=project.daily_profile('DAY_0079')
heating_operation_daily_profile=project.daily_profile('SYS_0207')
cooling_operation_daily_profile=project.daily_profile('DAY_0087')

heating_operation_list=[0,
[[0, hsb, '-'], [6, hsb, '-'], [6, hpt, '-'], [17, hpt, '-'], [17, hsb, '-'],[24, hsb, '-']],
[[0, hsb, '-'], [6, hsb, '-'], [6, hpt, '-'], [17, hpt, '-'], [17, hsb, '-'],[24, hsb, '-']],
[[0, hsb, '-'], [6, hsb, '-'], [6, hpt, '-'], [17, hpt, '-'], [17, hsb, '-'],[24, hsb, '-']],
[[0, hsb, '-'], [7, hsb, '-'], [7, hpt, '-'], [18, hpt, '-'], [18, hsb, '-'],[24, hsb, '-']],
[[0, hsb, '-'], [7, hsb, '-'], [7, hpt, '-'], [18, hpt, '-'], [18, hsb, '-'],[24, hsb, '-']],
[[0, hsb, '-'], [7, hsb, '-'], [7, hpt, '-'], [18, hpt, '-'], [18, hsb, '-'],[24, hsb, '-']],
[[0, hsb, '-'], [7.5, hsb, '-'], [7.5, hpt, '-'], [18.5, hpt, '-'], [18.5, hsb, '-'],[24, hsb, '-']],
[[0, hsb, '-'], [7.5, hsb, '-'], [7.5, hpt, '-'], [18.5, hpt, '-'], [18.5, hsb, '-'],[24, hsb, '-']],
[[0, hsb, '-'], [7.5, hsb, '-'], [7.5, hpt, '-'], [18.5, hpt, '-'], [18.5, hsb, '-'],[24, hsb, '-']]

cooling_operation_list=[0,
[[0, csb, '-'], [6, csb, '-'], [6, cpt, '-'], [17, cpt, '-'], [17, csb, '-'],[24, csb, '-']],
[[0, csb, '-'], [6, csb, '-'], [6, cpt, '-'], [17, cpt, '-'], [17, csb, '-'],[24, csb, '-']],
[[0, csb, '-'], [6, csb, '-'], [6, cpt, '-'], [17, cpt, '-'], [17, csb, '-'],[24, csb, '-']],
[[0, csb, '-'], [7, csb, '-'], [7, cpt, '-'], [18, cpt, '-'], [18, csb, '-'],[24, csb, '-']],
[[0, csb, '-'], [7, csb, '-'], [7, cpt, '-'], [18, cpt, '-'], [18, csb, '-'],[24, csb, '-']],
[[0, csb, '-'], [7, csb, '-'], [7, cpt, '-'], [18, cpt, '-'], [18, csb, '-'],[24, csb, '-']],
[[0, csb, '-'], [7.5, csb, '-'], [7.5, cpt, '-'], [18.5, cpt, '-'], [18.5, csb, '-'],[24, csb, '-']],
[[0, csb, '-'], [7.5, csb, '-'], [7.5, cpt, '-'], [18.5, cpt, '-'], [18.5, csb, '-'],[24, csb, '-']],
[[0, csb, '-'], [7.5, csb, '-'], [7.5, cpt, '-'], [18.5, cpt, '-'], [18.5, csb, '-'],[24, csb, '-']]

office_profile_list=[0,
[[0, 0, '-'], [7, 0, '-'], [7, 1, '-'], [12, 1, '-'], [12, 0.2, '-'],[13, 0.2, '-'],[13, 1, '-'], [17, 1, '-'], [17,
0, '-'],[24, 0, '-']],
[[0, 0, '-'], [7, 0, '-'], [7, 0.5, '-'], [8, 0.5, '-'], [8,1,-'],[12,1,-'],[12, 0.2, '-'],[13, 0.2, '-'],[13, 1,
'-'], [16,1,-'],[16,0.5,-'],[17,0.5,-'], [17, 0, '-'],[24, 0, '-']],
[[0, 0, '-'], [7, 0, '-'], [7, 1, '-'], [12, 1, '-'], [12,0.4,-'],[14,0.4,-'],[14, 1, '-'],[17, 1, '-'],[17, 0,
'-'],[24, 0, '-']],

```



```

[[0, 0, '-'], [8, 0, '-'], [8, 1, '-'], [12, 1, '-'], [12, 0.2, '-'], [13, 0.2, '-'], [13, 1, '-'], [18, 1, '-'], [18,
0, '-'], [24, 0, '-']],
[[0, 0, '-'], [8, 0, '-'], [8, 0.5, '-'], [9, 0.5, '-'], [9, 1, '-'], [12, 1, '-'], [12, 0.2, '-'], [13, 0.2, '-'], [13, 1,
'-'], [17, 1, '-'], [17, 0.5, '-'], [18, 0.5, '-'], [18, 0, '-'], [24, 0, '-']],
[[0, 0, '-'], [8, 0, '-'], [8, 1, '-'], [12, 1, '-'], [12, 0.4, '-'], [14, 0.4, '-'], [14, 1, '-'], [18, 1, '-'], [18, 0,
'-'], [24, 0, '-']],
[[0, 0, '-'], [8.5, 0, '-'], [8.5, 1, '-'], [12, 1, '-'], [12, 0.2, '-'], [13, 0.2, '-'], [13, 1, '-'], [18.5, 1, '-'],
[18.5, 0, '-'], [24, 0, '-']],
[[0, 0, '-'], [8.5, 0, '-'], [8.5, 0.5, '-'], [9, 0.5, '-'], [9, 1, '-'], [12, 1, '-'], [12, 0.2, '-'], [13, 0.2, '-'], [13,
1, '-'], [17.5, 1, '-'], [17.5, 0.5, '-'], [18.5, 0.5, '-'], [18.5, 0, '-'], [24, 0, '-']],
[[0, 0, '-'], [8.5, 0, '-'], [8.5, 1, '-'], [12, 1, '-'], [12, 0.4, '-'], [14, 0.4, '-'], [14, 1, '-'], [18.5, 1, '-'],
[18.5, 0, '-'], [24, 0, '-']]

```

```

canteen_profile_list=[0,
[[0,0,'-'],[12,0,'-'],[12,1,'-'],[13,1,'-'],[13,0,'-'],[24,0,'-']],
[[0,0,'-'],[12,0,'-'],[12,1,'-'],[13,1,'-'],[13,0,'-'],[24,0,'-']],
[[0,0,'-'],[12,0,'-'],[12,0.8,'-'],[14,0.8,'-'],[14,0,'-'],[24,0,'-']],
[[0,0,'-'],[12,0,'-'],[12,1,'-'],[13,1,'-'],[13,0,'-'],[24,0,'-']],
[[0,0,'-'],[12,0,'-'],[12,1,'-'],[13,1,'-'],[13,0,'-'],[24,0,'-']],
[[0,0,'-'],[12,0,'-'],[12,0.8,'-'],[14,0.8,'-'],[14,0,'-'],[24,0,'-']],
[[0,0,'-'],[12,0,'-'],[12,1,'-'],[13,1,'-'],[13,0,'-'],[24,0,'-']],
[[0,0,'-'],[12,0,'-'],[12,1,'-'],[13,1,'-'],[13,0,'-'],[24,0,'-']],
[[0,0,'-'],[12,0,'-'],[12,0.8,'-'],[14,0.8,'-'],[14,0,'-'],[24,0,'-']]

```

```

inlet_temperature_profile_list=[0,
[[0,14,'-'],[24,14,'-']],
[[0,15,'-'],[24,15,'-']],
[[0,16,'-'],[24,16,'-']],
[[0,17,'-'],[24,17,'-']],
[[0,18,'-'],[24,18,'-']]

```

```

office_daily_profile_data = office_profile_list[int(office_profile)]
canteen_daily_profile_data = canteen_profile_list[int(office_profile)]
heating_operation_daily_profile_data= heating_operation_list[int(office_profile)]
inlet_temperature_daily_profile_data = inlet_temperature_profile_list[int(inlet_profile)]
cooling_operation_daily_profile_data= cooling_operation_list[int(office_profile)]

```

```

office_daily_profile.set_data(office_daily_profile_data)
canteen_daily_profile.set_data(canteen_daily_profile_data)
heating_operation_daily_profile.set_data(heating_operation_daily_profile_data)

```

```

inlet_temperature_daily_profile.set_data(inlet_temperature_daily_profile_data)
cooling_operation_daily_profile.set_data(cooling_operation_daily_profile_data)

```

```

project = iesve.VEProject.get_current_project()
casual_gains = project.casual_gains()
templates = project.thermal_templates(False)
templates_iter = templates.values()

```

```

alltemplates=list(templates.values())
# then only change the templates called office, office is index 12 template
alltemplates[12].add_gain(casual_gains[int(occupancy)]) # data from sample excel
alltemplates[12].add_gain(casual_gains[int(light)]) # data from sample excel
alltemplates[12].add_gain(casual_gains[int(equipment)]) # data from sample excel
alltemplates[12].apply_changes()
# now add infiltration rate, loop each template
air_exchanges = project.air_exchanges()
for template in templates_iter:
    template.add_air_exchange(air_exchanges[int(infil)])# data from sample excel
    template.apply_changes()
# now add ventilation rate, loop determined templates, index 9,10,11,12,13,14
c=[9,10,11,12,13,14]
newarray = [alltemplates[int(i)] for i in c ]
for template in newarray:
    template.add_air_exchange(air_exchanges[int(auxi)])# data from sample excel
    template.apply_changes()

project = iesve.VEProject.get_current_project()
real_building = project.models[0]
templates = project.thermal_templates(False)
templates_iter = templates.values()
alltemplates=list(templates.values())

office_id_list = ['AIM50770', 'AIM23400', 'AIM39070', 'AIM75380', 'L0000018',
'AIM53640', 'AIM57610', 'AIM50450', 'AIM48520', 'AIM42260', 'L0000009', 'AIM44460',
'AIM23670', 'AIM59890', 'AIM61760', 'AIM21190', 'AIM21390', 'AIM64450', 'AIM69010',
'AIM44230', 'L0000003', 'AIM65820', 'AIM21870', 'AIM43090', 'AIM28200', 'AIM69740',
'AIM30500', 'AIM72360', 'AIM75480', 'AIM47240', 'AIM29140', 'AIM29370', 'AIM32180',
'AIM53350', 'AIM63510', 'AIM45370', 'AIM49800', 'AIM74800', 'AIM36760', 'AIM22070',
'AIM19080', 'AIM37530', 'AIM34260', 'AIM36950', 'L1000000', 'AIM69670', 'AIM60210',
'L0000005', 'AIM32980', 'AIM22450', 'AIM57200', 'AIM67360', 'AIM35220', 'AIM56250',
'AIM53780', 'AIM21040', 'AIM65180', 'AIM41390', 'AIM34230', 'AIM45870', 'AIM71080',
'AIM74210', 'AIM33620', 'AIM25490', 'AIM62740', 'AIM61200', 'AIM45190', 'AIM43690',
'AIM45230', 'AIM43880', 'AIM22530', 'AIM44420', 'AIM71720', 'AIM37390', 'AIM48430',
'AIM42150', 'AIM30050', 'AIM29320', 'AIM43650', 'AIM76680', 'AIM72020', 'AIM68900',
'AIM66320', 'AIM21230', 'AIM45960', 'AIM20170', 'AIM24810', 'AIM62170', 'AIM67460',
'AIM54920', 'AIM24120', 'AIM27080', 'AIM33480', 'AIM71290', 'AIM55330', 'AIM40230',
'AIM39800', 'AIM27010', 'AIM28150', 'AIM22780', 'AIM51070', 'AIM40570', 'AIM19940',
'AIM48790', 'AIM52500', 'AIM24020', 'AIM23250', 'AIM33640', 'AIM19230', 'AIM31190',
'AIM18890', 'AIM25400', 'AIM66730', 'AIM23460', 'AIM25040', 'AIM74280', 'AIM20850',
'AIM70880', 'AIM20280', 'AIM28080', 'AIM59390', 'AIM64280', 'AIM26520', 'AIM31640',
'AIM21740', 'AIM63310', 'AIM24730', 'AIM42920', 'AIM22880', 'AIM46700', 'AIM61030',
'AIM26300', 'AIM40180', 'AIM76650', 'AIM61970', 'AIM22250', 'AIM38260', 'AIM47650',
'AIM37270', 'AIM28230', 'AIM21920', 'AIM38300', 'AIM65590', 'L1000002', 'AIM27440',
'AIM55920', 'AIM42880', 'AIM49600', 'AIM49160', 'AIM17980', 'AIM32780', 'AIM73070',
'AIM40800', 'AIM42340', 'AIM70790', 'AIM67370', 'AIM23590', 'AIM29360', 'AIM58300',
'AIM77620', 'AIM25870', 'AIM54190', 'AIM40610', 'AIM39030', 'AIM23360', 'AIM22680',

```

```
'AIM58750', 'AIM38490', 'AIM45650', 'AIM56470', 'AIM54410', 'AIM73630', 'AIM70150',  
'AIM28760', 'AIM51910', 'AIM51500', 'L1000001', 'AIM73000', 'AIM62810', 'AIM60620',  
'AIM27090', 'AIM25950', 'AIM49710', 'AIM41570', 'AIM49070', 'AIM58200', 'AIM47550',  
'AIM66230', 'AIM54780', 'AIM35540', 'AIM60530', 'AIM72430', 'AIM31650', 'AIM47880',  
'AIM41950', 'AIM73160', 'AIM24290', 'AIM53050', 'AIM28910', 'AIM55400', 'AIM64040',  
'L0000004', 'AIM24840', 'AIM58340', 'AIM67870', 'AIM68600', 'AIM48540', 'AIM19790',  
'L0000002', 'AIM75840', 'AIM74200', 'AIM39260', 'AIM61670', 'AIM34510', 'AIM41480',  
'AIM41380', 'AIM20660', 'AIM22740', 'AIM56060', 'AIM49930', 'L0000001', 'AIM21310',  
'AIM57060', 'AIM76420', 'AIM30130', 'AIM57310', 'AIM59150', 'AIM47150', 'AIM38530',  
'AIM37720', 'AIM35020', 'AIM43110', 'AIM25160', 'AIM18400', 'AIM32290', 'AIM33170',  
'L0000006', 'AIM36250', 'AIM24350', 'AIM21810', 'AIM63950', 'AIM20930', 'AIM52210',  
'AIM36210', 'AIM47790', 'AIM35990', 'AIM33380', 'AIM27770', 'AIM27640', 'AIM65090',  
'AIM20600', 'AIM24330', 'AIM66590', 'L0000000', 'AIM42110', 'AIM46600', 'AIM62900',  
'AIM68130', 'AIM45640', 'AIM40030', 'AIM70440', 'AIM46510', 'AIM35110', 'AIM33920',  
'AIM30510', 'AIM39670', 'AIM71930', 'AIM41340', 'AIM39840', 'AIM28720', 'AIM44650',  
'AIM30400', 'AIM68510', 'AIM65050', 'AIM40810', 'AIM27190', 'AIM23210', 'AIM52640',  
'AIM51440', 'AIM50440', 'AIM69650', 'AIM25960', 'AIM26630']  
heated_id_list = ['AIM53910', 'AIM32460']  
noheated_id_list = ['AIM84890', 'AIM50600', 'AIM63820', 'AIM81550', 'AIM14150',  
'AIM66080', 'AIM61260', 'AIM87660', 'AIM83450', 'AIM10590', 'AIM00660', 'AIM43280',  
'AIM60890', 'AIM87490', 'AIM86720', 'AIM08440', 'AIM11560', 'AIM36390', 'AIM14790',  
'AIM17820', 'AIM08740', 'AIM10470', 'AIM09610', 'AIM10750', 'AIM16190', 'AIM08770',  
'AIM59200', 'AIM08920', 'AIM83110', 'AIM84290', 'AIM11330', 'AIM11890', 'AIM62040',  
'AIM33100', 'AIM08160', 'AIM58480', 'L000001E', 'AIM65870', 'AIM62440', 'AIM61080',  
'AIM86450', 'AIM14490', 'L0000008', 'L000001A', 'AIM80260', 'AIM65570', 'AIM64610',  
'AIM12730', 'L0000010', 'AIM09380', 'AIM80830', 'AIM62760', 'AIM86080', 'AIM84300',  
'AIM62360', 'AIM61930', 'L000000F', 'AIM82730', 'AIM65520', 'AIM51720', 'AIM63130',  
'AIM02630', 'AIM10550', 'AIM58760', 'AIM08660', 'AIM17330', 'AIM85550', 'AIM08860',  
'L000001D', 'AIM60700', 'AIM41310', 'L0000020', 'AIM59620', 'AIM13220', 'AIM46360',  
'AIM14540', 'AIM84580', 'AIM61510', 'L000001B', 'AIM65040', 'AIM13340', 'AIM09350',  
'AIM65120', 'AIM47950', 'AIM09300', 'AIM61640', 'AIM13020', 'AIM12700', 'AIM62230',  
'AIM34930', 'AIM08990', 'AIM19830', 'AIM61720', 'AIM24520', 'AIM10870', 'AIM39160',  
'AIM88760', 'AIM05650', 'L000000A', 'AIM65250', 'AIM06670', 'AIM03900', 'AIM16390',  
'AIM53230', 'AIM08430', 'AIM14130', 'AIM12500', 'AIM86980', 'L0000017', 'AIM10640',  
'AIM41790', 'AIM66210', 'AIM09680', 'AIM26240', 'AIM27040', 'AIM05390', 'AIM59940',  
'AIM64560', 'AIM12360', 'AIM27990', 'AIM82390', 'AIM63050', 'AIM08470', 'AIM09320',  
'AIM11030', 'AIM09780', 'AIM11840', 'AIM53710', 'AIM86230', 'AIM11610', 'AIM07960',  
'AIM33820', 'AIM66690', 'AIM59930', 'AIM08320', 'AIM09330', 'AIM07300', 'AIM60950',  
'AIM82270', 'AIM82960', 'AIM86650', 'AIM81790', 'AIM10390', 'AIM62380', 'AIM61980',  
'AIM35670', 'AIM11640', 'L0000007', 'AIM79660', 'AIM13570', 'AIM81150', 'AIM52490',  
'AIM04590', 'AIM80950', 'AIM63360', 'L000001C', 'AIM64910', 'AIM31580', 'AIM60340',  
'AIM44980', 'AIM84940', 'AIM59640', 'L000000E', 'AIM10140', 'AIM25600', 'AIM59570',  
'AIM61450', 'AIM44160', 'AIM10220', 'AIM07200', 'AIM11530', 'AIM14530', 'AIM07230',  
'AIM41420', 'AIM09120', 'AIM82040', 'AIM42590', 'AIM59440', 'AIM59160', 'L000000D',  
'AIM64640', 'AIM65730', 'AIM09910', 'L0000011', 'AIM83680', 'L0000012', 'AIM18900',  
'AIM09490', 'AIM28570', 'AIM12120', 'AIM60330', 'AIM09880', 'AIM07630', 'AIM13160',  
'AIM64130', 'AIM61100', 'AIM10160', 'AIM33600', 'AIM61820', 'AIM32190', 'AIM86760',  
'AIM66000', 'AIM12090', 'AIM60710', 'AIM16850', 'AIM57350', 'AIM14290', 'AIM58800',
```

```

'L000000B', 'AIM00320', 'AIM14260', 'AIM11760', 'AIM09970', 'AIM14550', 'AIM85270',
'AIM11050', 'AIM84820', 'AIM07680', 'AIM06820', 'AIM07150', 'AIM85710', 'AIM07910',
'AIM84170', 'AIM48670', 'AIM05280', 'AIM58040', 'AIM65600', 'AIM87500', 'AIM88230',
'AIM63340', 'AIM85590', 'AIM64480', 'AIM07730', 'AIM61160', 'L0000022', 'AIM08630',
'AIM13450', 'AIM10110', 'AIM81670', 'AIM62700', 'AIM08820', 'AIM58880', 'AIM59480',
'AIM15500', 'AIM12320', 'AIM62670', 'AIM08260', 'AIM85990', 'AI
M38680', 'AIM15180', 'AIM39930', 'AIM60390', 'AIM23110', 'AIM63450', 'L000001F',
'AIM83770', 'AIM09940', 'AIM12930', 'AIM63100', 'AIM07570', 'L0000014', 'L000000C',
'AIM62920', 'AIM65390', 'AIM45670', 'AIM32880', 'AIM64430', 'AIM13560', 'AIM63790',
'AIM66350', 'AIM09600', 'AIM06290', 'AIM15270', 'AIM63610', 'AIM58670', 'AIM60170',
'AIM58420', 'AIM18050', 'AIM34370', 'AIM11310', 'AIM06510', 'AIM10360', 'L0000021',
'L0000013', 'AIM01260', 'AIM83840', 'L0000015', 'AIM09550', 'AIM47180', 'AIM64140',
'AIM80430', 'AIM08880', 'AIM51080', 'AIM87180', 'L0000016', 'AIM61480', 'AIM11070',
'AIM10840']
skylounge_id_list= ['L1000003']
auditorium_id_list= ['AIM07690', 'AIM06330', 'AIM09370']
canteen_id_list= ['AIM19380', 'AIM36310', 'AIM29560', 'AIM17210', 'AIM17940',
'AIM12370', 'AIM18440', 'AIM17560', 'AIM20390', 'AIM17250', 'AIM29550', 'AIM17070',
'AIM16870', 'AIM17900', 'AIM16380', 'AIM18590', 'AIM17340', 'AIM19270', 'AIM15960',
'AIM18840', 'AIM16650', 'AIM19100', 'AIM18250', 'AIM18460', 'AIM17060', 'AIM17750',
'AIM17760', 'AIM20060', 'AIM19480', 'AIM19910', 'AIM20700', 'AIM18630', 'AIM21370']
atrium_id_list= ['L0000023', 'AIM03440', 'L0000026', 'RM000000', 'L0000024', 'L0000025',
'RM000002', 'RM000001']
meeting_id_list= ['AIM52250', 'AIM54560', 'AIM52220', 'AIM34900', 'AIM78900',
'AIM54500', 'AIM57240', 'AIM56270', 'AIM56020', 'AIM56480', 'AIM55600', 'AIM56440',
'AIM52940', 'AIM39460', 'AIM55680', 'AIM42180', 'AIM54160', 'AIM77690', 'AIM38420',
'AIM37220', 'AIM52480', 'AIM54880', 'AIM55470', 'AIM55220', 'AIM45590', 'AIM53200',
'L0000019', 'AIM51510', 'AIM51470', 'AIM52190', 'AIM79750', 'AIM53840', 'AIM78080',
'AIM54240', 'AIM78810', 'AIM35620', 'AIM31520', 'AIM34100', 'AIM47060', 'AIM55720',
'AIM32770', 'AIM56080', 'AIM52690', 'AIM36180', 'AIM40260', 'AIM77850', 'AIM49380',
'AIM55000', 'AIM52430', 'AIM55280', 'AIM40980', 'AIM53150', 'AIM51530', 'AIM53410',
'AIM44660', 'AIM54960', 'AIM56400', 'AIM54030', 'AIM78540', 'AIM48020', 'AIM77120',
'AIM43460', 'AIM54750', 'AIM50820']
auditorium_gardarobe_id_list= ['AIM15660', 'AIM15210', 'AIM15020', 'AIM15850',
'AIM20680', 'AIM15700', 'AIM14380', 'AIM13960', 'AIM14870', 'AIM15240', 'AIM15060',
'AIM16490', 'AIM16340', 'AIM16530', 'AIM14600', 'AIM15250', 'AIM17190', 'AIM15510',
'AIM16150', 'AIM15890']
print_id_list= ['AIM83200', 'AIM58520', 'AIM57550', 'AIM59080', 'AIM57120', 'AIM57860',
'AIM79500', 'AIM57920', 'AIM57880', 'AIM57300', 'AIM52550', 'AIM58320', 'AIM56720',
'AIM57040', 'AIM53270', 'AIM58240', 'AIM56660', 'AIM80140', 'AIM56910', 'AIM57360',
'AIM78930', 'AIM57760', 'AIM57680', 'AIM81400', 'AIM80710', 'AIM82510', 'AIM58110',
'AIM79620']

real_building.assign_thermal_template_to_rooms(alltemplates[12], office_id_list)
real_building.assign_thermal_template_to_rooms(alltemplates[7], heated_id_list)
real_building.assign_thermal_template_to_rooms(alltemplates[13], skylounge_id_list)
real_building.assign_thermal_template_to_rooms(alltemplates[9], auditorium_id_list)
real_building.assign_thermal_template_to_rooms(alltemplates[10], canteen_id_list)

```

```
real_building.assign_thermal_template_to_rooms(alltemplates[6], atrium_id_list)
real_building.assign_thermal_template_to_rooms(alltemplates[11], meeting_id_list)
real_building.assign_thermal_template_to_rooms(alltemplates[14],
auditorium_gardarobe_id_list)
real_building.assign_thermal_template_to_rooms(alltemplates[8], notheated_id_list)
real_building.assign_thermal_template_to_rooms(alltemplates[15], print_id_list)
```

2) Remove air exchange rate and internal gains

```
import xlrd
from xlrd import open_workbook
workbook=open_workbook('sampletorun0429.xlsx') #remember to put excel file in the same
folder of your ies model
sheet =workbook.sheet_by_index(0)# get sheet 1
import iesve
import pprint
import time
b=1 # sample number

for i in range(b,b+1):
    aps_sample_name=sheet.cell(i,0).value #aps.name
    infil=sheet.cell(i,4).value # infiltration index
    auxi=sheet.cell(i,5).value # auxiliary ventilation index
    occupancy=sheet.cell(i,8).value #occupancy gain index, remember to remove it before next
simulation
    light=sheet.cell(i,9).value #light gain index, remember to remove it before next simulation
    equipment=sheet.cell(i,10).value #equipment gain index, remember to remove it before
next simulation
    # remove gains remove air exchange before next simulation
    project = iesve.VEProject.get_current_project()
    casual_gains = project.casual_gains()
    templates = project.thermal_templates(False)
    templates_iter = templates.values()
    alltemplates=list(templates.values())
    alltemplates[12].remove_gain(casual_gains[int(occupancy)]) # data from sample excel
    alltemplates[12].remove_gain(casual_gains[int(light)]) # data from sample excel
    alltemplates[12].remove_gain(casual_gains[int(equipment)]) # data from sample excel
    alltemplates[12].apply_changes()
    air_exchanges = project.air_exchanges()
    for template in templates_iter:
        template.remove_air_exchange(air_exchanges[int(infil)])# data from sample excel
        template.apply_changes()
    c=[9,10,11,12,13,14]
    newarray = [alltemplates[int(i)] for i in c ]
    for template in newarray:
        template.remove_air_exchange(air_exchanges[int(auxi)])# data from sample excel
        template.apply_changes()
    # get each cell value(every time the same row)
```

3) Read data from aps file

```
import icsve      # the VE api
import numpy as np # numeric data series returned as numpy arrays
import sys

import xlswriter
workbook=xlswriter.Workbook('recording341400.xls')
worksheet=workbook.add_worksheet()
bold=workbook.add_format({'bold':1})

def find_variable(vista_display_name, var_level):

    for variable in aps_variables:
        if variable['display_name'] == vista_display_name and variable['model_level'] ==
var_level:
            return variable
    return None

def convert_units(value, units):
    return (value / units['divisor']) + units['offset']

def make_display_string(sum, units):
    return "{:,.2f} {}".format(
        convert_units(sum, units),

        units['display_name']
    )

for i in range(341,401) here define the samples you want to loop
def read_variable(result_reader, result_variable):
    assert result_variable is not None, "Error: missing variable data"

    units_for_this_variable = aps_units[result_variable['units_type']]
    units_metric = units_for_this_variable['units_metric']

    aps_data = result_reader.get_results(result_variable['aps_varname'],
result_variable['display_name'], result_variable['model_level'])

    if aps_data is None:
        print("Error reading variable: " + result_variable['display_name'], file=sys.stderr)
        return 0

    aps_data *= (24 / result_reader.results_per_day)

    annual_total = np.sum(aps_data)
    worksheet.write_number(i,0,annual_total)
    del aps_data

def read_variable_1(result_reader, result_variable):
```

```
assert result_variable is not None, "Error: missing variable data"

units_for_this_variable = aps_units[result_variable['units_type']]
units_metric = units_for_this_variable['units_metric']

aps_data = result_reader.get_results(result_variable['aps_varname'],
result_variable['display_name'], result_variable['model_level'])

if aps_data is None:
    print("Error reading variable: " + result_variable['display_name'], file=sys.stderr)
    return 0

aps_data *= (24 / result_reader.results_per_day)

annual_heat = np.sum(aps_data)
worksheet.write_number(i,1,annual_heat)

def read_variable_2(result_reader, result_variable):
    assert result_variable is not None, "Error: missing variable data"

    units_for_this_variable = aps_units[result_variable['units_type']]
    units_metric = units_for_this_variable['units_metric']

    aps_data = result_reader.get_results(result_variable['aps_varname'],
result_variable['display_name'], result_variable['model_level'])

    if aps_data is None:
        print("Error reading variable: " + result_variable['display_name'], file=sys.stderr)
        return 0

    aps_data *= (24 / result_reader.results_per_day)

    annual_cool = np.sum(aps_data)

    worksheet.write_number(i,2,annual_cool)
    del aps_data

def read_variable_3(result_reader, result_variable):
    assert result_variable is not None, "Error: missing variable data"

    units_for_this_variable = aps_units[result_variable['units_type']]
    units_metric = units_for_this_variable['units_metric']

    aps_data = result_reader.get_results(result_variable['aps_varname'],
result_variable['display_name'], result_variable['model_level'])

    if aps_data is None:
        print("Error reading variable: " + result_variable['display_name'], file=sys.stderr)
```

```
    return 0

    aps_data *= (24 / result_reader.results_per_day)

    annual_light = np.sum(aps_data)
    worksheet.write_number(i,3,annual_light)
    del aps_data

def read_variable_4(result_reader, result_variable):
    assert result_variable is not None, "Error: missing variable data"

    units_for_this_variable = aps_units[result_variable['units_type']]
    units_metric = units_for_this_variable['units_metric']

    aps_data = result_reader.get_results(result_variable['aps_varname'],
result_variable['display_name'], result_variable['model_level'])

    if aps_data is None:
        print("Error reading variable: " + result_variable['display_name'], file=sys.stderr)
        return 0

    aps_data *= (24 / result_reader.results_per_day)

    annual_equip = np.sum(aps_data)

    worksheet.write_number(i,4,annual_equip)
    del aps_data

if __name__ == "__main__":
    # Open APS file:\\Mac\\Home\\Desktop\\05 04 16 RED\\vista
    # \\Mac\\Home\\Desktop\\Final\\vista

    with iesve.ResultsReader.open('//Mac/Home/Desktop/Final
/vista/'+str(i)+'aps') as results_file_reader:
        assert results_file_reader is not None, "Error opening results file"

        aps_variables = results_file_reader.get_variables()
        aps_units = results_file_reader.get_units()

        read_variable(results_file_reader, find_variable('Total energy', 'e'))
        read_variable_1(results_file_reader, find_variable('Boilers energy', 'e'))
        read_variable_2(results_file_reader, find_variable('Chillers energy', 'e'))
        read_variable_3(results_file_reader, find_variable('Lights electricity', 'e'))
        read_variable_4(results_file_reader, find_variable('Equip electricity', 'e'))
```




LUND UNIVERSITY

Dept of Architecture and Built Environment: Division of Energy and Building Design
Dept of Building and Environmental Technology: Divisions of Building Physics and Building Services